CHAPTER FOURTEEN

TRANSACTINIDE ELEMENTS AND FUTURE ELEMENTS

Darleane C. Hoffman, Diana M. Lee, and Valeria Pershina

14.1 INTRODUCTION

This chapter gives a brief summary of the reported discoveries, confirmation, and nuclear properties of the claimed and confirmed transactinide elements through the year 2004. However, the primary emphasis is on the chemical properties – experimental, theoretical, and predicted – of the transactinides and a comparison of measured properties with theoretical predictions. The experimental studies of chemical properties are especially challenging because of the low production rates and the short half-lives and the need for very special facilities and the use of atom-at-a-time chemistry. The discovery of a new element must furnish evidence that its atomic number is different from those of all the currently known elements and first claims to discovery often lacked such positive identification. As a result, there were uncertainties and controversies over priority of discovery, nuclear and chemical properties, and assignment of names. The first *positive identification* of the atomic number of all these elements was accomplished using 'physical' rather than chemical techniques.

The authors of this chapter have made a conscientious effort to present a balanced view of research on the properties of the transactinides. The chapter also includes predictions of the nuclear and chemical properties of the

SuperHeavy Elements (SHEs). The term originally referred to an 'island of nuclear stability' around the predicted closed spherical shells at 112 to 114 protons and 184 neutrons. Revisions due to recent experiments and theoretical calculations are discussed.

As of 1997, discoveries of the transactinide elements 104 through 109 had been recognized by the International Union of Pure and Applied Chemistry (IUPAC) and the International Union of Pure and Applied Physics (IUPAP). The names and symbols for these elements as finally approved by IUPAC in 1997 (CNIC, 1997) and the year of discovery are given in Table 14.1.

Claims to the discovery of element 110 were made by researchers at the Lawrence Berkeley National Laboratory (LBNL) (Ghiorso *et al*., 1995a,b), by researchers at the Gesellschaft für Schwerionenforschung (GSI) in Darmstadt, Germany (Hofmann *et al*., 1995a), and by a Dubna/Livermore group working at the Joint Institute for Nuclear Research (JINR) in Dubna, Russia (Lazarev *et al*., 1996).

The published analysis of these claims by a Joint Working Party (JWP) of IUPAC/IUPAP (Karol *et al*., 2001) gave credit for the synthesis of element 110 to the GSI group and invited them to propose a name. They proposed the name 'Darmstadtium' with the symbol Ds after the place in Germany where the element 110 discovery experiments were conducted. The IUPAC Commission on Nomenclature of Inorganic Chemistry (CNIC) considered the proposal and in March 2003 (Corish and Rosenblatt, 2003) recommended to the IUPAC Bureau that it be accepted. It was officially approved by the IUPAC Council at the 42nd General Assembly in Ottawa, Canada, on August 16, 2003.

The discovery of elements 111 and 112 was reported by the GSI group in 1995 (Hofmann *et al*., 1995b, 1996) and confirmatory experiments were reported in 2002 (Hofmann *et al*., 2002). In mid-2003 the JWP assigned credit for discovery of element 111 to the GSI group and asked them to propose a name (Corish and Rosenblatt, 2003; Karol *et al*., 2003), but judged that the evidence for assigning

Table 14.1 *CNIC/IUPAC compromise recommendation for names of transactinide elements. Approved by IUPAC, August* 30, 1997, *Geneva, Switzerland.*

Element	*Name*	*Symbol*	*Discovery year*
104	Rutherfordium	Rf	1969
105	Dubnium (Hahnium)[a]	Db (Ha)[a]	1970
106	Seaborgium	Sg	1974
107	Bohrium	Bh	1981
108	Hassium	Hs	1984
109	Meitnerium	Mt	1982

[a] Many publications of chemical studies before 1997 use hahnium (Ha) for element 105.

credit for the discovery of element 112 was insufficient. The element 111 discovery team proposed the name 'Roentgenium' with symbol Rg after Wilhelm Conrad Roentgen, the discoverer of X-rays. A provisional recommendation for approval of the proposal was sent (Corish and Rosenblatt, 2004) to the IUPAC Bureau and Council and was approved in late 2004. A modern periodic table showing elements through $Z = 154$ is given in Fig. 14.1.

Evidence for elements 112 through 116 has been reported from 1999 to early 2004 by groups working at Dubna (Oganessian, 1999a–c, 2001, 2002; Lougheed *et al.*, 2000; Oganessian *et al.*, 2000a,b, 2002, 2004a–c). However, it should be emphasized that as yet there is no confirmation by other groups of the isotopes of these elements and their decay products. Nuclear properties of the transactinide elements including half-life, mode of decay, main radiations, and method of production based on reports published through early 2004 are given in Table 14.2 and in Appendix II. Nuclides for which only one decay chain has been reported are not listed. Charts of the isotopes of Lr (the last of the actinides) through 109 and for 110 through 116 are shown in Fig. 14.2(a) and (b).

The transactinide elements begin with element 104 (rutherfordium) and include all the elements beyond lawrencium, the element that ends the actinide series with the filling of the 5f electron shell. According to results of atomic relativistic calculations (Fricke, 1975), the filling of the 6d shell takes place in the

1																	18
1 H	2											13	14	15	16	17	2 He
3 Li	4 Be											5 B	6 C	7 N	8 O	9 F	10 Ne
11 Na	12 Mg	3	4	5	6	7	8	9	10	11	12	13 Al	14 Si	15 P	16 S	17 Cl	18 Ar
19 K	20 Ca	21 Sc	22 Ti	23 V	24 Cr	25 Mn	26 Fe	27 Co	28 Ni	29 Cu	30 Zn	31 Ga	32 Ge	33 As	34 Se	35 Br	36 Kr
37 Rb	38 Sr	39 Y	40 Zr	41 Nb	42 Mo	43 Tc	44 Ru	45 Rh	46 Pd	47 Ag	48 Cd	49 In	50 Sn	51 Sb	52 Te	53 I	54 Xe
55 Cs	56 Ba	57 La	72 Hf	73 Ta	74 W	75 Re	76 Os	77 Ir	78 Pt	79 Au	80 Hg	81 Tl	82 Pb	83 Bi	84 Po	85 At	86 Rn
87 Fr	88 Ra	89 Ac	104 Rf	105 Db (Ha)	106 Sg	107 Bh	108 Hs	109 Mt	110 Ds	111 Rg	*112*	*113*	*114*	*115*	*116*	(117)	(118)
(119)	(120)	(121)	(154)														

LANTHANIDES	58 Ce	59 Pr	60 Nd	61 Pm	62 Sm	63 Eu	64 Gd	65 Tb	66 Dy	67 Ho	68 Er	69 Tm	70 Yb	71 Lu
ACTINIDES	90 Th	91 Pa	92 U	93 Np	94 Pu	95 Am	96 Cm	97 Bk	98 Cf	99 Es	100 Fm	101 Md	102 No	103 Lr
SUPERACTINIDES	(122)	(123)	(124)	(125)	(126)									(153)

Fig. 14.1 *Periodic table showing placement of transactinides through element* 154. (*Italics indicate elements reported but not yet confirmed. Undiscovered elements are shown in parentheses.*)

Table 14.2 *Nuclear properties of transactinide elements.*

Mass number	*Half-life*	*Mode of decay*	*Main radiations* (MeV)	*Method of production*
rutherfordium (Rf)				
253	~48 μs	SF		^{206}Pb(^{50}Ti,3n)
254	22.3 μs	SF		^{206}Pb(^{50}Ti,2n)
255	1.64 s	α 48%	α 8.722 (94%)	^{207}Pb(^{50}Ti,2n)
		SF 52%		
256	6 ms	SF, α	α 8.79	^{208}Pb(^{50}Ti,2n)
257	4.7 s	α ~ 80%	α 9.012 (18%)	^{208}Pb(^{50}Ti,n)
		SF ~ 2%	8.977 (29%)	^{249}Cf(^{12}C,4n)
		EC ~ 18%		
258	12 ms	SF		^{246}Cm(^{16}O,4n)
259	3.1 s	α 93%	α 8.87 (~40%)	^{249}Cf(^{13}C,3n)
		SF 7%	8.77 (~60%)	^{248}Cm(^{16}O,5n)
260	20 ms	SF		^{248}Cm(^{16}O,4n)
261	75.5 s	α	α 8.28	^{248}Cm(^{18}O,5n)
	4.2 s	α, SF	8.52	
262	2.1 s	SF		^{248}Cm(^{18}O,4n)
	47 ms	SF		
dubnium (Db)				
256	1.6 s	EC, α	α 9.014 (~67%)	^{209}Bi(^{50}Ti,3n)
257	1.5 s	α, SF	α 8.967, 9.074	^{209}Bi(^{50}Ti,2n)
257 m	0.76 s	α, SF	9.163	^{209}Bi(^{50}Ti,2n)
258	4.4 s	α	α 9.19	^{262}Bh daughter
			9.07	
259	0.51 s	α	α 9.47	^{241}Am(^{22}Ne,4n)
260	1.5 s	α ≥ 90%	α 9.082 (25%)	^{249}Cf(^{15}N,4n)
		SF ≤ 9.6%	9.047 (48%)	^{243}Am(^{22}Ne,5n)
		EC ≤ 2.5%		
261	1.8 s	α ~ 75%	α 8.93	^{243}Am(^{22}Ne,4n)
		SF ~ 25%		^{249}Bk(^{16}O,4n)
262	34 s	α > 67%	α 8.66 (~20%)	^{249}Bk(^{18}O,5n)
		SF + EC < 33%	8.45 (~80%)	
263	27 s	α, SF	α 8.36	^{249}Bk(^{18}O,4n)
268	16 h	SF		115 decay product
seaborgium (Sg)				
258	2.9 ms	SF		^{209}Bi(^{51}V,2n)
259	0.48 s	α	α 9.62 (78%)	^{208}Pb(^{54}Cr,3n)
260	3.6 ms	α	α 9.77 (83%), SF	^{208}Pb(^{54}Cr,2n)
261	0.23 s	α, SF	α 9.56 (60%)	^{208}Pb(^{54}Cr,n)
262	6.9 ms	α ≤ 22%		^{270}110 decay
		SF ≥ 78%		product
263	0.9 s	α	α 9.06 (90%)	^{249}Cf(^{18}O,4n)
	0.3 s	α	α 9.25	
265	7.4 s	α	α 8.84 (46%)	^{248}Cm(^{22}Ne,5n)
266	21 s	α	α 8.77, 8.52	^{248}Cm(^{22}Ne,4n)

Table 14.2 (*Contd.*)

Mass number	*Half-life*	*Mode of decay*	*Main radiations* (MeV)	*Method of production*
bohrium (Bh)				
261	12 ms	α	α 10.10 (40%)	^{209}Bi(^{54}Cr,2n)
262	0.1 s	α	α 10.06, 9.91, 9.74	^{209}Bi(^{54}Cr,n)
	8.0 ms	α	α 10.37, 10.24	^{209}Bi(^{54}Cr,n)
264	1.0 s	α	α 9.48, 9.62	111 decay product
266	∼1 s	α	α 9.3	^{249}Bk(^{22}Ne,5n)
267	17 s	α	α 8.85	^{249}Bk(^{22}Ne,4n)
272	9.8 s	α	α 9.02	115 decay product
hassium (Hs)				
264	0.26 ms	α, SF	α 10.43	^{207}Pb(^{58}Fe,n)
265	1.7 ms	α	α 10.30 (90%)	^{208}Pb(^{58}Fe,n)
	0.8 ms	α	α 10.57 (63%)	^{208}Pb(^{58}Fe,n)
266	2.3 ms	α	α 10.18	^{270}110 daughter
267	59 ms	α	α 9.88, 9.83, 9.75	^{271}110 daughter
269	14 s	α	α 9.23, 9.17	112 decay product
270	∼4 s	α		^{248}cm(^{26}Mg,4n)
meitnerium (Mt)				
266	1.7 ms	α	α 10.46, 11.74	^{209}Bi(^{58}Fe,n)
268	42 ms	α	α 10.10, 10.24	111 daughter
276	0.72 s	α	α 9.71	115 decay product
darmstadtium (Ds)				
267	3.1 μs	α	α 11.6	^{209}Bi(^{59}Co,n)
269	0.17 ms	α	α 11.11	^{208}Pb(^{62}Ni,n)
270	0.10 ms	α	α 11.03	^{207}Pb(^{64}Ni,n)
	6.0 ms	α	α 12.15	^{207}Pb(^{64}Ni,n)
271	56 ms	α	α 10.71	^{208}Pb(^{64}Ni,n)
	1.1 ms	α	α 10.74, 10.68	
273	0.15 ms	α	α 11.08	112 daughter
280	7.6 s	SF		114 decay product
roentgenium (Rg)				
272	1.6 ms	α	α 11.0	^{209}Bi(^{64}Ni,n)
280	3.6 s	α	α 9.75	115 decay product
element 112				
277	0.6 ms	α	α 11.65, 11.45	^{208}Pb(^{70}Zn,n)
283	3 min	α, SF		^{238}U(^{48}Ca,3n); 114 daughter
284	0.75 min	α	α 9.15	114 daughter
element 113				
284	0.48 s	α	α 10.00	115 daughter
element 114				
287	5 s	α	α 10.29	^{242}Pu(^{48}Ca,3n)
288	2.6 s	α	α 9.82	^{244}Pu(^{48}Ca,4n)
element 115				
288	87 ms	α	α 10.46	^{243}Am(^{48}Ca,3n)
element 116				
292	53 ms	α	α 10.53	^{248}Cm(^{48}Ca,4n)

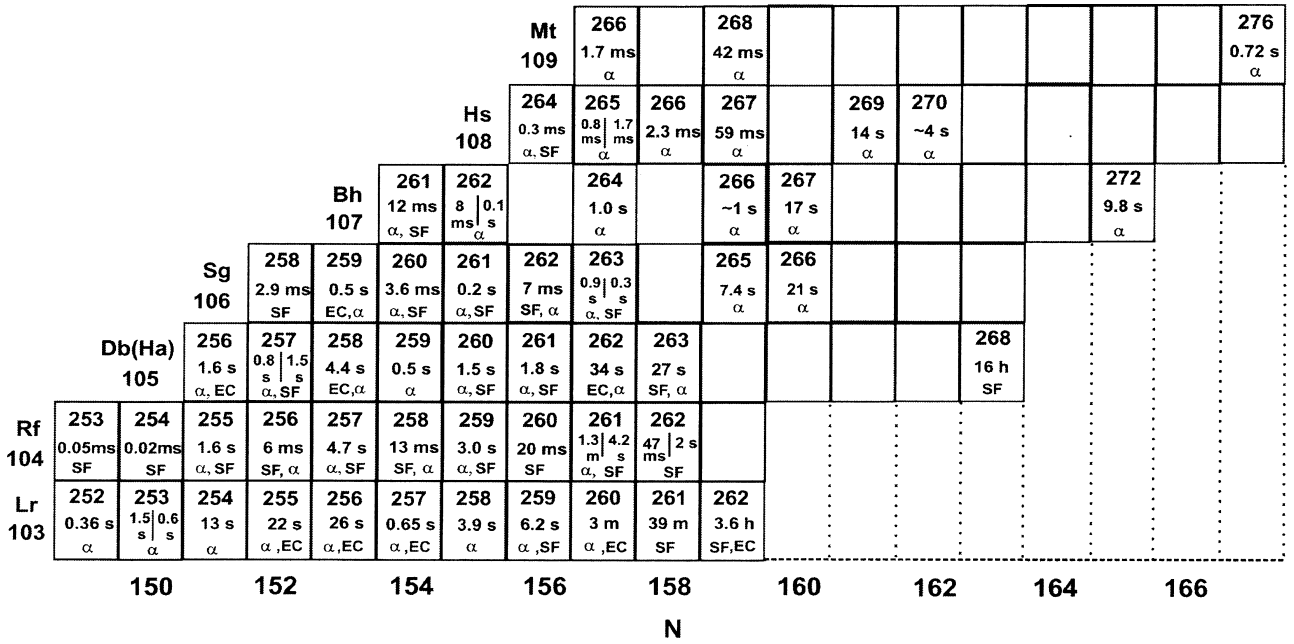

Fig. 14.2 (*a*) *Chart of all isotopes reported for elements* 103 *through* 109.

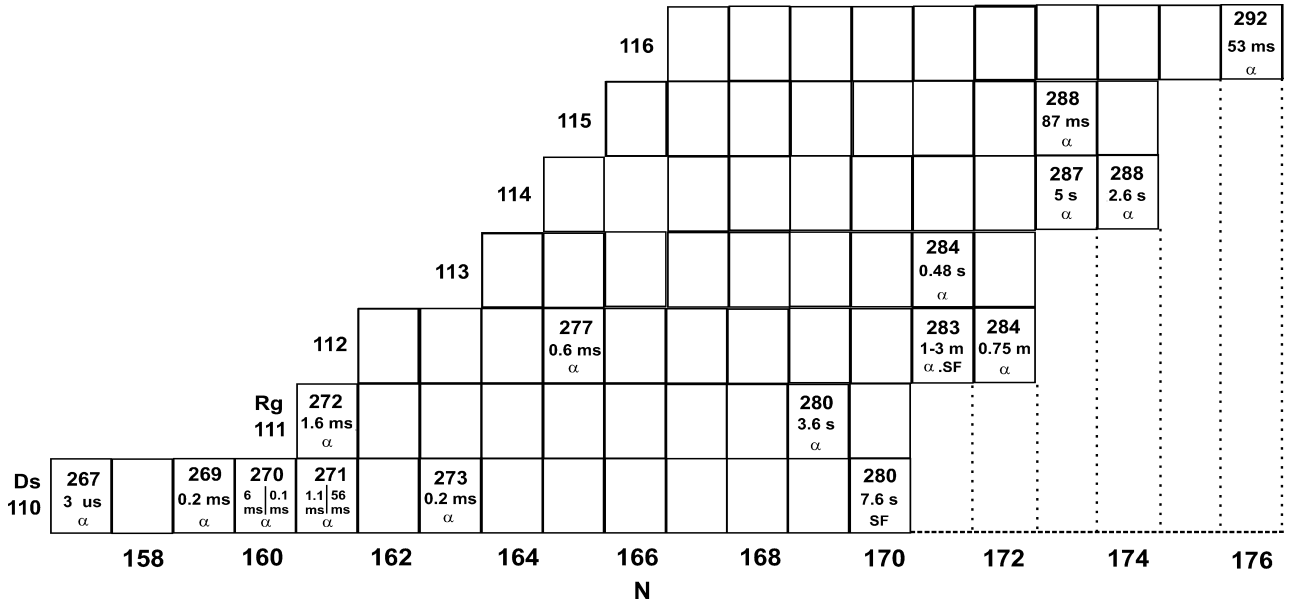

Fig. 14.2 (*b*) *Chart of all isotopes reported for elements* 110 *through* 116.

first nine of the transactinide elements ($Z = 104$ through 112). In elements 113 through 118 the 7p shell is being filled and element 118 is the heaviest member of the noble gas group. Filling of the 8s shell is expected to occur with elements 119 and 120, making them homologs of elements in groups 1 and 2. Accurate relativistic calculations (Eliav *et al.*, 1998a) show that element 121 will have an 8p electron in its ground state configuration in contrast to the 7d electron expected from simple extrapolation of the members of group 3 in the periodic table. A 7d electron will be added in element 122 to give it the [118] $8s^2 7d 8p$ configuration (Eliav *et al.*, 2002), in contrast to thorium, which has the configuration $[Rn]7s^2 6d^2$.

No accurate calculations exist beyond element 122 (Eliav *et al.*, 1992), where the situation becomes more complicated because the energy spacings for the 7d, 6f, and 5g levels and later on for the 9s, $9p_{1/2}$, and $8p_{3/2}$ become so close that in the region of $Z = 160$ the usual classification on the basis of a simple electronic configuration may become invalid. Clear structures on the basis of pure p-, d-, f-, and g-blocks are no longer distinguishable. Chemical properties of the elements influenced by these mixed electronic shells will then be so different from anything currently known that classification on the basis of the known periodic table will be impossible.

In order to positively identify a new element and place it in its proper position in the periodic table, its atomic number (proton number) must be determined or deduced in some way. For transactinide elements it became necessary to develop new methods for positive identification of atomic number. One widely used technique is that of correlation of the unknown element's decay to a known daughter and/or granddaughter, which can be identified either chemically or by its decay characteristics. The method of $\alpha-\alpha$ correlations has been widely used for elements that decay by alpha emission to subsequent known α emitters. Another definitive method is measurement of the characteristic X-rays of the new element. This technique was used by Bemis *et al.* (1973, 1977) to confirm the discovery and reported properties of elements 104 and 105, but it requires considerably larger samples than the α–α correlation method. Although detection of spontaneous fission (SF) is a very sensitive technique, determination of the Z of the parent fissioning nuclide is extremely difficult and depends on some other indirect method such as excitation functions, half-life systematics, production in other reactions, or determination of the atomic number of *both primary fragments* from the same SF event in order to add them together to get the Z of the fissioning new element. Detection of only SF decay has led to many controversies concerning discoveries of the transactinide elements.

In 1974, IUPAC and IUPAP appointed an *ad hoc* committee of neutral experts, consisting of three members from the USA, three from the USSR, and three from other countries (including the chairman), to consider the claims of priority to discovery of elements 104 and 105 and attempt to get agreement between the research groups at Berkeley (USA) and Dubna (USSR). The

committee was finally disbanded without finishing the report, but the American members eventually published their own in-depth report (Hyde *et al*., 1987) that summarized the claims and counterclaims together with a critical assessment of both the physical and the chemical evidence relating to discovery of these elements during the period 1960–77. Reference tables with all the known information for each element, a comprehensive bibliography including internal laboratory reports from Dubna and Berkeley, and all articles published in refereed journals related to the first synthesis and identification of the isotopes of elements 104 and 105, and a summary and conclusions were presented. They concluded that the information published for element 104 (Ghiorso *et al*., 1969) and element 105 (Ghiorso *et al*., 1970, 1971) was correct and fully met the criteria for discovery of new elements stated by Harvey *et al*. (1976) and Flerov and Zvara (1971) and that priority for discovery of elements 104 and 105 clearly belonged to the Berkeley group and endorsed their proposal that they be named rutherfordium (Rf) and hahnium (Ha).

However, the combined IUPAC and IUPAP Transfermium Working Group (TWG) came to different conclusions in their reports (Barber *et al*., 1991, 1992, 1993) on the final assignment of credit for discovery of elements 101 through 109. An immediate rebuttal to the initial assignments of credit for discovery (Barber *et al*., 1991) of element 102 to Dubna, and assignment of shared credit to Berkeley/Dubna for elements 104 and 105, and to GSI/Dubna for element 107 was sent in 1991 in a message from Ghiorso and Seaborg to the chairman of the joint IUPAC/IUPAP TWG. A longer response is found in Ghiorso and Seaborg (1993a), as part of the responses invited from Berkeley, Dubna (Oganessian and Zvara, 1993), and GSI (Armbruster *et al*., 1993). These were published immediately following the TWG report (Barber *et al*., 1993). The response from Ghiorso and Seaborg (1993b) was also published in *Progress in Particle and Nuclear Physics* because IUPAP had given them no opportunity to respond to the companion 'discovery' article published there (Barber *et al*., 1992). A long period of dissent ensued after the CNIC resolved that 'an element could not be named after a living person' and, therefore, the name seaborgium for element 106 already approved by the American Chemical Society could not be accepted. The names for elements 101 through 103 were accepted as mendelevium, nobelium, and lawrencium, but dubnium (Db), joliotium (Jl), rutherfordium (Rf), bohrium (Bh), hahnium (Ha), and meitnerium (Mt) were recommended for elements 104 through 109 by IUPAC/CNIC and approved by the IUPAC Bureau in September 1994. This resulted in protest and criticism from around the world as names that had been in common use were scrambled and the historical right of discoverers of a new element to name it was ignored. A long period of negotiation ensued and resulted in 1995 in the suggestion of still another 'compromise' set of names. This time nobelium (102) was replaced with the name flerovium (Fl), and dubnium, joliotium, seaborgium, nielsbohrium, hahnium, and meitnerium were suggested for elements 104 through 109. This slate did not meet with any more approval than the previous one and in an

unprecedented step the IUPAC Bureau rescinded the previously approved names and solicited comments over a 5-month period. Finally, the CNIC/IUPAC compromise recommendation shown in Table 14.1 was approved by the IUPAC Bureau on August 30, 1997. The long negotiations and final compromise that resulted in the naming of elements 104 through 106 as rutherfordium, dubnium, and seaborgium, and elements 107 through 109 as bohrium, hassium, and meitnerium have been described in detail in the book *The Transuranium People* (Hoffman *et al.*, 2000a).

14.2 NUCLEAR PROPERTIES OF THE TRANSACTINIDE ELEMENTS

All known isotopes of the transactinides are radioactive. The longest known confirmed half-life for these elements ranges from 75 s for ^{261}Rf to only 42.7 ms for ^{268}Mt, the daughter of ^{272}111 (see Fig. 14.2). No transactinide elements have been found in nature although early predictions (Myers and Swiatecki, 1966; Meldner, 1967) that an 'island of SHEs' well beyond uranium might exist around elements with atomic numbers 114 or 126 raised the tantalizing possibility that very long-lived SHEs might still exist on Earth after having been formed during the last nucleosynthesis in our solar system some 5 billion years ago. Later theoretical studies based on new theories of nuclear structure (Strutinsky, 1966; Nilsson *et al.*, 1969a,b; Fiset and Nix, 1972; Randrup *et al.*, 1974) confirmed that an island of nuclear stability stabilized by spherical nuclear shells should be centered around 110 to 114 protons and 184 neutrons. Some calculations even indicated that element 110 with 184 neutrons (^{294}110) should be the longest-lived, with a half-life in the range of hundreds of thousands to a billion years. These predictions sparked a host of experimental investigations to try to detect SHEs in a wide variety of natural sources, but by 1987 no credible evidence for SHEs in nature remained (Hoffman *et al.*, 2000b).

14.3 ONE-ATOM-AT-A-TIME CHEMISTRY

14.3.1 Challenges

Special challenges are involved in studying the chemical properties of the transactinide elements because of their short half-lives, low production rates, the presence of many other unwanted activities, the necessity for producing them in accelerators with high-intensity beams, and the need to build special radiochemistry laboratory and detection facilities nearby. In addition, it is often necessary to prepare and use highly radioactive and rare targets, e.g. ^{248}Cm, ^{249}Bk, ^{249}Cf. Techniques have been developed for detection of a single atom at a time, usually by measuring its radioactive decay. Often the longest-lived known isotope of the element that is used for chemical studies is not the isotope first

discovered. Knowledge of the nuclear decay properties and a measurement technique that positively shows that the detected decay arises from the element in question are required. The technique of α–α correlation to known daughter or granddaughter activities can provide such positive identification and has been widely used because many of the transactinide isotopes decay by alpha emission to known alpha-decaying daughter isotopes. Measurement of characteristic X-rays associated with the decay can also provide positive identification of atomic number, but the technique is difficult to apply when only a few atoms can be detected.

14.3.2 Production methods and facilities required

Chemical studies require use of an isotope with a half-life long enough to permit chemical separation and a reasonable production and detection rate, which for the transactinide elements may range from a few atoms per minute for Rf to only an atom per week in the case of Hs. In addition, the isotope must have unique decay characteristics so that it can be positively identified even on an atom-at-a-time basis in order to prove that it belongs to the element whose chemistry is being studied. The isotopes of elements Rf through Hs that were used in the first definitive chemical studies for each element, their production modes, approximate cross sections, and approximate detection rates for the initial experiments that had different overall efficiencies and transport times are listed in Table 14.3, together with those for Lr, the last of the actinides.

14.3.3 Chemical procedures

The chemical procedures used in atom-at-a-time studies must be fast enough to be accomplished in times comparable to the half-lives of the isotopes used in those studies and must give the same results for a few atoms as for macro

Table 14.3 *Isotopes used in first definitive chemical studies of Lr through Hs.*

Nuclide (half-life)	*Reaction*	*Cross section*	*Estimated rate*	*Year*
^{256}Lr (26 s)	^{249}Cf (^{11}B,4n)	~5 nb	3 min^{-1}	1970[a]
^{261}Rf (75 s)	^{248}Cm(^{18}O,5n)	~5 nb	3 min^{-1}	1970[b]
^{262}Ha (34 s)	^{249}Bk(^{18}O,5n)	~6 nb	1 min^{-1}	1988[c]
^{266,265}Sg (21 s, 7 s)	^{48}Cm(^{22}Ne,4n,5n)	0.03 nb	1-2 d^{-1}	1997[d]
^{267}Bh (17 s)	^{249}Bk(^{22}Ne,4n)	~60 pb	2 week^{-1}	2000[e]
^{270,269}Hs (~4 s, 14 s)	^{248}Cm(^{26}Mg,4,5n)	~5 pb	1 week^{-1}	2001[f]

[a] Silva *et al.* (1970a).
[b] Silva *et al.* (1970b).
[c] Gregorich *et al.* (1988).
[d] Schädel *et al.* (1997b).
[e] Eichler *et al.* (2000).
[f] Düllmann *et al.* (2002a,b); Kirbach *et al.* (2002).

amounts. Chemical methods in which a single atom rapidly participates in many identical chemical interactions in two-phase systems with fast kinetics that reach equilibrium quickly have proven to be valid. Adloff and Guillaumont (1993) have given a thorough discussion of the validity of conclusions about chemical behavior obtained from very small numbers of atoms. An equilibrium constant was defined for such reactions in terms of the probabilities of finding the species in one phase or the other. Adloff and Guillaumont concluded that it is valid to combine the results of many separate one-atom-at-a-time experiments in order to get statistically significant results. Thus the results obtained from many identical experiments, each performed with only a single atom, can be added together to obtain statistically significant information about chemical behavior (Guillaumont *et al*., 1989, 1991).

In early studies, activities recoiling from the target were deposited on a thin 'catcher' foil placed directly behind the target in the production chamber of the accelerator. The foil was then removed manually or remotely shuttled to a detection system without disturbing the accelerator vacuum, and its alpha and SF activity measured with appropriate radiation detectors. Alternatively, the collector foil was removed and chemically processed. In either case, the valuable target is not destroyed, and considerable decontamination from all of the activity remaining in the target itself is achieved. Later, gas transport systems using a variety of gases and aerosols were developed to rapidly and efficiently transport reaction products to collection sites outside the radiation field where chemistry can be carried out within a few seconds, either manually or with computer-controlled automated systems that have been developed for both aqueous- and gas-phase chemistry. Although the automated systems are not necessarily faster, they usually give more reproducible results and are more appropriate for carrying out the many repetitive, around the clock experiments lasting weeks at a time that are required to get statistically significant information. Several detailed reviews (Gäggeler, 1990; Hoffman, 1994; Wierczinski and Hoffman, 1996; Hoffman and Lee, 1999; Kratz, 1999a) of these methods have been given.

(a) Gas-phase chemistry

Both thermochromatographic and isothermal methods have been used to study gas-phase properties of the heaviest elements. These methods are particularly useful for short-lived isotopes because the lengthy process of evaporating liquid samples that is required in most aqueous chemistry experiments is avoided. Gas-phase chromatographic methods permit determination of the adsorption enthalpy, ΔH_{ads}, by using correlations between measured properties such as temperature of adsorption and ΔH_{ads}. The latter were shown to be linearly related to the sublimation enthalpy, ΔH_{sub} (Zvara *et al*., 1970), which is used to compare the volatilities with lighter homologs.

Pioneering studies of the volatilities of the halides of elements 104 and 105 were carried out in the late 1960s and 1970s by Zvara *et al*. (1974, 1976) using thermochromatographic separations. In this method, a longitudinal, negative temperature gradient is established along a chromatographic column through which a gas stream is conducted. It contains the volatile species of interest that deposit on the surface of the column according to their volatilities. Later, the deposition zones are determined from fission tracks registered in detectors positioned along the column. These fissions are associated with specific deposition temperatures, which are then correlated with ΔH_{ads}. The advantage of this method is that production and separation of the detected species takes place very rapidly and species with half-lives as short as a few seconds can be measured. It also has some disadvantages. Positions of the deposition zones are determined only after the experiments are finished. This makes the interpretation of the results very difficult because it is necessary to correct for the half-lives of the various species involved before their volatilities can be compared. Furthermore, real-time observation of the nuclear decay and the determination of the half-lives of the detected species are not possible. Another difficulty is that if only SF activity is measured in the experiments, it is difficult to prove what the atomic number of the detected species actually was because only the fission fragments are detected (see discussion in Section 14.1).

Improved gas thermochromatographic systems have now been developed in which volatile species are transported through a thermochromatographic column (TC) where they are deposited directly on the surface of the pairs of opposing (Si) photodiode detectors that form the column. Both the radiations from the radioactive species and their deposition positions as a function of temperature along the column can be determined simultaneously and recorded. In this way, the isotope (and element) being studied can be positively identified and its deposition temperature at various positions along the TC (Si) (subjected to an appropriate negative temperature gradient) can be determined. Such a cryogenic on-line TC system was used (Düllmann *et al*., 2002b) to perform the first successful chemical studies of element 108 (Hs) using the alpha-emitting isotopes ^{269,270}Hs and compare the behavior of Hs with Os, its lighter group 8 homolog. These investigations are described in detail in Section 14.6.4b.

Recent studies of gas-phase chemistry have utilized isothermal chromatographic systems such as the On-Line Gas Analyzer (OLGA) developed by Gäggeler (1994) and the Heavy Element Volatility Instrument (HEVI) developed by Kadkhodayan *et al*. (1996) and the alpha-emitting isotopes shown in Table 14.3 to compare the behavior of the halides and oxyhalides of elements 104 through 107 with those of their lighter homologs in groups 4 through 7 of the periodic table. In such systems the entire chromatographic column (usually quartz) is kept at a constant temperature. Volatile species pass through the column and undergo numerous sorption/desorption steps. Chromatographic experiments are carried out at a series of temperatures and the chemical yield of

the volatile, short-lived species is studied as a function of temperature. Retention time is indicative of the volatility at each isothermal temperature and can be deduced from the observed changes in the yield from low to high values. The half-life of the nuclide under investigation serves as an 'internal' clock for the process. Just half of the atoms introduced into the isothermal gas chromatographic column will exit from the other end when the time it takes for an atom to pass through the column (the retention time) corresponds to its half-life. That is, the retention time in the chromatographic column at the temperature where the yield is 50% ($T_{50\%}$) of this maximum value is equal to the half-life of the short-lived nuclide (Gäggeler, 1997) and can be used as a relative measure of volatility. If the retention time is very short compared to the known half-life, the yield through the column will approach 100%. A Monte Carlo program taking account of all the experimental conditions is used to deduce the ΔH_{ads} for the measured species. Examples of these studies are discussed in Section 14.6.

(b) Solution chemistry

The Automated Rapid Chemistry Apparatus (ARCA) and the microcentrifuge system SISAK (Special Isotopes Studied by the AKUFE, Swedish acronym for the centrifuge liquid–liquid extraction technique) are examples of automated, computer-controlled systems that have been used in studies of solution chemistry of the heaviest elements.

(*i*) *ARCA*

ARCA can be used to perform rapid, repeated, high-pressure liquid chromatography column experiments on a timescale of seconds. The separations usually are carried out using microscale ion-exchange resin columns. After sorption on the column, the absorbed species are eluted and distribution coefficients are determined from the retention times of the species on the column. The collected liquid samples must then be dried before measurement of alpha emission and/or SF decay with high-resolution solid-state detectors, thus limiting detection to nuclides with half-lives longer than ~30 s. However, longer-lived daughter products can be detected in subsequent steps and used to infer properties of the parent element. The ARCA system has been used successfully for separations of elements 104 through 106, as described in detail in several reviews (Hoffman, 1994; Schädel, 1995; Hoffman and Lee, 1999; Kratz, 1999a,b).

(*ii*) *SISAK*

SISAK is a well-established on-line technique that has been used for studies of gamma-emitting nuclides with half-lives as short as 0.8 s, e.g., ^{109,110}Tc (Alzitzoglou *et al.*, 1990) and was later adapted for use with alpha emitters (Alstad *et al.*, 1995). The SISAK system can be used to perform liquid–liquid

extractions on the timescale of a few seconds and has been coupled to a flowing liquid scintillation system to provide continuous separation and measurement of α–α correlations and SFs for nuclides as short as a few seconds (Omtvedt *et al.*, 1998). This permits chemical studies of shorter-lived nuclides, but the detection energy resolution is not as good. However, a recent experiment by Omtvedt *et al.* (2002) showed that rapid pre-separation by the Berkeley Gas-filled Separator (BGS) furnished sufficient decontamination from the extremely high background of unwanted activities so that the SISAK system could be used to obtain more detailed information about the chemical properties of Rf using 4.7-s ^{257}Rf produced in the ^{208}Pb(^{50}Ti,n) reaction. The same technique can be extended to studies of 4.4-s ^{258}Db produced via ^{208}Pb(^{51}V,n) or ^{209}Bi(^{50}Ti,n) reactions as well as to still heavier elements although the production rates are steadily decreasing as Z increases. Additional developments to increase production rates will be required. Another limitation will be the requirement to choose extraction systems with fast enough kinetics to achieve equilibrium.

14.4 RELATIVISTIC EFFECTS ON CHEMICAL PROPERTIES

14.4.1 Relativistic effects on atomic electronic shells

The relativistic mass increase can be expressed as $m = m_0\sqrt{1-(v/c)^2}$ where m_0 is the rest mass and v is the velocity of an electron. As the Z of the heavy elements increases, the stronger attraction to the core causes the electrons to move faster, and the resultant mass increase leads to a decrease in the Bohr radius of the hydrogen-like s and $p_{1/2}$ electrons: $a_B = \hbar^2/mc^2 = a_B^0\sqrt{1-(v/c)^2}$. The contraction and stabilization of these orbitals is the direct relativistic effect; it was shown to originate from the region of the inner K- and L-shells (Schwarz *et al.*, 1989; Baerends *et al.*, 1990). This effect was originally thought to be large only for the 'fast' electrons in inner core shells of heavy atoms. Later, it was also found to be large for the outer s and $p_{1/2}$ valence electrons. For example, the relativistic contraction for the 7s orbital in Db is $\Delta_R\langle r\rangle_{ns} = (\langle r\rangle^{nr} - \langle r\rangle^{rel}/\langle r\rangle^{nr}) = 25\%$, as shown in Fig. 14.3. As a consequence, the relativistic stabilization of this 7s orbital is 2.6 eV, as shown in Fig. 14.4.

The effect of the *n*s orbital contraction reaches its maximum in the 6th period with Au (17.3%) and in the 7th period with element 112 (31%); the phenomenon has been called the relativistic effect gold maximum and group 12 maximum, respectively (Pyykkö, 1988; Schwerdtfeger and Seth, 1998). The same maximum is, consequently, observed with the relativistic stabilization of the 6s and 7s orbitals (Fig. 14.5). The shift of the maximum to element 112 in the 7th period in contrast to gold in the 6th period is due to the fact that in both elements 111 and 112 the ground state electronic configuration is d^qs^2, while the electronic configuration changes from Au ($d^{10}s^1$) to Hg ($d^{10}s^2$). (See the discussion of relativistic effects in relation to electronic configurations by Autschbach *et al.* (2002).)

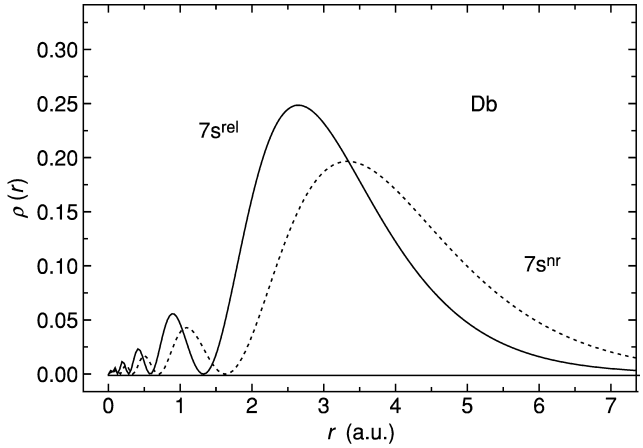

Fig. 14.3 *Relativistic* (*solid line*) *and nonrelativistic* (*dashed line*) *radial distribution of the* 7*s valence electrons in Element* 105, *Db.*

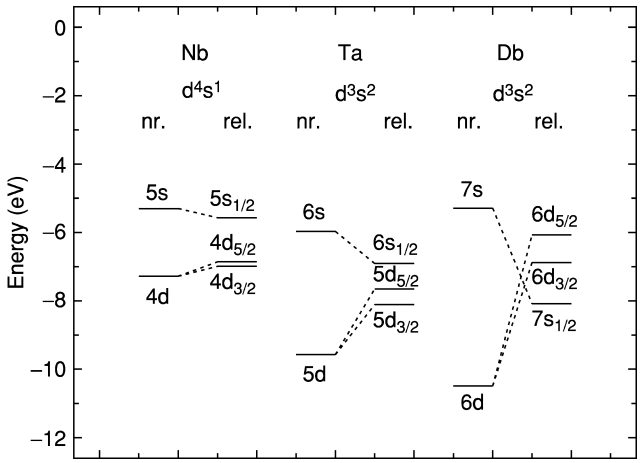

Fig. 14.4 *Relativistic stabilization of the* n*s orbitals, the destabilization of the* (n − 1)*d orbitals and their SO splitting for the group* 5 *elements. Dirac–Fock values are from Desclaux* (1973).

The contraction of the outer s and $p_{1/2}$ orbitals was recently explained as due to the admixture of higher bound and (partially) continuum orbitals due to relativistic perturbations (Schwarz *et al.*, 1989; Baerends *et al.*, 1990).

The relativistic contraction of the s and $p_{1/2}$ shells results in a more efficient screening of the nuclear charge so that orbitals of the outer d- and f-electrons, which never come close to the core, become more expanded and energetically destabilized. This is called the second or indirect relativistic effect. It was

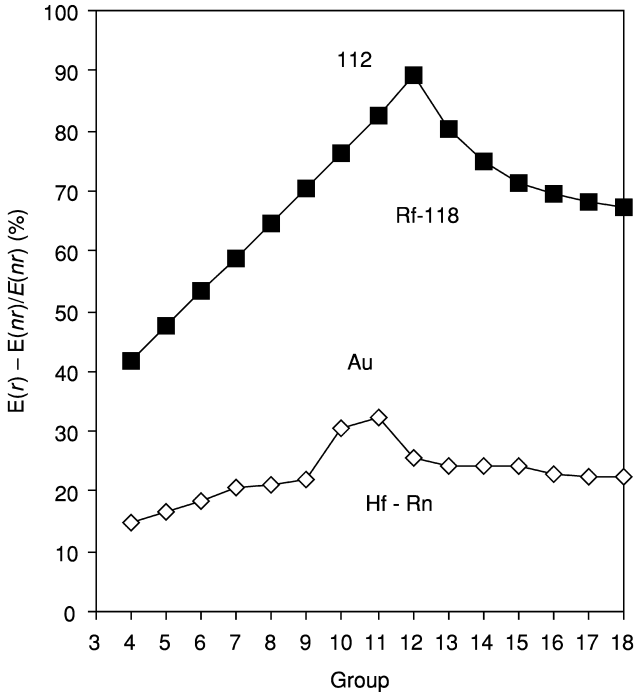

Fig. 14.5 *Relativistic stabilization of the* 6*s and* 7*s orbitals in the* 6*th and* 7*th periods of the periodic table. Redrawn from the data of Schwerdtfeger and Seth* (1998). *Relativistic Dirac–Fock data are from Desclaux* (1973). E(r) *is the relativistic orbital energy and* E(nr) *is the nonrelativistic orbital energy.* (*Figure from Pershina,* 2003).

realized that though contracted s and $p_{1/2}$ core (innermost) orbitals cause indirect destabilization of the outer orbitals, relativistically expanded d- and f-orbitals cause the indirect stabilization of the outer valence s- and p-orbitals. That partially explains the very large relativistic stabilization of the 6s and 7s orbitals in Au and in element 112, respectively (Fig. 14.5). Since both d-shells and f-shells become fully populated at the end of the d- and f-series, respectively, a maximum of indirect stabilization of the valence s- and p-orbitals will occur (Schwarz *et al.*, 1989) there. An example of the relativistic destabilization of the $(n - 1)$d orbitals is shown in Fig. 14.4 for the group 5 elements. This figure shows that trends in the relativistic and nonrelativistic energies of the valence electrons are opposite in going from the 5d to the 6d elements. Their spatial distributions show a similar effect (Fig. 14.3). Thus, only the relativistic description of the wave function can give the appropriate predictions of trends in properties within the chemical groups.

The third relativistic effect is the well-known spin–orbit (SO) splitting of levels with $l > 0$ (p-, d-, f-electrons, etc.) into $j = l \pm 1/2$. It also originates in

the vicinity of the nucleus. The SO splitting decreases with increasing l quantum number: $\mathrm{SO}(n\mathrm{p}_{1/2} - n\mathrm{p}_{3/2}) > \mathrm{SO}(n\mathrm{d}_{3/2} - n\mathrm{d}_{5/2}) > \mathrm{SO}(n\mathrm{f}_{5/2} - n\mathrm{f}_{7/2})$. All three of these effects are of the same order of magnitude and increase roughly as Z^2. The effects can be seen from the energies of one-electron levels of the 7th series of the elements shown in Fig. 14.6.

Breit effects (accounting for magnetostatic interactions) on energies of the valence orbitals and on ionization potentials (IPs) are usually small, e.g. 0.02 eV for element 121 (Eliav *et al.*, 1998a). They can, however, reach a few percent for the fine structure level splitting, e.g. 3.6% of the total amount of the Tl ^{2}P splitting. Quantum electrodynamic (QED) effects are known to be very important for the inner shells, e.g. in accurate calculations of x-ray spectra. The effects were shown to be small, but not negligible for the valence electron shells, and are of the order of 1–2% of the kinetic relativistic effects. That means that existing studies of relativistic effects have uncertainties of no more than 2% (Pyykkö *et al.*, 1998). Recent monographs are recommended for a discussion of relativistic effects on chemical properties (Schwarz, 1990; Wilson *et al.*, 1991).

14.4.2 Current relativistic quantum-chemical methods

Early predictions of chemical properties of the heaviest elements were made in the 1970s on the basis of relativistic atomic electronic structure calculations and extrapolations of properties from the lighter elements (Keller *et al.*, 1970, 1973; Fricke and Waber, 1971; Fricke, 1975; Penneman and Mann, 1976). Influenced by the success of chemical experiments on the heaviest elements and due to the further development of the quantum-mechanical theory, a new wave of predictions of chemical properties based on relativistic molecular calculations

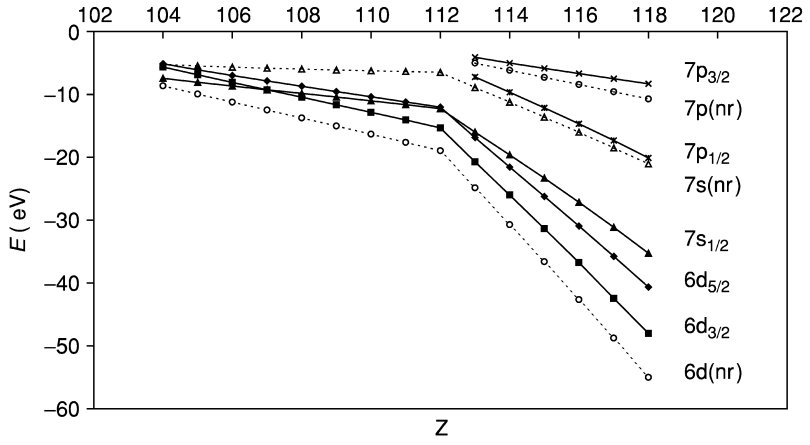

Fig. 14.6 *Relativistic* (*Dirac–Fock, solid lines*) *and nonrelativistic* (*Hartree–Fock, dashed lines*) *orbital energies for elements* 104 *through* 118. *The Dirac–Fock data are from Desclaux* (1973)*; Hartree–Fock data are from Schwerdtfeger and Seth* (1998).

appeared, beginning in the 1990s. These calculations were performed using the most advanced quantum-chemical methods at the time. Overviews of their application to transition elements are given by Pyykkö (1988), to actinides by Pepper and Bursten (1991), and to transactinides by Pershina (1996, 2003), Pershina and Hoffman (2003), and Schwerdtfeger and Seth (1998). All-electron *ab initio* methods based on the Dirac–Coulomb–Breit (DCB) Hamiltonian with some possible corrections such as the radiative correction, the extension of the finite nuclei, and coupling with nuclear spin offer fully relativistic treatment of any atomic system. Since the Dirac equation is written for one electron, the real problem of *ab initio* methods is the treatment of the instantaneous electron–electron interaction, called electron correlation. Correlation effects are taken into account by the configuration interaction (CI) technique, the many-body perturbation theory (MBPT) and currently, most accurately by the Fock-space coupled cluster (CC) procedure, called single double CC excitations (CCSDs) (Ishikawa and Kaldor, 1996; Kaldor and Eliav, 1998, 2000). However, the CCSD method is presently limited to treating electronic configurations with no more than two electrons or holes beyond the closed shell. The DCB CCSD calculations have been performed for elements as heavy as 103, 104, 111–115, 118–122 (Kaldor and Eliav, 2000; Eliav *et al*., 2002).

Atomic calculations using approximations of the DCB equations and some numerical techniques were very successful in the past. Calculations of the electronic structures of the heaviest elements up to very high Z were performed by Desclaux (1973), Mann and Waber (1970), Fricke and Waber (1971), and Fricke *et al*. (1971) using the one-configuration Dirac–Fock (DF) or the Dirac–Slater (DS) methods. (The DS method contains the Slater potential for the exchange-correlation term.) Later, a correlated method, the multi-configuration Dirac–Fock (MCDF) in some slightly different modifications (Desclaux, 1975; Grant, 1986; Parpia *et al*., 1996), was applied in calculations of the electronic structures of many of the heaviest elements up to $Z = 118$ (Desclaux and Fricke, 1980; Pyper and Grant, 1981; Glebov *et al*., 1989; Johnson *et al*., 1990, 1999, 2002; Fricke *et al*., 1993).

Molecular fully relativistic DF linear combination of atomic orbitals (DF-LCAO) codes including correlation effects are still under development (Grant, 1994; Grant and Quiney, 2000). Calculations are restricted to molecules with very few atoms, such as $(113)_2$ (Wood and Pyper, 1981), 111H, 117H, (113), (117), and $114H_4$ (Saue *et al*., 1996; Seth *et al*., 1996; Faegri and Saue, 2001). Algebraic solution of the molecular Dirac equation encounters difficulties due to the fact that the Dirac operator is unbound. Some special techniques like the projection operator technique are used to avoid the variational collapse connected with it. In contrast to nonrelativistic calculations, large basis sets are needed to describe accurately the inner-shell region where relativistic perturbation operators are dominant. The condition of kinetic balance relating the large and small components of the four-component wave function (Grant, 1986) must be observed. Kinetically balanced Gaussian type wave functions

with a Gaussian distribution for the nuclear potential are presently the best suited for these purposes. These methods place heavy demands on computer memory and computational time.

Some pseudopotentials (PPs) (Schwerdtfeger *et al.*, 1989; Schwerdtfeger and Seth, 1998) or relativistic effective core potentials (RECPs) (Ermler *et al.*, 1988; Nash *et al.*, 1997; Han and Lee, 1999) are used to solve the many-electron problem in an efficient way. According to these approximations, frozen inner shells are omitted and replaced in the Hamiltonian by an additional PP term. As a result, the number of basis functions is drastically reduced, and, hence the number of two-electron integrals is reduced. Then, the one-electron integrals are solved for the valence basis functions and this additional term by applying *ab initio* schemes at the self-consistent-field (SCF) level or with electron correlation (CI, MBPT, or CCSD) included. The RECP and the PP have been generated for the transactinides (Nash *et al.*, 1997; Schwerdtfeger and Seth, 1998) and quite a number of calculations have been performed for gas-phase compounds of the heaviest elements.

The next group of methods that can successfully be applied to the calculations of the ground state properties of large, chemically interesting systems are methods based on the density functional theory (DFT). This is a theory of the electronic ground state structure couched in terms of the electronic density distribution $\rho(r)$ (Kohn *et al.*, 1996; Rosen, 1997). It has become increasingly useful in calculations of the ground state density and energy of molecules, clusters, and solids, as well as of solvation and adsorption processes. It is an alternative and complementary approach to the traditional methods of quantum chemistry expressed in terms of the many-electron wave function $\psi(r_1, \ldots, r_N)$. The modern DFT is exact and the methods are accurate upon the introduction of the non-local effects via accurate exchange-correlation potentials, like the relativistic general gradient approximation (RGGA). The electronic structures of a number of the heaviest element compounds have been calculated (Bastug *et al.*, 1993; Varga *et al.*, 1999; Pershina and Bastug, 2000; Pershina *et al.*, 2001, 2002a,b) using the fully relativistic four-component RGGA DFT method. A slightly different Beijing DFT code (Liu *et al.*, 1997; Liu and van Wüllen, 1999) was used for some calculations on the simple heaviest systems. The DS discrete-variational (DS-DV) method, a predecessor of the RGGA DFT method which is intrinsically approximate, was extensively used previously by Pershina *et al.* Reviews of the systems for the heaviest elements are given in Pershina (1996), Pershina and Fricke (1999), Pershina and Hoffman (2003), and Pershina (2003).

There are many other theoretical methods appropriate for calculations of the electronic structures of the heaviest element systems, with some limitations. Their descriptions can be found elsewhere (Pepper and Bursten, 1991; Pershina, 1996; Schwerdtfeger and Seth, 1998). Presently, the combination of the PP (RECP) and DFT methods is the best way to study the electronic structures of the heaviest systems.

14.5 PREDICTIONS OF CHEMICAL PROPERTIES FOR ELEMENTS 104 THROUGH 112

14.5.1 Atomic properties

(a) Electronic configurations

Table 14.4 shows the current best calculations of the electronic configurations of the 6d element atoms and ions in comparison with their 5d homologs. The filling of the 6d shell takes place in the first nine of the transactinide elements, $Z = 104$ through 112. Relativistic changes in the energies of the 7s and 6d electrons (Fig. 14.6) result in the stabilization of the $7s^2$ electronic pair in the ground and first ionized states over the entire 7th period of the periodic table, which is different from the ground states of Pt($5d^9 6s$) and Au($5d^{10} 6s$) or from some of the 1+ and 2+ ionized states, as shown in Table 14.4. For example, the nonrelativistic configuration of element 111 is $6d^{10}7s$ according to Eliav *et al.* (1994). It was thought earlier that the relativistic stabilization of the $7p_{1/2}$ electrons of Rf (the $7s^2 7p6d$ ground state) indicated by MCDF calculations (Glebov *et al.*, 1989; Johnson *et al.*, 1990) would influence the properties of its compounds, but the $7s^2 7p6d$ electronic configuration was not confirmed by the more accurate CCSD calculations of Eliav *et al.* (1995a). Inclusion of dynamic correlation was required to obtain the correct $6d^2 7s^2$ ground state for Rf. However, the CCSD calculations of Eliav *et al.* (1995b) did confirm the $7s^2 7p_{1/2}$ ground state of Lr obtained earlier from the MCDF calculations of

Table 14.4 *Electronic configurations of 5d and 6d elements.*

5d elements[a]				*6d elements*			
Element	Atom	M^+	M^{2+}	Element	Atom	M^+	M^{2+}
Hf	$5d^2 6s^2$	$5d6s^2$	$5d^2$	Rf[b]	$6d^2 7s^2$	$6d7s^2$	$7s^2$
Ta	$5d^3 6s^2$	$5d^3 6s$	$5d^3$	Db[c]	$6d^3 7s^2$	$6d^2 7s^2$	$6d^3$
W	$5d^4 6s^2$	$5d^4 6s$	$5d^4$	Sg[d]	$6d^4 7s^2$	$6d^3 7s^2$	$6d^3 7s$
Re	$5d^5 6s^2$	$5d^4 6s^2$	$5d^5$	Bh[e]	$6d^5 7s^2$	$6d^4 7s^2$	$6d^3 7s^2$
Os	$5d^6 6s^2$	$5d^6 6s$	$5d^5 6s$[e]	Hs[e]	$6d^6 7s^2$	$6d^5 7s^2$	$6d^5 7s$
Ir	$5d^7 6s^2$	$5d^6 6s^2$?	$5d^7$?	109[f]	$6d^7 7s^2$	$6d^6 7s^2$	?
Pt	$5d^9 6s$	$5d^9$	$5d^8$	110[f]	$6d^8 7s^2$	$6d^7 7s^2$	?
Au	$5d^{10} 6s$	$5d^{10}$	$5d^9$	111[g]	$6d^9 7s^2$	$6d^8 7s^2$	?
Hg	$5d^{10} 6s^2$	$5d^{10} 6s$	$5d^{10}$	112[h]	$6d^{10} 7s^2$	$6d^9 7s^2$	$6d^8 7s^2$

[a] Experimental values (Moore, 1958).
[b] CCSD calculations (Eliav *et al.*, 1995a).
[c] MCDF calculations (Fricke *et al.*, 1993).
[d] MCDF calculations (Johnson *et al.*, 1999).
[e] MCDF calculations (Johnson *et al.*, 2002).
[f] DF calculations (Fricke, 1975).
[g] CCSD calculations (Eliav *et al.*, 1994).
[h] CCSD calculations (Eliav *et al.*, 1995b).

Desclaux and Fricke (1980). The relativistic stabilization of the $7p_{1/2}$ electrons manifests itself in some excited states of the transactinides that are different from those of their lighter homologs. For example, the first excited state of Rf is $6d7s^27p(^3D_2)$, only 0.3 eV above its $6d^27s^2(^3F_2)$ ground state (Eliav *et al.*, 1995a), in contrast to Hf, whose first excited state is $5d^26s^2(^3F_3)$, although its ground state is $5d^26s^2(^3F_2)$. Ionized states of elements 104 through 112 show no 7p character, so properties of their compounds in the most typical oxidation states also should not be influenced by this orbital.

(b) Stabilities of oxidation states and ionization potentials

The most accurate IPs calculated for the 6d elements are given in Table 14.5. IPs for elements of the 7th period are shown in Fig. 14.8 in comparison with those of elements of the 6th period. Earlier predictions of stable oxidation states were made on the basis of atomic DF calculations as given in the review of Fricke (1975). They indicated the 4+, 5+, and 6+ states as the most stable for gaseous compounds of Rf, Db, and Sg, respectively, although in solutions the 4+ state was suggested as the most stable for Sg, though not confirmed by later calculations (Pershina *et al.*, 1999). The close proximity of the energy levels of the 7s and 6d electrons (Fig. 14.6) is the reason for the increased stability of the maximum oxidation states of the 6d elements. Indeed, recent MCDF calculations for elements 104 through 108 (Johnson *et al.*, 1990, 1999, 2002; Fricke *et al.*, 1993) have shown a decrease in the multiple IP ($0 \rightarrow Z^+_{max}$) within the transition element groups 4 through 8, as illustrated in Fig. 14.7. This is also the reason that lower oxidation states are not stable at the beginning of the 6d series: the 7s and 6d levels are spatially so close to each other that the stepwise ionization process, for example, for Db or Sg, results in the $6d^2$ and not in the $7s^2$ configuration of Db^{3+} or Sg^{4+} (Pershina *et al.*, 1999). Since the 6d orbitals of the 6d elements are more destabilized than the 4d and 5d orbitals of the 4d and

Table 14.5 *Calculated ionization potentials for the* 6*d elements.*

IP	*Rf*[a]	*Db*[b]	*Sg*[b]	*Bh*[b]	*Hs*[b]	109[c]	110[c]	111	112
IP_1	6.01	6.89	7.85	7.7	7.6	8.3	9.9	10.6[a]	11.97[a]
IP_2	14.4	16.03	17.96	17.5	18.2	(18.9)	(19.6)	(21.5)	22.49[a]
IP_3	23.8	24.65	25.74	26.6	29.3	(30.1)	(31.4)	(31.9)	(32.8)
IP_4	31.9	34.19	35.40	37.3	37.7	(40)	(41)	(42)	(44)
IP_5		44.62	47.28	49.0	51.2	(51)	(53)	(55)	(57)
IP_6			59.24	62.1	64.0				
IP_7				74.9	78.1				
IP_8					91.8				

[a] CCSD calculations: 104 (Eliav *et al.*, 1995a), 111 (Eliav *et al.*, 1994), and 112 (Eliav *et al.*, 1995b).
[b] MCDF calculations; 104 (Johnson *et al.*, 1990), 105 (Fricke *et al.*, 1993), 106 (Johnson *et al.*, 1999), 107, and 108 (Johnson *et al.*, 2002).
[c] DF calculations, best expectation value (Fricke, 1975). Values in parentheses are estimates.

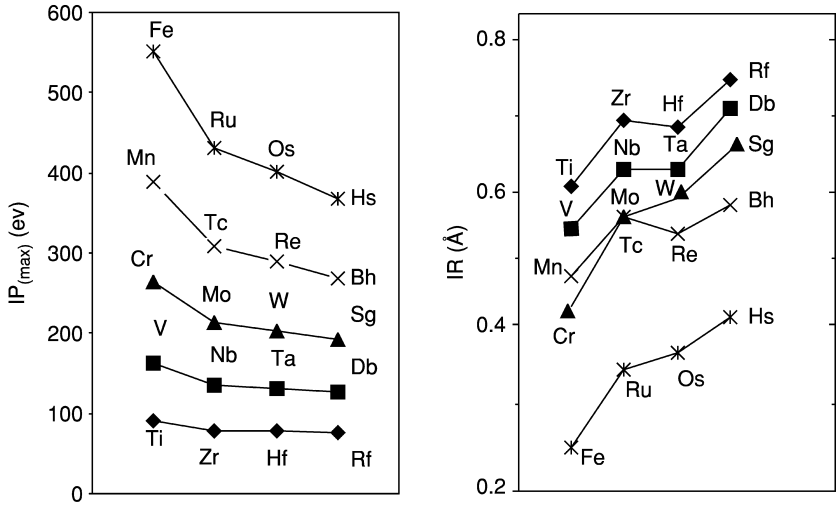

Fig. 14.7 *Ionization potentials (IP_{max}) and ionic radii (IR) for elements* 104 *through* 108 *in their maximum oxidation states obtained as a result of the MCDF calculations* (*Johnson* et al., 1990, 1999, 2002; *Fricke* et al., 1993).

5d elements, respectively, Db^{3+} and Sg^{4+} will be even less stable than Ta^{3+} and W^{4+}. Redox potentials estimated on the basis of these MCDF calculations, as discussed in Section 14.5.3a, indicate that the 6+ state of Sg will also be the most stable in solutions (Pershina *et al.*, 1999).

Predicted stable oxidation states of elements 107 through 110 vary widely. They were discussed in an early paper of Penneman and Mann (1976) that used relativistic Hartree–Fock calculations of the gaseous ion and the hydration parameters of Jorgensen to predict that the most stable oxidation states of elements 107 through 110 in aqueous solutions would be 3+, 2+, 1+, and 0. Earlier, Cunningham (1969) predicted 7+, 8+, 6+, 6+, respectively, for oxidation states of these elements, based on extrapolation by group in the periodic table. Since the Jorgensen hydration parameters did not consider the stabilizing effects of oxyanion formation as observed experimentally for W(VI) and for Re and Os, the higher oxidation states suggested by Cunningham are probably more realistic for solutions where oxyanions can be formed. No predictions based on modern relativistic calculations have been reported for elements 107 through 110.

A most stable oxidation state of 3+ was suggested for element 111, predicted to be a noble metal. It was considered to be as reactive as Au^{3+}, but with more extensive complex formation. Oxidation state 1− was also thought to be possible by analogy to Au^-, while 1+ was predicted to be less stable than for Au. The destabilization of the 6d orbitals at the end of the transactinide series is a reason for the 6d electrons to be chemically active. As a consequence, an enhanced

stability of higher oxidation states can be expected, for example, of the 5+ states of element 111, and of the 4+ state of element 112 (Fricke, 1975; Schwerdtfeger and Seth, 1998).

It was suggested that the 2+ oxidation state of element 112 would be less stable than that of Hg as its IP_2 of 22.49 eV is larger than that for Hg of 18.75 eV (see Table 14.5). The 1+ state of element 112 also will be less stable than that of Hg (see Fig. 14.8) and probably will not be realized in element 112 at all, since compounds of Hg(I) exhibit the diatomic species $(Hg–Hg)^{2+}$. Higher oxidation states such as 4+ will surely be important in aqueous solutions and in compounds. The neutral state of element 112 is also likely to be very stable due to the inertness of the $7s^2$ electrons.

(c) Ionic radii and polarizability

The ionic radii (IR) of elements are defined by the maximum of the radial charge density, r_{max}, or the expectation values $\langle r_{nj} \rangle$ of an outer valence orbital of an ion. The DF $\langle r_{nj} \rangle$ values for elements up to $Z = 120$ were tabulated by Desclaux (1973). The MCDF r_{max} for elements 104 through 108 in various oxidation states were calculated by Johnson *et al.* (1990, 1999, 2002) and by Fricke *et al.* (1993). Using these r_{max}, IR of elements 104 through 108 were estimated by these workers using a linear correlation between r_{max} and the experimentally known IR for the lighter group 4 to 8 elements (Shannon, 1976). The predictions

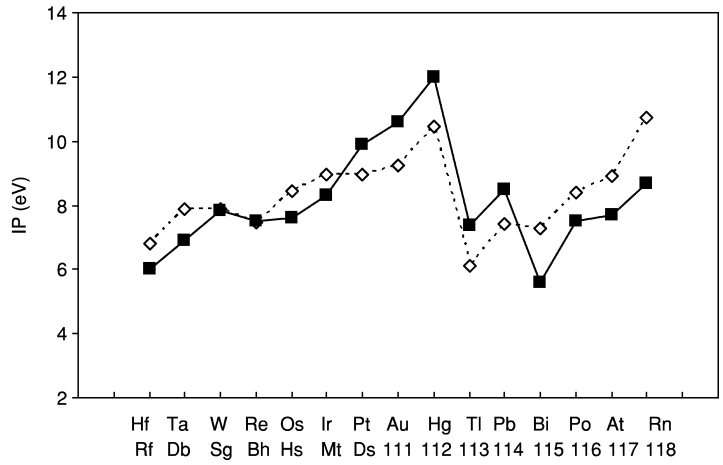

Fig. 14.8 *First ionization potentials for the* 7*th period* (*calculated, solid line*) *and the* 6*th period elements* (*experimental, dashed line*). *CCSD calculations for Rf and elements* 111 *through* 115 (*Eliav* et al., 1994, 1995*b*, 1996*a*, 1998*a*,*b*; *Landau* et al., 2001); *MCDF for elements* 105 *through* 108 (*Fricke* et al., 1993; *Johnson* et al., 1999, 2002; *Pyper and Grant*, 1981).

for the IR of Rf through Hs in their highest oxidation states are summarized in Table 14.6 and Fig. 14.7 together with experimental values for the lighter elements.

The indicated IR of the 4d and 5d elements are almost equal due to the lanthanide contraction, which is 86% a nonrelativistic effect, while the IR of the transactinides are about 0.05 Å larger than the IR of the 5d elements due to an orbital expansion of the $6p_{3/2}$ orbitals, the outer orbitals for the maximum oxidation state. Nevertheless, they are still smaller than the IR of the actinides due to actinide contraction (of 0.030 Å), which is mostly a relativistic effect. Relativistic effects on polarizability (α) change roughly as Z^2 and α should be the smallest in group 12 and in the 7th period for element 112. Its α is relativistically decreased from 74.66 to 25.82 a.u., as shown by PP CCSD(T) calculations (Seth *et al.*, 1997). As a consequence, element 112 is expected to have the weakest van der Waals bond and be extremely volatile.

14.5.2 Gas-phase compounds

(a) Electronic structures of Rf through element 112 and role of relativity

(*i*) *Rf through Hs*

A large series of calculations were performed for halides, oxides, and oxyhalides of Rf through Hs using the DFT and RECP methods: MCl_4 (M = Zr, Hf, and Rf), MCl_5 and MBr_5, $MOCl_3$, and $MOBr_3$ (M = V, Nb, Ta, and Db), MF_6 and MCl_6, $MOCl_4$, MO_2Cl_2, and MO_4^{2-} (M = Mo, W, and Sg) (Pershina, 1996, Pershina and Fricke, 1999), MO (M = Nb, Ta, and Db) (Dolg *et al.*, 1993), $M(CO)_6$ (M = Mo, W, and Sg) (Nash and Bursten, 1995; Nash and Bursten, 1999b), MO_3Cl (M = Tc, Re, and Bh) (Pershina and Bastug, 2000), and MO_4 (M = Ru, Os, and Hs) (Pershina *et al.*, 2001). Various electronic structure

Table 14.6 *MCDF values of IR* (*in* Å) *for the coordination number CN* = 6 *of elements* 104 *through* 108 *in the maximum oxidation states estimated by Johnson* et al. (1990, 1999) *and Fricke* et al. (1993). *Experimental data* (*Shannon,* 1976) *where available are given for the lighter elements*.

Group 4		*Group* 5		*Group* 6		*Group* 7		*Group* 8[a]	
Ti^{4+}	0.61	V^{5+}	0.54	Cr^{6+}	0.44	Mn^{7+}	0.46	Fe^{8+}	0.23
Zr^{4+}	0.72	Nb^{5+}	0.64	Mo^{6+}	0.59	Tc^{7+}	0.57	Ru^{8+}	0.36
Hf^{4+}	0.71	Ta^{5+}	0.64	W^{6+}	0.60	Re^{7+}	0.53	Os^{8+}	0.39
Rf^{4+}	0.79[b]	Db^{5+}	0.74[b]	Sg^{6+}	0.65	Bh^{7+}	0.58	Hs^{8+}	0.45

[a] For CN = 4.
[b] More realistic values obtained from the geometry optimization of molecular compounds are IR = 0.76 Å for Rf^{4+} (Varga *et al.*, 2000) and 0.69 Å for Db^{5+} (Han *et al.*, 1999a).

properties such as IP, electron affinity (EA), electron transition energies, charge density distribution and bonding, as well as their trends in the groups, have been predicted.

Bonding in the compounds of Rf through Hs was shown to be typical of d-element compounds. The bonding is dominated by the large participation of both $6d_{3/2}$ and $6d_{5/2}$ orbitals. The 7s orbital, as well as both $6p_{1/2}$ and $6p_{3/2}$ orbitals, each contribute about 15% to the bonding, and this contribution is increased relative to that of the lighter homologs. The contribution of the $7p_{1/2}$ orbital of 9.4% in $DbCl_5$ is, for example, 50% larger than the contribution of the $5p_{1/2}$ orbital of Nb in $NbCl_5$ (Pershina *et al.*, 1992a). The contribution of the 6d orbitals with respect to that of the 7s and $7p_{1/2}$ orbitals is thus decreased, although it does not change the d-character of the chemical properties.

Molecular orbital (MO) levels for the highest chlorides of Rf, Db, and Sg are shown in Fig. 14.9. They are similar to those of d-element compounds. The group of binding (occupied) levels (with the upper MOs of predominantly 3p character of Cl) is separated from the group of the unoccupied levels of d-character by the energy gap ΔE. A decrease in ΔE from $RfCl_4$ to $SgCl_6$ is indicative of a decrease in the metal–ligand overlap of the atomic wave functions.

The most common feature found in the calculations for all these compounds is an increase in covalence, i.e. a decrease in the effective charge, Q_M, and an increase in the overlap population (OP), as shown in Figs. 14.10 and 14.11. The OP is the amount of the electronic density localized on the bond between atoms in a molecule and is a direct counterpart of the covalent contribution to the

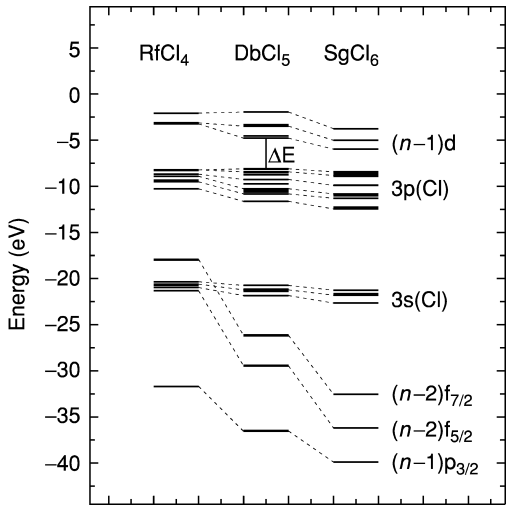

Fig. 14.9 *MO levels for $RfCl_4$, $DbCl_5$, and $SgCl_6$* (*Pershina and Fricke*, 1994).

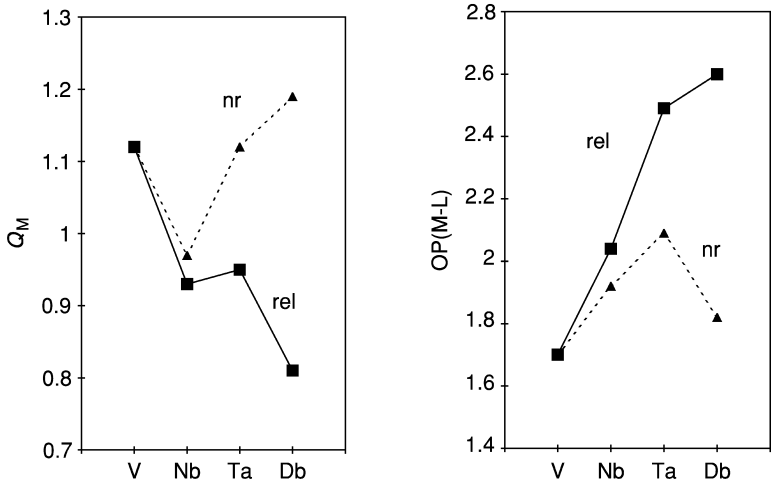

Fig. 14.10 *Relativistic* (*rel*) *and nonrelativistic* (*nr*) *values of the effective charge* (Q_M) *and overlap population* (*OP*) *in* MCl_5, *where* $M = V$, *Nb, Ta, and Db* (*Pershina and Fricke,* 1993).

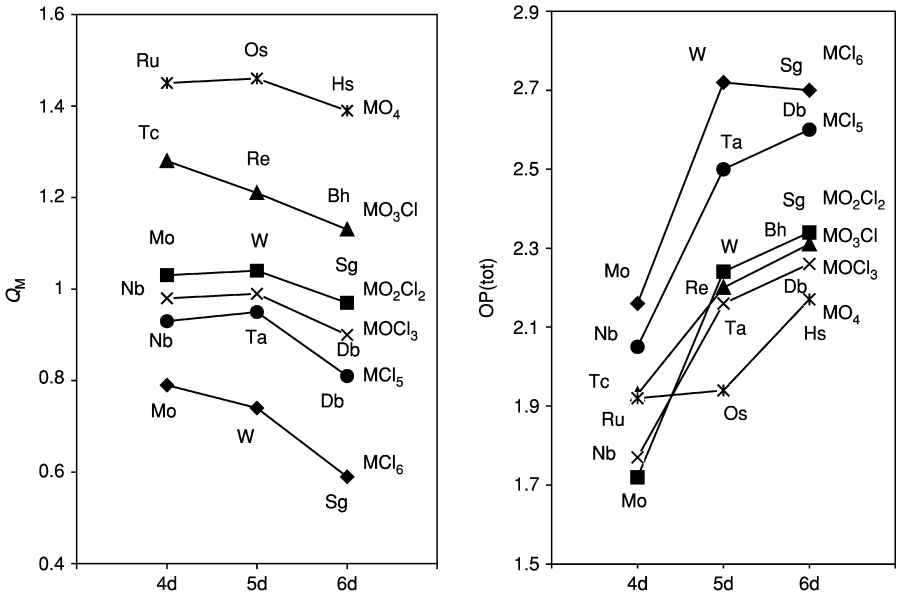

Fig. 14.11 *Effective charges* (Q_M) *and total overlap populations* (*OPs*) *for group* 4 *through* 8 *halides and oxyhalides obtained in various calculations* (*Pershina,* 2003).

binding energy (Mulliken, 1955). Comparison of the relativistic with nonrelativistic calculations (Fig. 14.10) shows this increase to be a purely relativistic effect due to the increasing contribution of the relativistically stabilized and contracted 7s and $7p_{1/2}$ atomic orbitals (AOs), as well as of the expanded 6d AOs in bonding (Pershina and Fricke, 1993).

Calculated molecular properties of gas-phase chlorides, oxychlorides, and oxides of groups 4 through 8 elements and of their homologs studied experimentally are summarized in Table 14.7. Results of molecular calculations (Pershina and Fricke, 1993; Pershina, 1996) have shown that relativistic effects increase IP, decrease EA, and increase the stability of the maximum oxidation state in each compound of the *n*d transition elements, with these effects increasing with increasing Z within the chemical groups. As a consequence, IP, ΔE, and the stabilities of the maximum oxidation states increase from the 4d to the 6d compounds, while the EAs decrease. Nonrelativistically, trends in all these properties would just be reversed from the 5d to the 6d compounds, similarly to the Q_M and OP shown in Fig. 14.10.

Trends in binding energies, D_e, and equilibrium bond distances, R_e, for various types of compounds are depicted in Fig. 14.12. There is a decrease in D_e for almost all of the 6d relative to the 5d element compounds except for MO_4 (M = Ru, Os, and Hs) and MCl_6 (M = Mo, W, and Sg). Within all the groups, relativistic effects enhance bonding of the compounds with increasing Z, though increasing SO splitting of the d-orbitals partially diminishes the binding energy, reaching a decrease of about 1.5 eV for 6d element compounds like SgO_2Cl_2, as shown by RECP calculations (Han *et al.*, 1999a). This is one of the reasons that most of the transactinide compounds have atomization energies lower than those of the homologous 5d elements. The other reason is a decrease in the ionic contribution to bonding, which is also a relativistic effect. The calculated R_e (Fig. 14.12) reflect the experimentally known similarities of bond lengths for the 4d and 5d compounds (due to the lanthanide contraction) and they show an increase in R_e of about 0.05 Å in the transactinide compounds compared to the 5d compounds.

Another important trend is the decrease in the metal–ligand single bond strength in going from the group 4 to the group 6 halides, as well as a decrease in the relative stability of the maximum oxidation state. As a consequence, volatile species such as $SgCl_6$ and $SgOCl_4$ are expected to decompose (a weak Sg–Cl bond) into compounds of Sg(v) at high temperatures by analogy with $MoCl_6$ and $MoOCl_4$. SgO_2Cl_2 was found to be the most stable of all the halides or oxyhalides and was, therefore, recommended (Pershina, 1996) for gas-phase chromatography experiments (Schädel *et al.*, 1997a). An increase in dipole moment, μ, of the low-symmetry molecules within the transition element groups was predicted for all the group 4 to 7 compounds (Table 14.7). The μ and α, as well as the molecular sizes, are decreased by relativistic effects. The PP calculations performed for the gas-phase MO (M = Nb, Ta, and Db) (Dolg *et al.*, 1993) have shown that relativistic effects stabilize the $^2\Delta$ ground state by 2.74 eV

Table 14.7 *Calculated molecular properties of transactinide compounds and of some lighter homologs experimentally studied: ionization potentials (IPs), electron affinities (EAs), energies of the lowest charge-transfer transitions* ($E_{\pi\rightarrow d}$), *equilibrium bond lengths* (R_e), *bond strengths* (D_e), *or dissociation energies* (ΔH_{diss}), *and dipole moments* (μ).

Compound	*IP* (eV)	*EA* (eV)	$E_{\pi\rightarrow d}$ (eV)	R_e (Å)	D_e (eV) (ΔH_{diss})	μ (D)	*Reference*
$ZrCl_4$				2.32[a]	20.32[b]		Girichev *et al.* (1981) (exp.)
$HfCl_4$				2.318[a]	20.53[b]		Girichev *et al.* (1981) (exp.)
$RfCl_4$				2.36	18.97		Han *et al.* (1999a)
				2.38	18.8		Varga *et al.* (2000)
$NbCl_5$	10.77	2.04	2.98	2.34/2.24[c]	19.25[b]		Pershina *et al.* (1992a)
$TaCl_5$	10.73	1.53	3.41	2.37/2.23[c]	19.47[b]		Pershina *et al.* (1992a)
$DbCl_5$	10.83	1.49	3.70	2.42/2.26[c]	17.76		Pershina *et al.* (1992a)
$NbOCl_3$	11.60	0.77	4.57	1.66/2.24[c]		0.91	Pershina *et al.* (1992b)
$TaOCl_3$	11.57	0.29	4.98	1.67/2.25[c]		0.99	Pershina *et al.* (1992b)
$DbOCl_3$	11.64	0.45	4.94	1.72/2.30[c]		1.27	Pershina *et al.* (1992b)
$MoCl_6$	11.06		1.92	2.25	19.29[b]		Pershina and Fricke (1994)
WCl_6	11.13		2.37	2.36[d]	21.65[b]		Pershina and Fricke (1994)
			2.32		19.9		Han *et al.* (1999a)
$SgCl_6$	11.17		2.65	2.38	20.05		Pershina and Fricke (1994)
				2.36	19.9		Han *et al.* (1999a)
$MoOCl_4$				1.658/2.279[e]	20.5[b]	0.14	Pershina and Fricke (1995)
$WOCl_4$				1.685/2.280[e]	22.1[b]	0.49	Pershina and Fricke (1995)
				1.670/2.317	21.5	0.24	Han *et al.* (1999a)

$SgOCl_4$				21.2	1.03	Pershina *et al.* (1995)
			1.720/2.364	21.0	0.77	Han *et al.* (1999a)
MoO_2Cl_2		4.06	1.698/2.259[f]	21.08[b]	1.04	Pershina and Fricke (1996)
WO_2Cl_2		4.48	1.710/2.27[g]	23.5[b]	1.35	Pershina and Fricke (1996)
			1.70/2.28	22.2	1.51	Han *et al.* (1999a)
SgO_2Cl_2		4.33		21.8	1.83	Pershina *et al.* (1996b)
			1.75/2.34	21.0	2.39	Han *et al.* (1999a)
TcO_3Cl	12.25		1.69/2.30[c]	23.12	0.93	Pershina and Bastug (2000)
ReO_3Cl			1.761/2.23			Amble *et al.* (1952) (exp.)
	12.71		1.71/2.28	24.30	1.29	Pershina *et al.* (2000)
BhO_3Cl	13.05		1.77/2.37	22.30	1.95	Pershina *et al.* (2000)
RuO_4	12.19[i]		1.706[h]	27.48		Pershina *et al.* (2001)
OsO_4	12.35[i]		1.711[h]	27.71		Pershina *et al.* (2001)
HsO_4	12.28		1.775	28.44		Pershina *et al.* (2001)

[a] Exp. (Girichev *et al.*, 1981).
[b] From a Born–Haber cycle.
[c] Estimated from IR.
[d] Exp. (Brown, 1973).
[e] Exp. (Lijima and Shibata, 1974, 1975)
[f] Exp. (Zharskii *et al.*, 1975).
[g] Exp. (Jampolskii, 1973).
[h] Exp. (Krebs and Hasse, 1976).
[i] Exp. (Burroughs *et al.*, 1974).

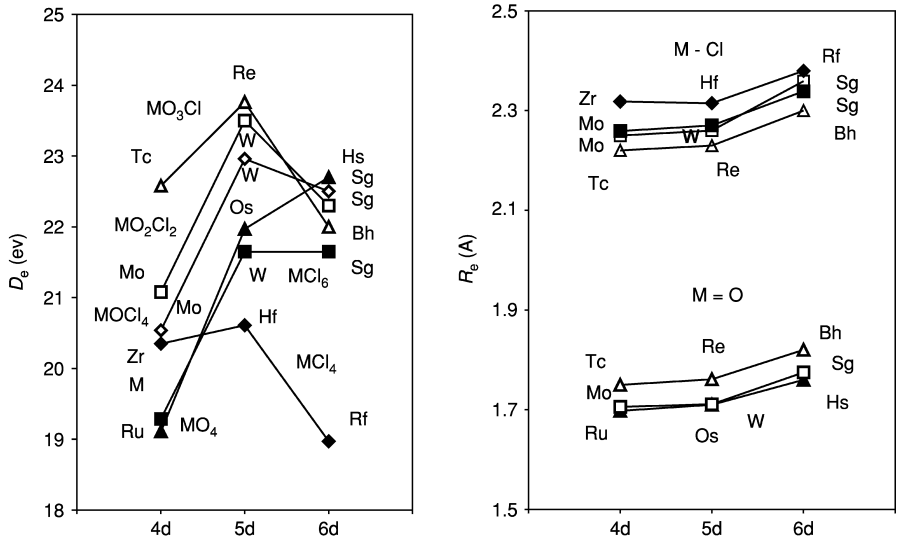

Fig. 14.12 *Binding energies* (D_e, *the dissociation energy of the molecule into its atoms*) *and optimized bond lengths* (R_e) *for various halides, oxides, and oxyhalides of group* 4 *through* 8 *elements* (*Pershina,* 1996*; Han* et al., 1999*a; Pershina and Bastug,* 2000*; Pershina* et al., 2001). *Symbols for both* D_e *and* R_e *are open triangles* = MO_3Cl, *open squares* = MO_2Cl_2, *open rhomboids* = $MOCl_4$, *solid rhomboids* = MCl_4, *solid triangles* = MO_4, *solid squares* = MCl_6.

(the nonrelativistic configuration is $^4\Sigma^-$) in contrast to the $^4\Sigma^-$ state observed for NbO. The relativistic effects also stabilize the binding energy of DbO by 1.93 eV. (Σ and Δ denote molecular spectroscopic states.)

(*ii*) *Mt through element* 112

Elements 109 (Mt) and 110 (Ds) have received little attention in recent years. The position of these elements in the periodic table indicates that they should be noble metals. Volatile hexafluorides and octafluorides might be produced and used for chemical separations. The relativistic DS-DV molecular calculations of Rosen *et al.* (1979) and of Waber and Averill (1974) performed for DsF_6 have shown that its electronic structure is very similar to that of PtF_6, with similar values of IP.

Earlier detailed predictions of chemical properties of element 111 based on atomic calculations were made by Keller *et al.* (1973). Due to the fact that the maximum of relativistic effects in the *n*s shell in group 11 occurs at element 111, there has been widespread interest in the electronic structure of its compounds. The effect of the 7s orbital contraction was investigated for the simplest molecule, 111H, whose electronic structure was calculated by a variety of methods including the fully relativistic DCB *ab initio* method (Seth *et al.*, 1996; Liu and

van Wüllen, 1999). The bonding was shown to be considerably increased by relativistic effects, which doubled the dissociation energy, though the SO splitting diminished it by 0.7 eV. Calculations (Liu and van Wüllen, 1999) were also performed for other dimers, AuX and 111X where X = F, Cl, Br, O, Au, and 111.

The stability of higher oxidation states of element 111 was examined in calculations of energies of the decomposition reactions $MF_6^- \rightarrow MF_4^- + F_2$ and $MF_4^- \rightarrow MF_2^- + F_2$ using the relativistic PP method (Seth *et al.*, 1998a,b). The results support the earlier predictions that the 3+ and 5+ oxidation states will be more stable for this element than they are for Au (due to a larger participation of the 6d orbitals in bonding) and that the 1+ oxidation state of element 111 may be difficult to prepare. The SO coupling was shown to stabilize the molecules in the following order: $MF_6^- > MF_4^- > MF_2$. This order is consistent with the relative involvement of the $(n-1)$d electrons in bonding for each type of molecule.

The most interesting among the heaviest elements from the chemical point of view is element 112, where the maximum of relativistic effects on the 7s shell in the entire 7th period and within group 12 occurs (see Fig. 14.5). Due to the strong relativistic contraction and stabilization of the 7s orbitals (and accordingly its highest IP in group 12) and its closed-shell configuration, it is expected to be rather inert and may be a distinctly noble metal. It was suggested that the interatomic interaction in the metallic state will be small, possibly even leading to high volatility as in the noble gases. Pitzer (1975a) estimated that the very high excitation energy of about 8.6 eV for the $6d^{10}7s^2 \rightarrow 6d^{10}7s7p$ transition into the configuration of the metallic state will not be compensated by the energy gain of the metal–metal bond formation. An extrapolation of the sublimation enthalpy from its homologs, Zn, Cd, and Hg, also suggests that element 112 should be quite volatile (Eichler, 1974). Recently, a similar conclusion was obtained by using a more sophisticated empirical model (Ionova *et al.*, 1996).

Estimates of adsorption enthalpies of element 112 on various metal surfaces using some adsorption models suggest, nevertheless, that element 112 can be deposited on some metals, like Ag, Au, Pd, or Pt (Eichler and Rossbach, 1983). The ability of element 112 to form a metal–metal bond was also predicted by recent relativistic MO calculations for 112M, where M = Cu, Pd, Pt, Ag, and Au (Pershina *et al.*, 2002a). Element 112 was calculated to form a rather strong bond with the above-mentioned transition elements, only about 15–20 kJ mol^{-1} weaker than that of HgM, with the D_e of 112Pd being the largest.

Molecular relativistic PP calculations (Seth *et al.*, 1997) have predicted that the 2+ oxidation state of element 112 will be less stable than that of Hg. They have calculated that $112F_2$ is, indeed, less stable than HgF_2 and that it will decompose readily into 112 and F_2. Seth *et al.* (1997) also came to the conclusion that element 112 should exhibit a typical transition element character in higher oxidation states, because its 6d orbitals are relativistically destabilized and, therefore, should participate more in coordination bonding. Thus, for

example, the 4+ oxidation state of element 112 as in $112F_4$ may be accessible while the 2+ state may not. In combination with an appropriate polar solvent, the species $112F_5^-$ and/or $112F_3^-$ should be formed rather than $112F_4$ or $112F_2$, although these compounds will probably undergo strong hydrolysis in aqueous solutions, and perhaps bromides or even iodides will be more stable and would be better for experimental investigations.

(b) Predictions of volatilities

A more extensive series of the DFT calculations (Pershina, 1996; Pershina and Bastug, 2000; Pershina *et al.*, 2001) permitted establishment of some relationships between molecular properties such as covalence or dipole moment and volatility. Because covalent compounds are typically more volatile than ionic compounds, the higher covalence of high-symmetry halides or oxides of the transactinides is expected to result in their higher volatilities compared with those of their 4d and 5d homologs. For example, $RfCl_4$ is expected to be more volatile than $HfCl_4$ since it is more covalent and is expected to have the T_d symmetry shown by $HfCl_4$ in the vapor phase. Low-symmetry compounds, e.g. oxyhalides of C_n symmetry, have dipole moments and, therefore, are attracted more strongly to the surface of a chromatographic column due to an additional electrostatic (dipole moment–surface charge) interaction than are high-symmetry compounds of the same element such as pure halides. Therefore, one expects that $DbCl_5$ (D_{3h} symmetry) will be more volatile than $DbOCl_3$ (C_{3v} symmetry). For low-symmetry compounds, a trend in volatility in a chemical group will be opposite to the trend in μ, since larger dipole moments cause stronger electrostatic interactions with the surface of a chromatography column. Accordingly, the following decreasing trends in volatility were predicted: $MoO_2Cl_2 > WO_2Cl_2 > SgO_2Cl_2$ and $TcO_3Cl > ReO_3Cl > BhO_3Cl$. These trends are opposite to the increasing dipole moments. Indeed, these trends were confirmed experimentally by the observations (Kadkhodayan, 1993; Kadkhodayan *et al.*,1996; Türler *et al.*, 1998b; Sylwester *et al.*, 2000) that $RfCl_4$ is more volatile than $HfCl_4$, while $DbOCl_3$ (Türler *et al.*, 1996), SgO_2Cl_2 (Schädel *et al.*, 1997a; Türler *et al.*, 1999), and BhO_3Cl (Eichler *et al.*, 2000) are less volatile than the corresponding compounds of their lighter homologs in the respective chemical groups.

In addition, enthalpies of adsorption, $\Delta H_{ads}(BhO_3Cl) = -78.5$ kJ mol^{-1} compared to $\Delta H_{ads}(TcO_3Cl) = -48.2$ kJ mol^{-1} and ΔH_{ads} $(ReO_3Cl) = -61$ kJ mol^{-1}, on the quartz surface of the chromatography column were predicted by Pershina and Bastug (2000) using a model of physisorption and by performing calculations of the electronic structures of those molecules. The obtained adsorption enthalpies indicate that volatility decreases as $TcO_3Cl > ReO_3Cl > BhO_3Cl$, in excellent agreement with the experimental value $\Delta H_{ads}(BhO_3Cl) = -77.8$ kJ mol^{-1} (Eichler *et al.*, 2000). In a similar way, $\Delta H_{ads} = -(36.7 \pm 1.5)$ kJ mol^{-1} on a quartz surface was predicted by Pershina *et al.* (2001) for HsO_4

as compared to $\Delta H_{ads}(RuO_4) = -(40.4 \pm 1.5)$ kJ mol^{-1} and ΔH_{ads} $(OsO_4) = -(38.0 \pm 1.5)$ kJ mol^{-1}. Thus, the volatility of group 8 tetroxides in the specific experiments is expected to change as $RuO_4 < OsO_4 \leq HsO_4$. Such a sequence is also expected from an extrapolation of this property within the group (Düllmann *et al.*, 2002b). This trend is in accord with the idea of increasing volatility with increasing covalence of compounds.

14.5.3 Solution chemistry

(a) Redox potentials

Some earlier estimates of oxidation states of the transactinides made on the basis of empirical modifications of the Born–Haber cycle were reviewed by Fricke (1975). They were mostly related to simple M^{z+} ions, and the results were rather inconsistent. Recently, redox potentials (E°) for complex species of Rf, Db, and Sg in aqueous solutions were estimated (Ionova *et al.*, 1992; Pershina and Fricke, 1994; Pershina *et al.*, 1999) using correlations between the MCDF-calculated IPs (Johnson *et al.*, 1990; 1999; Fricke *et al.*, 1993) and the tabulated redox potentials for group 4, 5, and 6 elements (Bratsch, 1989). Two correlation plots for groups 5 and 6 are shown in Fig. 14.13.

These estimates indicate that the stability of the maximum oxidation state increases with Z within groups 5 and 6, while that of lower oxidation states decreases. Thus, the 5+ and 6+ states of Db and Sg will be more stable than their 3+ and 4+ states, respectively. The 3+ state of Db will be less stable than the 3+ states of Nb or Ta, and the 4+ state of Sg will be less stable than the 4+ states of Mo and W.

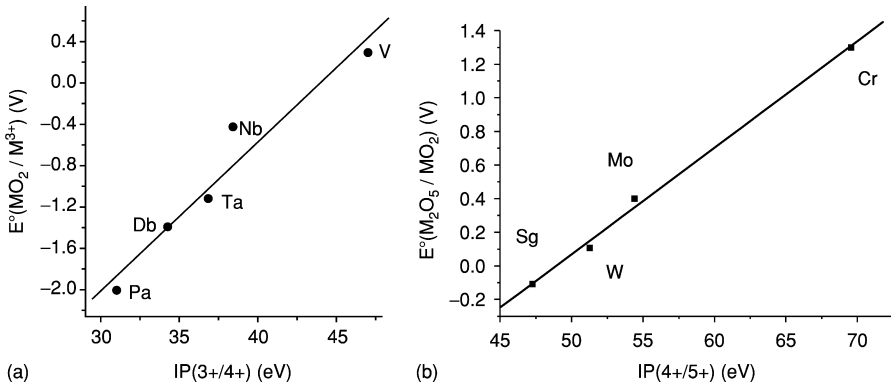

Fig. 14.13 (*a*) *Correlation between IP*(3+/4+) *and the standard potentials* $E^o(MO_2/M^{3+})$ *where M = V, Nb, Ta, Db, Pa. The standard potential for Db is from Ionova* et al. (1992). *The standard potentials for Nb, Ta, and Pa are from Bratsch* (1989). (*b*) *Correlation between IP*(4+/5+) *and the standard potentials* $E^o(M_2O_5/MO_2)$ *where M=Cr, Mo, W, and Sg* (*Pershina* et al., 1999).

The increasing stability of the maximum oxidation state and the decreasing stability of lower oxidation states at the beginning of the 6d series is a relativistic effect caused by destabilization of the 6d orbitals, as discussed earlier. Along the 6d series, the stability of the maximum oxidation state decreases in the order: $Lr^{3+} > Rf^{4+} > Db^{5+} > Sg^{6+}$. For comparison, the results are summarized in Table 14.8, together with those for Lr, the last of the actinides.

(b) Hydrolysis

Aqueous ions of transition elements undergo strong hydrolysis, as do their heaviest homologs. In acidic solutions, hydrolysis involves either the cation $M(H_2O)_n^{Z+} \Leftrightarrow MOH(H_2O)_{n-1}^{(Z-1)+} + H^+$ or the anion, or both. The hydrolysis of cations of a given oxidation state is known to decrease within groups 4, 5, and 6 as one proceeds down the periodic table and it increases from group 4 to group 6 (Baes and Mesmer, 1976). Hydrolysis/protonation of group 4, 5, and 6 cations and of their compounds was considered theoretically on the basis of relativistic DFT calculations (Pershina, 1998a,b; Pershina and Kratz, 2001; Pershina *et al*., 2002b).

For group 4 elements, about 50% of each type of the species indicated in the following equilibrium exists in aqueous solutions at pH = 0: $M(H_2O)_8^{4+} \Leftrightarrow MOH(H_2O)_7^{3+}$. For this reaction, the following trend in hydrolysis of the group 4 elements was predicted from the calculated Gibbs energy changes: Zr > Hf > Rf (Pershina *et al*., 2002b). The first hydrolysis constant

Table 14.8 *Calculated redox potentials of Lr, Rf, Db, and Sg in aqueous acidic solutions.*

Potential	*Lr*[a]	*Rf*	*Db*[b]	*Sg*[c]
$E^\circ(M^{6+}/M^{5+})$	–	–	–	–0.046 (MO_3/M_2O_5) –0.05 (M^{6+}, H^+/M)
$E^\circ(M^{5+}/M^{4+})$	–	–	–1.0 (M_2O_5/MO_2) –1.13 (MO_2^+/MO^{2+})	0.11 (M_2O_5/MO_2) –0.35 (M^{5+}, H^+/M^{4+}, H^+)
$E^\circ(M^{4+}/M^{3+})$	8.1	–1.5 (M^{4+}/M^{3+})[d]	–1.38 (MO_2/M^{3+})	–1.34 (MO_2/M^{3+}) –0.98 ($M(OH)_2^{2+}/M^{3+}$)
$E^\circ(M^{3+}/M^{2+})$	–2.6	–1.7 (M^{3+}/M^{2+})[d]	–1.20	–0.11
$E^\circ(M^{3+}/M)$	–1.96[e]	–1.97 (M^{3+}/M)[f]	–0.56	0.27
$E^\circ(M^{4+}/M)$	–	–1.85 (M^{4+}/M)[g] –1.95 (MO_2/M)[g]	–0.87 (MO_2/M)[f]	–0.134 (MO_2/M) –0.035 ($M(OH)_2^{2+}/M$)
$E^\circ(M^{5+}/M)$	–	–	–0.81 (M_2O_5/M)	–0.13 (M_2O_5/M)[f]
$E^\circ(M^{6+}/M)$	–	–	–	–0.12 (MO_3/M) –0.09 (M^{6+}, H^+/M)

[a] Bratsch and Lagowski (1986).
[b] Ionova *et al*. (1992).
[c] Pershina *et al*. (1999).
[d] Johnson and Fricke (1991).
[e] Bratsch (1989).
[f] Roughly estimated from the other E°.
[g] Pershina *et al*. (1994).

$\log K_{11}(\mathrm{Rf}) \approx -4$ was then calculated and compared to $\log K_{11}(\mathrm{Zr}) = 0.3$ and $\log K_{11}(\mathrm{Hf}) = -0.25$. This hydrolysis sequence is in agreement with the order of extraction of group 4 elements into thenoyltrifluoroacetone (TTA) obtained in the experiments described in Section 14.6.1c(iv).

For group 5 elements and Pa, hydrolysis proceeds very rapidly, with the ultimate formation of products such as $M(OH)_5(aq)$. Hydrolysis of group 5 cations was studied theoretically for the following reaction: $M(H_2O)_6^{5+} \Leftrightarrow M(OH)_6^- + 6H^+$ where M = Nb, Ta, Db, and Pa. Calculations (Pershina, 1998a) of the Gibbs energy changes of this reaction showed that the trend toward decreasing hydrolysis is continued with Db, giving the sequence Nb > Ta > Db >> Pa.

Hydrolysis of group 6 elements proceeds even further than that of the group 5 elements, with the formation of MO_4^{2-} at higher pH according to the following scheme: $M(H_2O)_6^{6+}$ (this species is not observed) $\Leftrightarrow \ldots \Leftrightarrow [M(OH)_4(H_2O)]^{2+}$ $\Leftrightarrow [MO(OH)_3(H_2O)_2]^+ \Leftrightarrow MO_2(OH)_2(H_2O)_2 \Leftrightarrow [MO_3(OH)]^- \Leftrightarrow MO_4^{2-}$. The protonation process, the reverse of the reaction shown above, was considered theoretically (Pershina and Kratz, 2001). The resulting relative values of Gibbs energy changes suggest that for the first two protonation steps (see Table 14.12) the trend in group 6 should be W > Sg ≥ Mo rather than Sg > W > Mo. For the third and subsequent protonation processes, the trend should be Sg > W > Mo. The values of log *K* were defined for Sg, as shown in Table 14.9. The predicted trends in log *K* are in agreement with experiments on Mo and W at various pH values (Baes and Mesmer, 1976) and with Sg for the protonation/hydrolysis of the positively charged complexes (Schädel *et al.*, 1998).

(c) Complexation

If one molecular complex ML_i, among many others, is extracted into an organic phase, the distribution coefficient, K_d (expressed in terms of the complex formation constant β_i), is a good measure of its stability and the sequence in the K_d values for a given series should reflect the sequence in the stability of the complexes (Ahrland *et al.*, 1973). Thus, by predicting $\log\beta_i = \Delta G^r/2.3RT$ one

Table 14.9 *Values of log* K *for the stepwise protonation of* MO_4^{2-} (*M = Mo, W, and Sg*) (*Pershina and Kratz*, 2001).

	log K_n		
Reaction	*Mo*	*W*	*Sg*
$MO_4^{2-} + H^+ \Leftrightarrow MO_3(OH)^-$	3.7	3.8	3.74
$MO_3(OH)^- + H^+ + 2H_2O \Leftrightarrow MO_2(OH)_2(H_2O)_2$	3.8	4.3	4.1 ± 0.2
$MO_4^{2-} + 2H^+ + 2H_2O \Leftrightarrow MO_2(OH)_2(H_2O)_2$	7.50	8.1	8.9 ± 0.1
$MO_2(OH)_2(H_2O)_2 + H^+ \Leftrightarrow MO(OH)_3(H_2O)_2^+$	0.93	0.98	1.02

can predict sequences in the extraction of complexes into an organic phase or their sorption by cation- or anion-exchange resins.

Complex formation is known to increase within the transition element groups with increasing Z. However, in aqueous solutions it competes with hydrolysis as described by the following equilibrium: $x\mathrm{M(H_2O)}_{w^\circ}^{z+} + y\mathrm{OH}^- + i\mathrm{L}^- \Leftrightarrow \mathrm{M}_x\mathrm{O}_u\mathrm{(OH)}_{z-2u}\mathrm{(H_2O)}_w\mathrm{L}_a^{(xz-y-i)} + (xw^\circ + u - w)\mathrm{H_2O}$. This may change trends in the stabilities of the complexes and, consequently, their extraction into an organic phase.

(*i*) *Rf through Sg*

Complexation of group 4 elements in HF solutions is described by the following equilibria:

$$\mathrm{M(H_2O)}_8^{4+} \Leftrightarrow \mathrm{MF(H_2O)}_7^{3+} \Leftrightarrow \mathrm{MF_3(H_2O)}_5^- \Leftrightarrow \tag{14.1}$$

$$\mathrm{MF_4(H_2O)_4} \Leftrightarrow \mathrm{MF_5(H_2O)}^- \Leftrightarrow \mathrm{MF}_6^{2-}. \tag{14.2}$$

Results of DFT calculations of the relative Gibbs energy changes of these equilibria (Pershina *et al.*, 2002b) suggest that the trend in the formation of the positively charged complexes according to equation (14.1) should be Zr $\geq$ Hf $>$ Rf. This means that the K_d values for sorption by a cation resin of the positively charged complexes formed at HF concentrations below $<$0.01 M will have the following trend in group 4: Rf $>$ Hf $\geq$ Zr. (In the case of the formation of positively charged complexes of a lower charge from complexes with a higher charge (equation (14.1)), the sequence in the K_d values is opposite to the sequence in the complex formation, since complexes with a lower positive charge are more poorly sorbed on cation exchange resin than those with a higher charge.) For the formation of anionic complexes (equation (14.2)) sorbed by an anion-exchange resin, the trend becomes more complicated depending on the pH, i.e. depending on whether the fluorination process starts from the hydrated or the hydrolyzed species. Thus, for experiments conducted at HF concentrations above 0.001 M where some hydrolyzed or partially fluorinated species are present, the trend for the formation of MF_6^{2-} (equation (14.2)) and hence of K_d should be reversed in group 4: Rf $\geq$ Zr $>$ Hf.

The predicted sequences are in agreement with experiments on cation- and anion-exchange resin separations of Zr, Hf, and Rf from mixed HF/HCl solutions, where fluorinated complexes were sorbed on the resin and Cl^- ions served as counter-ions competing for its active centers (Trubert *et al.*, 1999). At high HCl concentrations, where no hydrolysis takes place, the complexation reaction is $\mathrm{M(H_2O)}_8^{4+} + 6\mathrm{HCl} \Leftrightarrow \mathrm{MCl}_6^{2-}$. Results of the DFT calculations of Gibbs energy changes for this reaction (Pershina *et al.*, 2002b) suggest that the trend in complex formation and in the K_d values should definitely be continued with Rf to give the sequence Zr $>$ Hf $>$ Rf.

Group 5 elements form a large variety of complexes, such as $M(OH)_2Cl_4^-$, $MOCl_4^-$, $MOCl_5^{2-}$, and MCl_6^- (M = Nb, Ta, Db, and Pa), in HCl solutions with different degrees of hydrolysis. Their formation is described in a general form by the following equilibrium reactions: $M(OH)_6^- + iL^- \Leftrightarrow MO_u(OH)_{z-2u}L_i^{(6-i)-}$. The DFT calculations of Gibbs energy changes for these reactions (Pershina, 1998b) showed the following trend in the complex formation and extraction of group 5 elements: Pa >> Nb $\geq$ Db > Ta. Thus, a reversal of the trend from Ta to Db was predicted for group 5 elements. The following sequence in the formation of various types of complexes as a function of increasing acid concentration was predicted (Pershina and Bastug, 1999): $M(OH)_2Cl_4^- > MOCl_4^- > MCl_6^-$. For the acids of interest, the sequence was predicted as: $MF_6^- > MCl_6^- > MBr_6^-$.

Complex formation of the group 6 elements, Mo, W, and Sg, in HF solutions is described as: MO_4^{2-} (or $MO_3(OH)^-$) + HF $\Leftrightarrow$ $MO_3F^- \Leftrightarrow MO_2F_2(H_2O)_2 \Leftrightarrow MO_2F_3(H_2O)^- \Leftrightarrow MOF_5^-$. The calculated Gibbs energy changes of these reactions show a very complicated dependence of trends in the complex formation on HF concentration and pH. Thus, at low [HF] $< \sim$0.1 M, a reversal of the trend from W to Sg should occur, while at high [HF] > 0.1 M, the trend is continued with Sg: Sg > W > Mo. It should be noted that such complicated trends could not be obtained by any extrapolation of properties within the group, but are the result of considering complex formation in equilibrium with hydrolysis and by calculating relativistically the electronic structure of the complexes.

(*ii*) *Bh through element* 112

The aqueous chemistry of these elements promises to be very interesting and should provide extensive information about complexing ability as well as information about the potential reduction reactions. Some general considerations on the basis of atomic calculations are presented by Fricke and Waber (1971); Fricke (1975). Some aspects of the complex formation of elements 107 through 112 in aqueous solution were discussed by Keller and Seaborg (1977) and Seaborg and Keller (1986). It is expected that element 112 will have extensive complex-ion chemistry, as do other elements of the second half of the 6d transition series. From early relativistic atomic calculations, Pitzer (1975a) postulated some very interesting properties for element 112 caused by relativistic effects on the $7s^2$ shell. He suggested that element 112, eka-Hg, would be more noble than Hg, and even though the oxide, the chloride, and the bromide would be unstable, $112Cl_4^{2-}$ and $112Br_4^{2-}$ would exist in solution, and $112F_2$ would be stable.

Recently, Seth *et al.* (1997) have considered the possibility of formation of $112F_5^-$ and $112F_3^-$, by analogy with Hg where the addition of F^- to HgF_2 or HgF_4 was found to be energetically favorable. However, in aqueous solutions these complexes probably undergo strong hydrolysis. Thus, experiments might only be possible with $112Br_5^-$ or $112I_5^-$.

14.6 MEASURED CHEMICAL PROPERTIES FOR ELEMENTS 104 THROUGH 112

The experimental results for Rf, Db, and Sg, the results of the first experimental investigations for Bh and Hs, and a preliminary report of experiments designed to study element 112 are briefly reviewed. Several more detailed reviews of the experimental techniques, measured chemical properties of Rf, Db (Ha), and Sg, and prospects for studies of still heavier elements are available and should be consulted for additional information (Schädel, 1995, 2002; Gregorich, 1997a; Hoffman and Lee, 1999; Kratz, 1999b).

A summary of some predicted chemical properties of elements 104 through 112 is given in Table 14.10. First experimental investigations of the chemical properties of the transactinides focused on the most fundamental and simplest properties. For example, the determination that the most stable oxidation states of elements 104 and 105 in aqueous solutions were 4+ and 5+, respectively, allowed their placement at the bottom of groups 4 and 5 in the periodic table as members of the 6d transition series. In later experiments, attempts were made to perform more complex studies of transactinide properties for comparison with their lighter homologs in the periodic table. Such studies present even greater challenges because of the need to investigate the transactinides and their lighter homologs under exactly the same chemical conditions – the ideal situation being to measure them all in the same on-line experiments conducted at the accelerators where they are produced.

14.6.1 Chemistry of rutherfordium (104)

(a) Historical

In early gas-phase studies at Dubna, Zvara *et al.* (1969, 1970) reported that the chloride of a 0.3-s SF activity produced in the ^{242}Pu(^{22}Ne,4n) reaction and initially assigned to ^{260}Rf formed a chloride, presumably $RfCl_4$, that was less volatile than $HfCl_4$. However, the existence of such an isotope has never been confirmed (see Fig. 14.2) and these claims were apparently incorrect as discussed in detail by Kratz (1999b). Zvara *et al.* (1972) later proposed that they were actually measuring the SF branch of the known alpha-emitting 3-s ^{259}104, which was produced in the same experiments via the ^{242}Pu(^{22}Ne,5n) reaction. They then reported that the volatility of the Rf tetrachloride was similar to that of $HfCl_4$ and much more volatile than the chlorides of the actinides and Sc. They concluded from their results that Rf properly belonged to group 4 of the periodic table. However, only SF events were measured and there is still some doubt about the magnitude of the SF branch of ^{259}104, which decays predominantly by alpha emission. The results could not be considered definitive because positive identification of the element being studied was not possible since only SF decay was detected.

Table 14.10 *Predicted chemical properties of elements* 104 *through* 112.

	Rf	Db	Sg	Bh	Hs	Mt	110	111	112
chemical group	4	5	6	7	8	9	10	11	12
stable oxidation states[a,b]	**4**,3	**5**,4,(3)	**6**,5,4,(3)	**7**,5,4,3	**8**,6,4,3	6,3,1	6,4,2,0	5,**3**,–1	**4**,2,**0**
first ionization potential (eV)[c]	6.01	6.89	7.85	7.7	7.6	8.7	9.6	10.6	11.97
standard electrode potential in aqueous solution (V)[d]	(4+→0)	(5+→0)	(6+→0)	(5+→0)	(4+→0)	(3+→0)	(2+→0)	(3+→0)	(2+→0)
	–1.85	–0.81	–0.12	+0.1	+0.4	+0.8	+1.7	+1.9	+2.1
ionic radius of indicated ion (Å)[e]	0.76(4+)	0.69(5+)	0.65(6+)	0.83(5+) 0.58(7+)	0.80(4+) 0.45(8+)	0.83(3+)	0.80(2+)	0.76(3+)	0.75(2+)
atomic radius (Å)[f]	1.50	1.39	1.32	1.28	1.26	1.22	1.18	1.14	1.10
density (g cm^{-3})[f]	23	29	35	37	41	37.4	34.8	28.7	23.7
ΔH_{sub} (kJ mol^{-1})[g]	694	795	858	753	628	594	481	335	29
boiling point (K)[g]	5800								
melting point (K)[g]	2400								

[a] Bold type: most stable in gas phase; underlined = most stable in aqueous solutions; non-bold: less stable; ( ) = least stable.
[b] Fricke (1975), Pershina *et al.* (1999), Schwerdtfeger and Seth (1998).
[c] See Table 14.5.
[d] See Table 14.8 for Rf through Sg; see Seaborg and Keller (1986) for elements Bh through 112.
[e] See Table 14.6 for maximum oxidation states of Rf through Hs; see Seaborg and Keller (1986) for Mt through 112.
[f] See Seaborg and Keller (1986) for Rf through Hs and Fricke (1975) for Mt through 112.
[g] Seaborg and Keller (1986).

Studies of the solution chemistry of element 104 were conducted in 1970 by Silva *et al.* (1970b) using 75-s ^{261}Rf (see Table 14.3). Positive identification of ^{261}Rf was made by measuring its known half-life and characteristic alpha-decay sequence. Elutions with α-hydroxyisobutyrate solutions from cation-exchange resin columns were used to compare the behavior of ^{261}Rf with No^{2+}, trivalent actinides, Hf^{4+}, and Zr^{4+}. In several hundred repetitive experiments in which 100 atoms were produced for study, the behavior of element 104 was shown to be similar to that of the group 4 elements Zr and Hf, which did not sorb on the column. Its behavior was entirely different from that of No^{2+} and the trivalent actinides that did sorb on the column at pH 4.0.

Some time later, Hulet *et al.* (1980) used ^{261}Rf to perform further experiments to compare the anionic chloride complexes of Rf with those of Hf, Cm, and Fm. Extraction chromatography with a column containing trioctylmethylammonium chloride on an inert fluorocarbon powder was used rather than an ion-exchange resin column because of the faster kinetics. The products recoiling from the nuclear reaction were transported to a fast computer-controlled apparatus that performed the many repetitive experiments necessary to get statistically significant information. The results showed that in 12 M HCl solutions the anionic chloride complexes of Rf and the Hf tracer were strongly extracted by the quaternary amine while the trivalent actinides were not and ran through the column. The chloride complexation of Rf was clearly similar to Hf and much stronger than that of the trivalent actinides, again confirming its position in group 4 of the periodic table. This experiment is especially noteworthy in that it was the first sophisticated, computer-controlled automated system to be used to perform very rapid solution chemistry experiments on an atom-at-a-time basis.

Following these pioneering studies of Rf, a rather long period of time elapsed before additional experiments were conducted in the late 1980s. MCDF calculations (Desclaux and Fricke, 1980; Glebov *et al.*, 1989) indicated that relativistic effects might cause replacement of the expected 6d orbital in Lr by $7p_{1/2}$ orbitals. Spurred by Keller's (1984) extrapolation that Rf might have the configuration $7s^27p^2$ rather than $6d^27s^2$ as expected by analogy to the $5d^26s^2$ configuration of Hf, experimental investigations of relativistic effects in Rf were undertaken. In 1989, Zhuikov *et al.* (1989) examined the volatility of 3-s ^{259}Rf relative to Au, Tl, and Pb tracers in on-line measurements in a quartz column at 1170°C. Under reducing conditions using Ar/H_2 carrier gas, they found that Hf and Rf did not pass through the column while the other elements did. They deduced a lower limit of 370 kJ mol^{-1} for the sublimation enthalpy of metallic 104, much higher than for Pb and other heavy 'p-elements'. Later MCDF relativistic calculations (Glebov *et al.*, 1989; Johnson *et al.*, 1990) indicated that the ground state of Rf is 80% [$6d7s^27p$] while the $7s^27p^2$ state is 2.9 eV above the ground state. Zhuikov *et al.* (1990) and Ryzhkov *et al.* (1992) further concluded that there was no basis for expecting any distinct 'p-character' in the chemical properties of Rf and evaluated various experimental approaches for investigating relativistic effects, including volatilities in the elemental state,

thermochromatography of tetrahalides, and the stability of lower oxidation states. Zhuikov *et al*. warned that gas chromatography experiments that depend on Rf or Hf in the atomic state are not useful for investigating relativistic effects because of the difficulty in stabilizing the atomic states at the temperatures above 1500°C that are needed for chromatography columns. However, they suggested that thermochromatography of the tetrahalides appeared promising.

(b) Gas-phase chemistry

In the late 1980s an international team of scientists from Switzerland, Germany, and the USA studied the gas-phase properties of the tetrahalides of Rf using the automated isothermal systems OLGA (Türler *et al*., 1996) and HEVI (Kadkhodayan *et al*., 1992). The alpha-emitting isotope 75-s ^{261}Rf (see Table 14.3), produced at the LBNL 88-Inch Cyclotron, was used in the experiments and was positively identified by using surface barrier detectors to measure α–α correlations from its known decay scheme. The Zr and Hf activities were identified via gamma spectroscopy. A schematic diagram of HEVI and the arrangement used in some of the gas-phase studies of element 104 tetrachlorides and tetrabromides at LBNL is shown in Fig. 14.14.

The adsorption enthalpies on the SiO_2 surface of the column were calculated from Monte Carlo fits to the measurements of the relative yields as a function of the isothermal temperature between about 100 and 600°C. The Monte Carlo model was introduced by Zvara (1985) and adapted for use with isothermal gas chromatography by Türler (1996). The calculation takes account of the flow rate, half-life of the isotope, temperature, and other variables to generate yield curves as a function of temperature. A rather complete description of this model has been given by Gäggeler (1997). The adsorption enthalpies resulting from the most recent experiments on the tetrabromides (Sylwester *et al*., 2000) are shown, together with those for the tetrachlorides (Kadkhodayan *et al*., 1996), in Fig. 14.15.

Under these conditions, Rf produced volatile $RfCl_4$ at about the same temperature as $ZrCl_4$, indicating their similar volatilities. $HfCl_4$ was unexpectedly less volatile. The analysis of the data using the Monte Carlo model gave the following ΔH_{ads} for group 4 chlorides on SiO_2: –(74 ± 5) kJ mol^{-1} for Zr, –(96 ± 5) kJ mol^{-1} for Hf, and –(77 ± 6) kJ mol^{-1} for Rf (Fig. 14.14). $RfCl_4$ showed about the same volatility as $ZrCl_4$ within the error bars as expected from relativistic calculations (Pershina and Fricke, 1994). 'Nonrelativistic' extrapolations gave lower volatility for $RfCl_4$ (Türler *et al*., 1996). The observation of the relatively high volatily of $RfCl_4$ was a confirmation of the influence of relativistic effects. Experiments with the bromides showed that they are generally less volatile than the chlorides and that $RfBr_4$ is more volatile than $HfBr_4$ (Fig. 14.14), in agreement with theoretical predictions (Pershina and Fricke, 1999). No attempts to measure the volatilities of the fluorides have yet been reported.

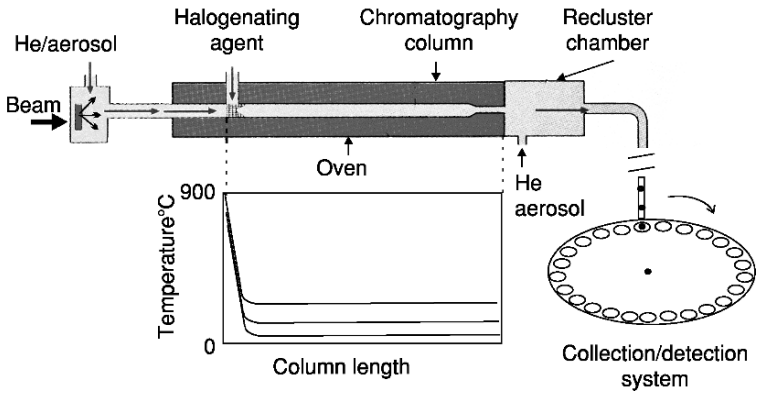

Fig. 14.14 *Schematic diagram of a system used for gas-phase studies is shown. The recoiling products from the reaction are attached to either KCl, KBr, or* MoO_3 *aerosols and transported in He gas to the entrance to HEVI where they were deposited on a quartz wool plug and halogenated at* 900°C. *Volatile products are transported through the quartz column in flowing He gas and are again attached to aerosols and transported in a gas-jet system and deposited on thin polypropylene films placed on the periphery of a horizontal wheel that is rotated so as to position the foils successively between pairs of surface barrier detectors for* alpha *and SF spectroscopy.*

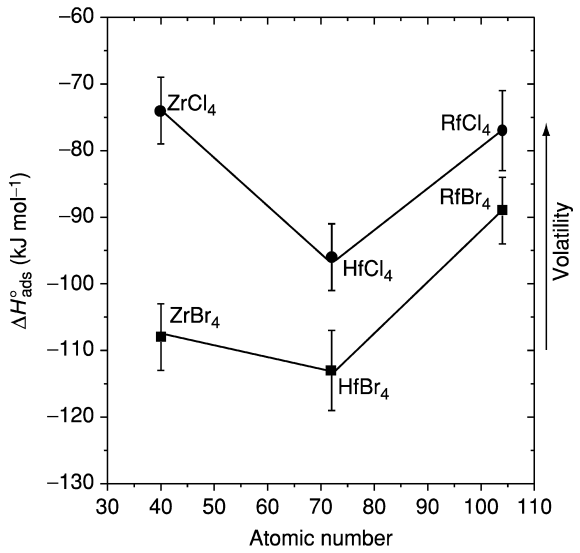

Fig. 14.15 *Adsorption enthalpy values on* SiO_2 *for Zr, Hf, and Rf chlorides and bromides* (*Kadkhodayan,* 1993*; Kadkhodayan* et al., 1996*; Sylwester* et al., 2000).

(c) Solution chemistry

Additional experimental investigations of the solution chemistry of Rf were initiated in the late 1980s. Manual studies to compare the extraction from aqueous solutions into triisooctylamine (TIOA), tri-*n*-butylphosphate (TBP), and TTA of 75-s ^{261}Rf, its lighter homologs Zr and Hf, and the pseudohomologs Th(IV) and Pu(IV) were reported by the Berkeley group (Czerwinski, 1992b; Czerwinski *et al*., 1994a,b; Bilewicz *et al*., 1996; Kacher *et al*., 1996a,b; Hoffman and Lee, 1999). A comprehensive review and summary, as of 1997, of the results from experiments on the extraction behavior of Rf was given by Gregorich (1997a). Later studies used ARCA for repeated chromatographic studies and SISAK for very rapid automated liquid–liquid extractions (Alstad *et al*., 1995; Omtvedt *et al*., 2002).

(*i*) *Extraction of anionic species*

Batch extractions

In repeated manual extractions taking about a min each and using only microliters of each phase, the effect of chloride concentration and pH on extractions into TIOA were investigated. In general, these extractions (Czerwinski *et al*., 1994a,b; Kacher *et al*., 1996a,b) confirmed the earlier results (Hulet *et al*., 1980), showing that Rf generally behaves as a group 4 element, and unlike the trivalent actinides, forms negatively charged complexes in concentrated HCl that are extracted efficiently. Rf is nearly 100% extracted into TIOA from 12 M HCl, as are Zr and Nb, while Th and trivalent actinides and lanthanides are poorly extracted.

Extractions into TIOA/xylene from HF solutions were also performed (Kacher *et al*., 1996b). Although there were some experimental difficulties with the experiments, they clearly showed that Rf was extracted from 0.5 M HF but not from 4 M HF. This was attributed to the extraction of F^- at the higher fluoride concentrations, which complexes all of the TIOA, thus limiting the extraction of the anionic metal fluoride complexes. The extractability of the group 4 elements was found to decrease in the order: Ti > Zr ~ Hf > Rf. This behavior was cited as evidence that the equilibria for the group 4 elements are the same and that Rf is extracted in the chemical form RfF_6^{2-} similarly to Ti, Zr, and Hf, which are extracted as MF_6^{2-} complexes.

Column separations

Pfrepper *et al*. (1998) produced ^{261}Rf and $^{165–169}$Hf isotopes (few-minute half-lives) simultaneously at the Dubna U-400 cyclotron and devised a multi-column technique for continuous on-line processing and detection of ^{253}Es, the long-lived descendant of ^{261}Rf. Using an anion-exchange column with 0.27 M HF/0.1–0.2 M HNO_3 as the eluant, Es was eluted and measured to obtain the K_d values for Rf, which were nearly the same as those for Hf. The ionic charge of

the Rf complex was obtained from measurements of K_d vs. [HNO_3]. The ionic charge was calculated to be –(1.9 ± 0.2), similar to that of Hf, indicating formation of RfF_6^{2-}. This again indicates that Rf is similar to Hf and to other members of group 4. The technique, though extremely complex, ensures that equilibrium has been attained and has the virtue of measuring both Rf and Hf in the same experiment. However, it does not give any additional information about specific differences in the chemical behavior of Rf and of its lighter homologs and pseudohomologs.

Other researchers (Haba *et al.*, 2002) used batch extractions with an anion-exchange resin (CA08Y) to determine K_d values for the Rf homologs Zr and Hf, and the pseudohomologs Th(IV) and Pu(IV) as a function of HCl and HNO_3 concentrations in order to determine appropriate conditions for on-line studies with ^{261}Rf and ^{169}Hf at the same time. They then performed on-line measurements of ^{261}Rf and ^{169}Hf produced in ^{18}O-induced reactions with a ^{248}Cm target containing natural Gd, to study their sorption behavior on this anion-exchange resin in solutions of 1.0–11.5 M HCl and in 8 M HNO_3 using an automated ion-exchange separation apparatus coupled to an alpha-spectroscopy detection system. They found that the adsorption of Rf increased steeply with increasing HCl concentration between 7.0 and 11.5 M, as did the adsorption of Zr and Hf, indicating that like Zr and Hf, anionic complexes such as $Rf(OH)Cl_5^{2-}$ or $RfCl_6^{2-}$ are formed. Their results are consistent with previous experiments with Aliquat 336 (Hulet *et al.*, 1980) and TIOA (Czerwinski *et al.*, 1994a). The adsorption order in the region of 9 M HCl was Rf > Zr > Hf. This behavior is quite different from that of Th(IV), whose distribution coefficients are less than 1 and further decrease in this region. In 8 M HNO_3, more than 80% of Rf, Hf, and Zr were eluted while 99% of the pseudohomolog Th(IV) was retained, indicating that Rf, like Hf and Zr, formed cationic or neutral species, unlike Th(IV) or Pu(IV).

(*ii*) *Extraction of neutral complexes with TBP*

It is well known that TBP extracts neutral complexes by forming adducts with neutral metal salts that are extractable into the TBP organic phase. The adduct is presumed to have the form $ML_4 \cdot xTBP_{(org)}$ where x can be determined by measuring the slope of log K_d as a function of log [TBP]. If the TBP concentration is too high, aggregation of the TBP molecules may give erroneous results. Furthermore, there are very large statistical uncertainties in determination of K_d values when the small number of atoms produced is measured only in the organic phase. The calculation of K_d = (extraction yield)/(1−extraction yield) is probably only accurate for relatively small K_d values because if the K_d values are high the denominator becomes a very small difference between two very similar numbers with large errors. Extractions from HCl into TBP are also unusually dependent on both [H^+] and [A^-], indicating that hydrolysis plays an important role.

Batch extractions

Extractions of ^{261}Rf, Hf, Zr, Th, and Pu into TBP were first studied by Czerwinski *et al*. (1994b) using manual extractions from aqueous solutions of 8, 10, and 12 M HCl, with $[H^+]$ held constant at 8, 10, and 12 M and $[Cl^-]$ adjusted with LiCl to 8, 10, and 12 M. The Zr, Th, and Pu(IV) results were obtained from off-line tracer experiments. In pure HCl solutions, the extraction of Pu, Th, and Zr was nearly 100% at all three molarities, consistent with previously reported (Peppard *et al*., 1956) data for Zr and Th, while extraction of Rf and Hf was low at 8 M and increased to higher values at 10 and 12 M HCl. Extraction of Hf remained lower than that of Rf at all molarities. With $[H^+]$ held at 8 M, an increase in $[Cl^-]$ to 10 and 12 M resulted in significant decreases of both Rf and Pu extraction into TBP/benzene while extraction of Zr, Hf, and Th remained high. This was interpreted as indicating that chloride complexation is stronger for Rf than for Zr, Hf, and Th, and that Rf, similarly to Pu(IV), forms anionic species of the type MCl_6^{2-}, which does not extract into TBP. The trends in extraction yields vs. $[H^+] = 8$, 10, and 12 M for $[Cl^-]$, which are constant at 12 M, show that the Hf yields are independent of $[H^+]$ and remain nearly constant between 75 and 80% while the extraction yields for Rf sharply increase, indicating different extraction mechanisms for Rf and Hf. At the highest $[Cl^-]$ concentrations, the extraction yield for Hf follows that of Th, which does not form anionic chloride complexes, while the trend for Rf follows Pu(IV), which does. Problems with losses of Rf and Hf on Teflon collector foils used in some of the on-line studies resulted in absolute values that were probably too low for the higher K_d values. Nevertheless, much useful information can be obtained from an examination of relative extraction yields.

The extractability decreases in the order Zr > Pu > Rf > Hf > Th for 8 M HCl, in the order Zr > Pu > Rf ~ Th > Hf for 10 M HCl, and in the order Zr ~ Rf ~ Pu > Th > Hf for 12 M HCl. A striking observation that needs to be investigated further is that with $[H^+]$ held constant at 8 M the extraction of Rf increases to ~80% when $[Cl^-]$ is increased to 10 M and then decreases sharply to ~25% when $[Cl^-]$ is increased to 12 M, similar to the extraction of Pu(IV), which decreases to less than 20% while that of Zr remains at ~100% and Hf and Th increase to 80–90%. This would indicate formation of an anionic species of Rf similar to $PuCl_6^{2-}$ and unlike all the other group 4 elements and Th. Extraction as a function of $[H^+]$ between 8 and 12 M with $[Cl^-]$ constant at 12 M indicated little effect on the extraction of Zr and Hf, but the extraction of Rf increased from 25 to ~100%. The extracted complex might be of the type $RfCl_4 \cdot x HCl \cdot y TBP$, where x is 1 or 2, values that have been observed in extraction of other elements into TBP.

Kacher *et al*. (1996a) conducted studies to compare extractions of these elements from HBr solutions into TBP with the results of the previous HCl/TBP experiments. They expected the stability of the bromide complexes to differ from that of the HCl complexes because bromide is a larger and more polarizable anion than chloride. They found that the most likely extracted form of Zr

was $ZrBr_4 \cdot \sim 1TBP$ for the HBr/TBP system and $\sim 2TBP$ for the HCl/TBP system. In general, the extraction of these elements from HBr is much lower than from HCl, and 0.35 M TBP was used to obtain increased extraction. At 9 M HBr, essentially no Rf was extracted but increasing $[Br^-]$ with LiBr to 10, 12, and 13 M resulted in more than 88% extraction of Zr and Rf and ~80% extraction of Th throughout this range while extraction of Pu(IV) increased from about 25 to 70%. In these experiments, Pt collection foils were used to avoid losses of the on-line cyclotron-measured isotopes Rf and Hf. (The Pu tracer was fumed with $NaNO_2$ to make sure it was in the tetravalent state.) Extraction as a function of [HBr] from 7.75 to 9 M HBr solutions was investigated, but without addition of LiBr neither Th nor Rf was extracted. Zr begins to extract at a somewhat lower concentration than Hf, indicating a somewhat stronger tendency to form neutral complexes; Ti extracted only above 9 M HBr. Thus the order of extractability is Zr > Hf >> Ti ~ Rf, a reversal in the trend Zr > Rf > Hf seen in the HCl/TBP extractions. Experiments to examine the extraction at concentrations up to 12 M HBr are necessary to confirm this trend.

Column experiments

In order to check and resolve some of the differences in the previously reported results for the TBP/HCl system, Brüchle *et al*. (1998) and Günther *et al*. (1998) measured K_d values for the TBP/HCl system for the carrier-free radionuclides ^{98}Zr (from fission), and ^{169}Hf and ^{261}Rf produced on-line at the Paul Scherrer Institute (PSI) cyclotron. The recoiling products were transferred via He(KCl) jet to ARCA II whose 40 microchromatographic columns (1.6-mm diameter × 8-mm long) were filled with the inert support Voltalef™ (Lehmann & Voss, Hamburg, Germany) coated with undiluted TBP. The use of undiluted TBP is expected to shift the complete extraction of both Zr and Hf to higher HCl concentrations, as shown earlier (Czerwinski *et al*., 1994b), and prior batch experiments from >10 M HCl confirmed this. From 8 M HCl, 80% Zr and only 20% Hf extraction was found. Chromatographic separations of Zr and Hf were then conducted with ARCA. The radioactive ions were sorbed from 12 M HCl. Most (75%) of the Hf and no Zr were eluted with 8 M HCl and then the remaining Hf and Zr were stripped with 2 M HCl. The K_d for Hf was calculated to be 53 from the relationship, $K_d = [(100)(\%aq)^{-1}–1][vol_{aq}/vol_{org}]$, consistent with batch measurements. Subsequent experiments to determine the K_d for Rf in 8 M HCl were conducted at the PSI cyclotron in the same way. After 90 s collection times, the reaction products were sorbed on the columns in 12 M HCl. Hf and Zr fractions were eluted with 8 and 2 M HCl, respectively, and analyzed for alpha decays from ^{261}Rf and its daughter ^{257}No. Two α–α mother–daughter correlations were observed in the Hf fraction and three in the Zr fraction, indicating that Rf extraction is somewhere between that of Hf and Zr in 8 M HCl. After lengthy and complex considerations of contributions from random and background effects, they (Günther *et al*., 1998) concluded that the K_d for Rf is 150 compared to the K_d of 1180 for Zr and of 60 for Hf obtained

from the batch experiments with 8 M HCl, giving the order of decreasing extraction Zr > Rf > Hf. The percentage extraction in their work, 52% for Rf and 25% for Hf from 8 M HCl, appears to be consistent with that of ~60% for Rf and ~25% for Hf obtained by Czerwinski *et al.* (1994b). In a detailed discussion of corrections for the differences in volumes used in the two studies and the dependence of the equilibrium constant on the differences in the TBP concentrations in the organic phase, they finally concluded that Czerwinski's K_d values for Hf and probably for Rf are significantly too low (probably due to sorption on the Teflon collection foils), but that their K_d values were also lower than expected for undiluted TBP because of aggregation effects.

Thus it appears that measurements of relative extractability can be obtained for experiments carried out under exactly the same conditions, but that determination of absolute K_d values is subject to numerous difficulties. The inconsistencies in the K_d results reported by various researchers are probably due in large part to differences in the exact details of the experimental conditions and can greatly affect the measurements, as pointed out above. In addition, results of on-line experiments for the transactinides often are compared with results of off-line tracer studies of their homologs. Furthermore, in the very rapid separations with ion-exchange resin columns required in the study of short-lived isotopes it is necessary to make sure that equilibrium is attained in order to obtain valid results. Some evidence of non-equilibrium effects was reported by Paulus *et al.* (1999) for most amines other than Aliquat 336 and will require further study. Care must be taken in batch experiments to remove any fluoride ion that may have been present in stored tracer solutions. Kacher *et al.* (1996b) found that fluoride ion concentrations as low as 0.02 M reduced the K_d values for extraction into TBP from HBr by about 2 for Hf and 10 for Zr.

(*iii*) *Extraction of fluoride complexes*

Cationic complexes

The fluoride complexation of Zr, Hf, ^{261}Rf, and Th in mixed HNO_3/HF solutions was investigated (Strub *et al.*, 2000) by studying K_d values for both anion- and cation-exchange resins using ARCA. A detailed study of the complexation as a function of fluoride- and nitrate-ion concentrations was performed. They found all four elements to be strongly sorbed on the cation-exchange resin Aminex A6 at HF concentrations below 0.001 M. The K_d values for Zr and Hf decreased between 0.001 and 0.01 M HF, presumably due to the formation of fluoride complexes. Those for Rf and Th decreased at an order of magnitude higher HF concentrations, and the K_d for Rf remained very high even in 0.01 M HF. The K_d for Rf was found to be >148 in 0.1 M HNO_3/5×10^{-4} M HF while under these conditions ^{265}Sg had been found to elute (Türler *et al.*, 1998a). As discussed in Section 14.5.3c (Eqs. 14.1 and 14.2) at [HF] < 0.01 M, positively charged complexes of higher charge will be formed, which will sorb on the cation resin. The observed order of sorption Rf > Hf ≥ Zr

corresponds to the opposite trend in the complex formation, as discussed in Section 14.5.3c, in agreement with theoretical predictions.

Anionic complexes

Trubert *et al.* (1999) determined distribution coefficients for Zr, Hf, and Rf on the macroporous anion exchanger Bio-Rad (Bio-Rad Laboratory, Hercules, CA, USA) AG® MP-1 from HF/HCl media with concentrations between 0.02 M and concentrated HF and [HCl] $\leq$ 0.8 M. They used batch experiments with Zr and Hf tracers and examined the K_d values as a function of free H^+, Cl^-, and F^- species in solution. They performed on-line column experiments using their automated system at the tandem accelerator at Orsay where ^{261}Rf and ^{167}Hf were produced.

A rather complicated two-column technique (Pfrepper *et al.*, 1998) was used in which the Rf or Hf parents were partially sorbed on a first anion-exchange resin column and the remainder plus the trivalent decay products Fm and Lu are sorbed on a subsequent cation-exchange resin column. One-hour irradiation times were used and the longer-lived ^{253}Fm–^{253}Es granddaughters of ^{261}Rf were finally measured to deduce the K_d for Rf. The one K_d value for Rf obtained for 0.02 M HF/0.4 M HCl was slightly higher than those for Zr and Hf, respectively, in agreement with the theoretically predicted trend Rf $>$ Hf $\geq$ Zr (Section 14.5.3c), but more data are needed before any conclusions can be drawn.

An increase in K_d values for Zr and Hf was observed by Strub *et al.* (2000) with the anion-exchange resin (similar to Bio-Rad AG®1-X8) and solutions between 0.001 and 0.01 M HF, consistent with the observation of decreasing values in the HF range for the cation-exchange resin. Surprisingly, the results of the experiments showed that again Rf and Th behaved differently from Zr and Hf and did not show the high K_d values expected for anionic fluoride complexes even at HF concentrations as high as 1 M. Rf seemed to resemble Th rather than Zr and Hf, which was different from the theoretical predictions (Pershina *et al.*, 2002b). There were indications that the action of the counter-ion was responsible for the unexpected behavior, and by varying the NO_3^- concentration Strub *et al.* (2000) were able to show that Rf did form anionic species, but apparently NO_3^- competed more effectively than F^- for the binding sites on the anion resin. Additional experiments are needed to investigate the effect of varying [NO_3^-] at constant [F^-] and varying [F^-] at much lower [NO_3^-].

(*iv*) *Extraction of cationic complexes*

TTA batch extractions

The chelating agent TTA extracts cationic species from aqueous solutions. Its electron donor groups are oxygen atoms and the tendency for different metals to be extracted is a measure of their affinity for oxygen atoms. This affinity should have a strong correlation with the log of the first hydrolysis constants of the metal ions. Thus TTA can be used to obtain information about hydrolysis of the group 4 ions.

The Berkeley group (Czerwinski, 1992b) performed some preliminary measurements of the extraction of the group 4 elements, Th, and Pu from 0.1 and 0.4 M HCl into 0.5 M TTA/benzene. The initial measurements gave K_d values, decreasing in the order Zr > Hf ~ Pu > Rf > Th, similar to the decreasing values of the logs of the first hydrolysis constants that have been measured for Zr, Hf, Th, and Pu (Baes and Mesmer, 1976). These extraction results are discussed by Gregorich (1997b), who states that on this basis the tendency for Rf to hydrolyze should be between that for Th and Pu and less than that for Zr and Hf. This prediction is in agreement with the theoretical calculation for the hydrolysis of group 4 elements (Pershina *et al.*, 2002b). However, more tracer measurements of the effect on extraction as a function of [HCl] and [TTA] are needed to determine if the equilibria involved in the extraction of Pu and Th are the same as for the group 4 elements. The kinetics of TTA extractions are relatively slow so they may not be the best choice for rapid separations of short-lived species.

HDBP extractions with SISAK

The SISAK microcentrifuge liquid–liquid extraction system described in Section 14.3.3b was used to study extraction of 4.7-s ^{257}Rf [1] from 6 M HNO_3 and 0.25 M dibutylphosphoric acid (HDBP) in toluene. ^{257}Rf was produced at the LBNL 88-Inch Cyclotron in the ^{208}Pb(^{50}Ti,n) reaction, with a cross section of ~10 nb.[1] In preliminary test experiments, ^{257}Rf was pre-separated in the BGS, which reduced unwanted background activities by more than three orders of magnitude, and then transferred to the specially designed Recoil Transfer Chamber (RTC) attached at the BGS focal plane (Kirbach *et al.*, 2002). The Rf ions passed from the BGS detector chamber (held at a pressure of only 1.3 mbar) through a thin Mylar window into the RTC containing He gas whose pressure could be varied from 480 to 2000 mbar, as appropriate, to stop the separated ions. The positive identification of Rf atoms entering the RTC was accomplished by measuring their α decay with an array of Si-strip detectors and six to seven ^{257}Rf–^{253}No α–α correlations per hour were found in these experiments. They were then sorbed on aerosols in a He/KCl gas-jet system and transported without chemical separation directly to the SISAK liquid scintillation detection cells. The transport time was measured with $^{170-x}$Hf isotopes (half-lives > 1 min) produced at the same time in ^{120}Sn(^{50}Ti,xn) reactions. An alpha event in the appropriate preset energy range caused the cell to close and to switch to daughter mode. The cell remained closed for more than five ^{253}No ($t_{1/2}$ = 1.6 min) daughter half-lives. In this way an α–α correlation matrix was successfully obtained and clearly showed that the SISAK liquid scintillation system could detect nuclides at a rate of less than one atom per hour. A number

[1] ^{257}Rf has been reported (Hessberger *et al.*, 1997) to have a metastable state with a half-life of ~4.0 s from which ~60% of the α-decay is estimated to originate and a ground state that α-decays with a half-life of ~3.5 s, but this has not yet been confirmed. Both decay primarily by α-emission so for the purposes of this experiment it makes very little difference.

of other important improvements including pulse-shape discrimination to reduce the beta-background, real-time scintillation yield monitoring by continuous measurement of the Compton edge of ^{137}Cs γ-rays, and improvements in the detection cell efficiencies were also made. Experimental details of the system have been published (Omtvedt *et al.*, 2002). The pre-separation thus permits designing studies of the chemical properties of Rf without the necessity for adding time-consuming and yield-loss steps to remove radioactive isotopes that would interfere with its detection and measurement.

After this successful demonstration, liquid–liquid extraction experiments were performed to compare the extraction behavior of Rf from 6 M HNO_3 into 0.25 M HDBP/toluene with that of its lighter homologs Zr and Hf. A schematic diagram of the setup is shown in Fig. 14.16. The activity-containing aerosols in the He jet are dissolved in the 'de-gasser' centrifuge containing 6 M HNO_3 and the He gas is removed. The main extraction is performed in the next centrifuge. An important step is to wash any dissolved HNO_3 from the organic phase before adding the scintillator ingredients because the acid will cause degradation of the energy resolution, as will any O_2. It is removed by sparging with He, which is removed in the last centrifuge. Flow rates of the order of 0.4–0.8 ml s^{-1} were used and the centrifuges typically operate at 25000–40000 rpm. This was the first time a transactinide, Rf, was extracted and unequivocally identified by the SISAK liquid scintillation system and demonstrates that this method can be used to investigate the chemical properties of the transactinides. The results indicate that Rf behaves similarly to Zr and Hf, as expected. In this demonstration, the conditions were chosen to maximize extraction of Rf and the other group 4 elements rather than to investigate possible differences among them. The next step will be to use the pre-separation technique to conduct experiments with chemical systems designed to distinguish differences in the behavior of individual elements within a periodic table group.

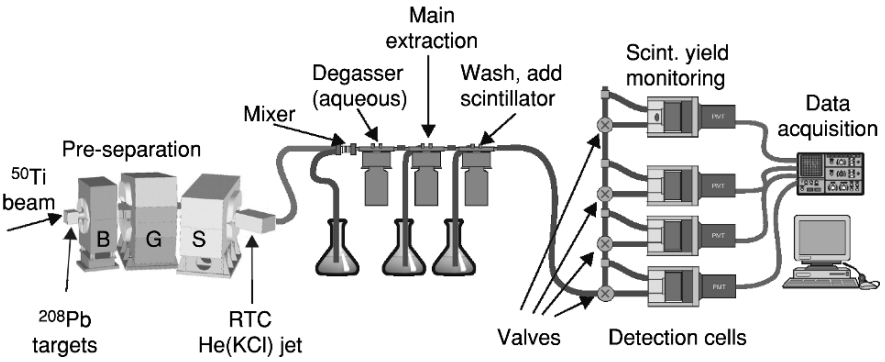

Fig. 14.16 *Schematic diagram of a typical SISAK liquid–liquid extraction configuration with BGS as a pre-separator.*

14.6.2 Chemistry of dubnium/(hahnium) (105)

As discussed in Section 14.5 and shown in Tables 14.4–14.6, the ground state configuration for element 105 is predicted to be $6d^37s^2$ although the relativistic destabilization of the 6d electrons and the close proximity of the 7s and 6d levels should stabilize the higher oxidation states of the 6d elements relative to their 5d homologs. Thus, the most stable oxidation state of Db is expected to be 5+ and the 3+ and 4+ states are even less stable than in its lighter homolog Ta.

(a) Historical

In the only published studies of the early chemistry of element 105, Zvara *et al.* (1974, 1976) reported investigations of the volatilities of the chlorides and bromides of element 105 with 1.8-s ^{261}Db compared to those of Nb and Hf. They used a thermochromatographic system similar to that used in the studies of Rf. Again, they detected SF events from the SF branch in mica track detectors placed along the chromatography column. After corrections for the much shorter half-life of ^{261}Db, the distribution of the fission tracks was compared with the adsorption zones of the tracers (3.3-min ^{169}Hf and 14.6-h ^{90}Nb). From these experiments, Zvara *et al.* concluded that the volatility of Db bromide was less than that of Nb bromide and about the same as that of Hf bromide. Again, only SF events were detected and because the SF branch ($\leq$18%?) is still not well known, it is not certain that the detected fissions belonged to element 105. A complete discussion of these early results was given by Hyde *et al.* (1987), who interpreted these results as indicating that Db behaved more like the group 4 element Hf than like Nb and Ta.

(b) Solution chemistry

No further studies of element 105 chemistry were reported until 1988 when Gregorich *et al.* (1988) reported the very first study of its behavior in aqueous solutions. These experiments were undertaken simply to show whether its most stable oxidation state in aqueous solution was 5+. At that time it had been postulated (Keller, 1984) that Ha might have a $7s^26d7p^2$ rather than a $6d^37s^2$ valence configuration expected by analogy with Ta, whose most stable state in aqueous solution is 5+. The α-emitting, 35-s ^{262}Db (then called Ha), produced in the reaction of ^{18}O with the radioactive target, 320-d ^{249}Bk (see Table 14.3) at the LBL 88-Inch Cyclotron, was used. The recoiling reaction products attached to KCl aerosols were transferred from the target system and outside the cyclotron shielding via a He gas-jet system to a 4-position collection site in a fume hood located outside the radiation area. Here very simple 'manual' chemistry was performed using only a few microliters of solution. The sorption of Ha on glass cover slips after fuming twice with concentrated nitric acid and washing

with 1.5 M HNO_3 was compared with that of tracers of the group 5 elements Nb and Ta and with the group 4 elements Zr and Hf produced on-line under similar conditions. These group 5 elements are known to sorb on glass surfaces while the group 4 elements do not. Measurements of the energy and time distribution of the alpha decay and of time-correlated pairs of alphas from ^{262}Db and its 4-s daughter ^{258}Lr were recorded and analyzed to provide positive identification that element 105 was detected. Some 800 manual extractions taking about 50-s each were performed and a total of 26 alpha and 26 SF events were recorded. Element 105, like its group 5 homologs Nb(V) and Ta(V), was found to sorb on the glass surfaces while Zr and Hf and the trivalent actinides did not. This confirmed the group 5 character of Ha and demonstrated that it properly belonged in the periodic table as the heaviest member of group 5. Its extraction behavior into methylisobuytlketone from mixed HNO_3/HF solutions under conditions in which Ta was extracted but Nb was not was also investigated (Gregorich *et al.*, 1988). Surprisingly, it was found that element 105 did not extract and that its behavior was more like Nb than Ta, indicating that details of complexing behavior cannot be predicted based only on simple extrapolations of trends within a group in the periodic table. This behavior was explained much later (Pershina, 1998b), as discussed in detail in Sections 14.5.3b and 14.5.3c.

This surprising result provided the impetus for further exploration of the complex behavior of element 105. Chromatographic experiments using ARCA II to carry out the thousands of required repetitive experiments were performed jointly by the GSI/Mainz, PSI/Bern, and LBL/Berkeley groups in 1988, 1990, and 1993 at LBL, and in 1992 at GSI. In the first extraction chromatography column separations with the anion exchanger TIOA on inert supports, all the group 5 elements and Pa(V) were extracted from concentrations of HCl > 10 M. At lower concentrations of HCl, small amounts of added HF gave selective back extraction, showing different chemical behavior for these elements (Kratz *et al.*, 1989; Zimmermann *et al.*, 1993). Element 105 showed a marked non-Ta-like behavior at concentrations below 12 M HCl and follows the behavior of Nb and the pseudohomolog Pa(V). Because of this similarity to Nb and Pa, it was concluded that the complex was $DbOX_4^-$ or $[Db(OH)_2X_4]^-$. ARCA was also used to investigate the extraction of Db from HBr into diisobutyl carbinol (DIBC), a specific extractant for Pa, with subsequent elutions with mixed HCl/HF and HCl. The extraction sequence Pa > Nb > Db was obtained and attributed to the increasing tendency to form non-extractable polynegative complexes (Gober *et al.*, 1992). Due to the difficulties encountered in the theoretical interpretation of the results of these experiments because of the small amounts of HF added to the various halide solutions (long recommended for reducing hydrolysis of group 5 elements to prevent them from unwanted sorption on containers, etc.), it was recommended that future experiments be carried out in pure rather than mixed halide solutions (Pershina, 1998b).

Experiments conducted with ARCA also showed that Ha was eluted promptly from cation-exchange columns with α-hydroxyisobutyrate (Kratz *et al.*, 1992;

Schädel *et al.*, 1992) together with Nb, Ta, and Pa, whereas trivalent and tetravalent ions were retained, again confirming that Ha is most stable in aqueous solution as a pentavalent species. The new isotope 27-s ^{263}105 was also identified in these experiments.

Subsequently, Pershina (1998b) and Pershina and Bastug (1999) predicted the sequence Pa >> Nb ≥ Db > Ta for extraction into the anion exchanger TIOA from halide solutions. Paulus *et al.* (1999) remeasured K_d values for Nb, Ta, and Pa in new batch extraction experiments with the quaternary ammonium salt Aliquat-336 and pure HCl, HBr, and HF solutions. New chromatographic column separations with ARCA II were then conducted to study chloride and fluoride complexation separately. The Aliquat-336/HCl experiments confirmed the extraction sequence Pa >> Nb ≥ Db > Ta, as theoretically predicted. In the Aliquat 336/HF system the K_d value for element 105 in 4 M HF was >570, close to those for Nb and Ta of >1000 and different from that of ~10 for Pa.

In his review of transactinide chemistry, Kratz (1999b) discussed all the results for the ARCA experiments on element 105 in detail and concluded that the amine extraction behavior of dubnium halide complexes is always close to Nb, consistent with the predicted inversion of the trend in properties between the 5d and the 6d elements. In pure HF solution, Db differs most from Pa, and in pure HCl solution, it differs from both Pa and Ta. In mixed HCl/HF solutions, it differs markedly from Ta. The experimental results are in agreement with the calculated Gibbs energy changes (see Section 14.5.3c) of 12, 20, and 22 eV for the reactions for complex formation (Pershina *et al.*, 2002b) of the fluorides, chlorides, and bromides, respectively. For example, the equilibrium between hydrolysis and halogenation always favors formation of an extractable fluoride complex rather than the hydrolyzed species even at very low HF concentrations, whereas [HCl] > 3 M is required for formation of extractable chloride complexes, and [HBr] > 6 M is required for the formation of extractable bromide complexes.

(c) Gas-phase chemistry

The first on-line isothermal gas chromatography experiments were performed by an international group (Gäggeler *et al.*, 1992; Türler *et al.*, 1992) using OLGA II with 35-s ^{262}Db. The volatile species were deposited on a moving tape that was subsequently stepped in front of six large-area-passivated implanted planar Si detectors to measure alpha particles and SF events to identify element 105. From the yields as a function of isothermal temperature measured for the bromides of Nb, Ta, and Db, adsorption enthalpies of –88, –94, and –155 kJ mol^{-1}, respectively, were obtained from least-squares fits of Monte Carlo simulations to the isothermal yield curves. Within the error limits, the adsorption enthalpies (volatilities) are nearly the same for Nb and Ta, but Db appears to be significantly less volatile. It was postulated that traces of oxygen in the system might have led to formation of the oxytribromide of Db,

which was predicted to be less volatile than the pentabromide (Pershina *et al*., 1992b), and Db was also predicted to have a much stronger tendency to form oxyhalides than Nb or Ta, as discussed in Section 14.5.2b.

Investigations (Kadkhodayan *et al*., 1996; Türler, 1996) of the volatility of the chlorides of the group 5 elements showed that they were more volatile than their respective bromides, with element 105 being similar to Nb, but for Ta, only a species with much lower volatility, presumably $TaOCl_3$, was observed. In more recent experiments conducted by Türler *et al*. (1996) the volatilities of Db and Nb chlorides were studied as a function of controlled partial pressures of O_2. It was shown that the concentrations of O_2 and oxygen-containing compounds were extremely important in determining whether or not the oxychlorides were formed and in determining the resultant volatilities of the Nb and Db compounds. The results showed that for pO_2 between 1 ppm (vol.) and 80 ppm (vol.) both a volatile species and a less volatile species, presumably MCl_5 and $MOCl_3$, were formed in about equal amounts. The more volatile species, $NbCl_5$, was shown to be the major component at $pO_2 \leq 1$ ppm (vol.). Subsequent experiments with Db were conducted under similar conditions and a two-step yield curve was obtained indicating that both $DbCl_5$ and $DbOCl_3$ were present. Adsorption enthalpies of –80 and –99 kJ mol^{-1} for the Nb species and –98 and –117 kJ mol^{-1} for the Db species were deduced, indicating that the Db species are less volatile than those of Nb. As predicted, the oxychlorides are less volatile than the chlorides, but the experiments need to be extended to lower temperatures for Db with pO_2 kept as low as possible to see if $DbCl_5$ can be measured as a single component, and the measurements need to be extended to Ta.

14.6.3 Chemistry of seaborgium (106)

(a) Historical

Early attempts were made to study the chemistry of Sg using 0.9-s ^{263}Sg produced in the $^{249}Cf(^{18}O,4n)$ reaction at the U-400 cyclotron at Dubna (Timokhin *et al*., 1996; Yakushev *et al*., 1996). Recoiling reaction products were thermalized and carried in Ar gas from the target chamber into a fast on-line TC consisting of a 3.5 mm i.d. by 120 cm long tube of fused SiO_2 where air saturated with $SOCl_2$ was used as a chlorinating agent. The inner surface of the silica column served as a solid-state detector for SF events. In two experiments, Timokhin *et al*. (1996) found a total of 29 fission tracks in zones in the temperature region of 150–250°C, close to the deposition temperature of 16-s ^{166}W. No tracks were found in the start zone or outside the indicated region while alpha activities from actinide products were seen mostly in the start zone. They claimed that this was the first chemical identification of element 106 as SgO_2Cl_2 and that it formed an oxychloride similar to that of W. However, the assignment of the fissions to element 106 based on detection of a small

fission branch of ^{263}Sg is uncertain because it was not shown that the observed fissions did not belong to elements 104 or 105. Kratz (1999b) gave a detailed critique of the Timokhin reports and concluded that their conclusions were not justified.

The discovery by a Dubna–Lawrence Livermore National Laboratory (LLNL) collaboration (Lazarev *et al*., 1994; Lougheed *et al*., 1994) of the longer-lived isotopes ^{266}Sg and ^{265}Sg in ^{248}Cm(^{22}Ne,4n,5n) reactions with cross sections of ~80 and 260 pb for 116 and 121 MeV ^{22}Ne projectiles, respectively, made chemical studies of element 106 much more feasible. These new isotopes were separated and identified using the gas-filled recoil separator at the Dubna U-400 cyclotron. The partial alpha half-lives of 2–30 s for ^{265}Sg and 10–30 s for ^{266}Sg had to be estimated from the measured alpha-decay energies because the time intervals between the Sg isotopes and their Rf daughters were not measured as the signals from the implanted Sg isotopes were below the threshold of their detector system. On-line procedures for studying the chemistry of element 106 with both OLGA and ARCA were developed using W and Mo, the presumed lighter group 6 homologs of element 106.

(b) Gas-phase chemistry

Theoretical predictions (Pershina and Fricke, 1996) based on relativistic MO calculations indicated that SgO_2Cl_2 was the most stable of the Sg oxychlorides. Based on this prediction, the gas-phase chromatography experiments discussed in Section 14.5.2b were conducted under conditions designed to study and identify SgO_2Cl_2. The trend in volatilities of these oxychlorides within group 6, which was predicted using relationships between molecular properties such as covalence or dipole moment and volatility, was $MoO_2Cl_2 > WO_2Cl_2 > SgO_2Cl_2$. Eichler *et al*. (1999) estimated the thermochemical quantities for chlorides, oxychlorides, and oxides of Sg by extrapolation. By the use of empirical correlations, they also found SgO_2Cl_2 to be the most suitable compound for the gas-phase chemistry experiments and expected its standard sublimation enthalpy to be between 125 and 144 kJ mol^{-1}, resulting in an adsorption enthalpy between –97 and –108 kJ mol^{-1} and less volatile than its W homolog.

OLGA III was used in experiments to study the behavior of fission-product Mo isotopes and short-lived W isotopes produced at the PSI Philips cyclotron in preparation for studies of element 106 (Gärtner *et al*., 1997). The reactive gas mixture O_2, Cl_2, and $SOCl_2$ at 900°C was used; adsorption enthalpies of −90 and −100 kJ mol^{-1} were measured for MoO_2Cl_2 and WO_2Cl_2, respectively, in agreement with predictions. The isothermal yield curve was measured for 58-min ^{229}U produced in the ^{232}Th(α,7n) reaction and the resulting adsorption enthalpy of −91 kJ mol^{-1} was interpreted as indicating formation of UCl_6.

The first chemical experiments on Sg were conducted in 1995 and in 1996 at the Universal Linear Accelerator (UNILAC) at GSI using the ^{248}Cm

(^{22}Ne,4n,5n) reactions to produce ^{266,265}Sg. The reaction products recoiling out of the target were thermalized in helium gas containing carbon aerosols ($\sim 0.1 - 1$ μm diameter, generated using a spark discharge generator). In about 3 s, the flowing helium gas continuously transported the reaction products attached to the carbon aerosols through a capillary to a quartz wool plug in the reaction chamber (900–1000°C) at the inlet of OLGA III. There the reactive chlorinating gas consisting of O_2, Cl_2, and $SOCl_2$ was added to form volatile compounds, which were transported through the 1.5-mm i.d. × 1.8 m long isothermal quartz chromatography column to a recluster chamber where the chemically separated volatile Sg compounds were again attached to aerosol particles. They were transported within about 6 s to a rotating wheel system and collected on thin polypropylene foils placed in the 64-collection positions located around the periphery of a wheel that was stepped every 10 s to move the collected activity consecutively between pairs of Passivated Ion-implanted Planar Silicon (PIPS) detectors for measurement of alpha and SF activities. The times, energies, and positions of all events were recorded in list mode by a computer. A mother–daughter stepping mode was used to avoid interference from 45-s ^{212}Po^{m} contamination in the alpha energy region of interest (8.8 MeV). In this mode every other position on the 64-position wheel was left empty. When an alpha particle with the decay energy of ^{265,266}Sg was detected in a bottom detector, the daughter Rf nucleus was assumed to have recoiled out of this aerosol deposit onto the top detector. This initiated the daughter mode, causing a single step that positioned the empty collection sites between the detector pairs. The system waited for 2 min to permit the Rf daughter on the detector to decay in an environment clean of contamination. In the first experiment, two decays of ^{265}Sg were identified in daughter mode, one triple correlation was observed in parent mode, and one $\alpha-\alpha$ correlation from ^{266}Sg–^{262}Rf was recorded (Schädel *et al.*, 1997a).

The isothermal temperature was varied in the second experiment conducted in 1996 (Türler *et al.*, 1999) to obtain the adsorption enthalpy for Sg. The experimental conditions were similar except that a 200 s wait in the daughter mode was used. The yield of short-lived W isotopes produced from ^{22}Ne reactions with ^{152}Gd incorporated in the ^{248}Cm target was measured with a high-purity Ge detector and used to monitor the yield of the chemical separation. An adsorption enthalpy of $-(96 \pm 1)$ kJ mol^{-1} was obtained for $^{168}WO_2Cl_2$, in agreement with the previous measurement. The isothermal yield curves obtained for SgO_2Cl_2 along with those for the Mo and W compounds are shown in Fig. 14.17. Based on detection of 11 events attributable to Sg, an adsorption enthalpy of $-(100 \pm 4)$ kJ mol^{-1} was derived. Adsorption enthalpies of $-(90 \pm 3)$ kJ mol^{-1} and $-(96 \pm 1)$ kJ mol^{-1} were obtained for Mo and W oxychlorides, respectively. Thus the volatility sequence is $MoO_2Cl_2 > WO_2Cl_2 > SgO_2Cl_2$, as theoretically predicted. Türler *et al.* (1998a) analyzed the decay properties of the 13 correlated chains of ^{265}Sg and ^{266}Sg observed in these experiments and recommended the following half-lives and cross sections for

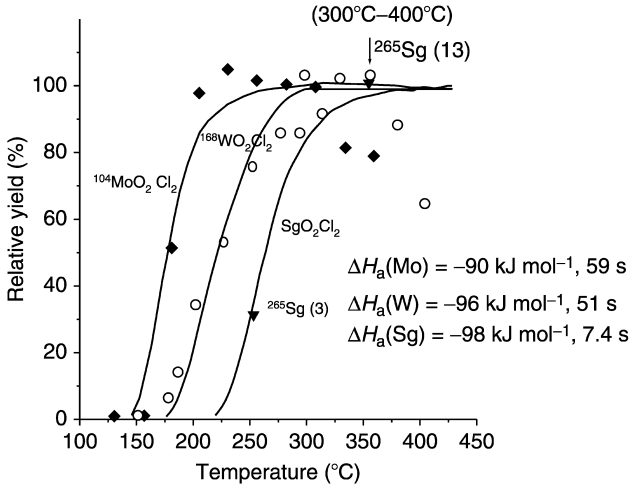

Fig. 14.17 *Relative yields vs. isothermal temperatures for* MoO_2Cl_2 (*solid diamonds*), WO_2Cl_2 (*open circles*), *and* SgO_2Cl_2 (*solid triangles*). (*Data from Türler* et al., 1999).

^{22}Ne energies between 120 and 124 MeV: ^{265}Sg, $t_{1/2} = 7.4^{+3.3}_{-2.7}$ s, cross section ~240 pb; ^{266}Sg, $t_{1/2} = 21^{+20}_{-12}$ s, cross section ~25 pb.

Hübener *et al.* (2001) reported that Sg forms volatile oxide-hydroxides similar to those of U and the group 6 elements Mo and W. They used high-temperature on-line isothermal gas chromatography with quartz columns to study Sg and W in the O_2–H_2O(g)/SiO_2 system. ^{266}Sg, produced as above, was transported in a He/MoO_3 gas-jet system into the chromatography system. Group 6 elements formed oxide-hydroxides that were volatile at a temperature of 1325 K upon addition of O_2. ^{266}Sg was unambiguously identified by measuring its decay chain. They postulated a dissociative adsorption and associative desorption process to explain their results.

(c) Solution chemistry

The first successful studies of the chemical properties of Sg in aqueous solution were reported by Schädel *et al.* (1997a,b) using ^{265,266}Sg produced in the reaction of 121 MeV ^{22}Ne projectiles with ^{248}Cm targets of 0.15 mg cm^{-2} in the first experiment and 0.95 mg cm^{-2} in the second experiment at the UNILAC at GSI. The emphasis in these experiments was on rapid preparation of samples for alpha spectroscopy with decontamination from the high-energy Bi and Po alpha activities and of trivalent actinides, and efficient separation of the Rf and No daughter activities from Sg. If these conditions are met, Rf and No isotopes observed later in the chemically separated Sg fraction can be presumed to be daughters of Sg precursor nuclei. A system with anionic or possibly neutral oxy- and oxyfluoride compounds was chosen because the formation of neutral and

anionic complexes with F^- ions is a characteristic property of group 4, 5, and 6 elements, with distinct differences between the behaviors of the three groups. Based on previous on-line tracer experiments, a solution of 0.1 M HNO_3/5 × 10^{-4} M HF was used to elute the activity from the columns of the cation-exchange resin Bio-Rad AG Aminex A6. The recoiling activities attached to KCl aerosols were swept from the recoil chamber with He gas into a capillary and transported in flowing He some 18 m to ARCA II where they were collected, dissolved, and fed into the 1.8-mm i.d. × 8-mm chromatographic columns filled with the cation-exchange resin Aminex A6. The transport and collection efficiency of about 45% was monitored frequently by checking the production rate of $^{252-255}$Fm isotopes of known cross section. Although the mean separation time of Sg from Rf and No took only 5 s, the evaporation of the eluted samples took about 20 s and on the average, α-particle and SF measurements using a system of eight PIPS detectors were not begun until 38 s after the end of the collection. The energies, times, and detector positions were recorded in list mode on a magnetic disk and tape for later data analysis and identification of the Sg isotopes. Collections times of 45 s were used for most of the 3900 collection and elution cycles. Observation of three correlated α−α events identified as the ^{261}Rf(78 s)→^{257}No(26 s)→decay sequence indicated the decay of ^{265}Sg in the chemically separated Sg fractions. From this observation, it was concluded that Sg behaved as a typical hexavalent group-6 element as did W studied previously in similar on-line experiments. This indicated the formation of SgO_2F_2 by analogy to its Mo and W homologs and showed behavior different from the pseudohomolog U(VI), which remained on the column, presumably as UO_2^{2+}.

An investigation of the fluoride complexation of Zr, Hf, Rf, and Th in mixed HNO_3/HF solutions was undertaken (Strub *et al.*, 2000) to verify experimentally that under the conditions of the first experiments on the solution chemistry of Sg using ARCA, ^{261}Rf would not be eluted from the cation-exchange resin. These detailed studies of sorption on both cation- and anion-exchange resins using ARCA confirmed the validity of the assumption in the Sg experiments that Rf would remain on the Aminex A6 cation-exchange resin column. Therefore, it was concluded that Rf could only have been in the Sg fraction as a result of the alpha decay of 7-s ^{265}Sg.

A new series of 4575 experiments was conducted (Schädel *et al.*, 1998) with ARCA using the same Aminex A6 cation-exchange resin to determine if Sg would form SgO_4^{2-} under the same conditions as before if fluoride ions were not present. The activity was dissolved in 0.1 M HNO_3 without any HF; subsequent analysis of the effluent showed that Sg still remained on the column while W was eluted with 0.1 M HNO_3. This non-tungsten-like behavior of Sg was tentatively attributed to its weaker tendency to hydrolyze in dilute HNO_3 so that its hydrolysis stopped at $M(OH)_4(H_2O)_2^{2+}$ or $MO(OH)_3(H_2O)_2^+$ while hydrolysis of Mo and W proceeded to the neutral species $MO_2(OH)_2$. Thus, in the previous experiments in the presence of fluoride ions, Sg might have been eluted from the

cation-exchange column as neutral or anionic fluoride complexes of the type SgO_2F_2 or $SgO_2F_3^-$ rather than as SgO_4^{2-}.

This hypothesis has been examined theoretically by considering hydrolysis of group 6 elements, as described in Sections 14.5.3b and 14.5.3c. The calculations (Pershina and Kratz, 2001) show that between a pH of 0 and 1, Sg forms complexes with charges of 1+ or 2+ while W forms neutral complexes. Hydrolysis of group-6 elements proceeds even faster at higher pH and a reversal of the trend in group-6 should be observed at pH > 4 (see Section 14.5.3b). Theoretical considerations of complex formation in HF solutions (Pershina *et al.*, 2002b) indicate that it competes with hydrolysis in aqueous solutions, that the dependence on pH and HF concentrations is very complicated, and that reversals of the trends occur. Further experiments can be planned based on the theoretical predictions that cover a wide range of pH values. These reversals of trends among the group 6 elements and U(IV) should be investigated experimentally.

14.6.4 Chemistry of bohrium (107) and hassium (108)

(a) Bohrium

The isotope, 17-s ^{267}Bh (Wilk *et al.*, 2000), produced in the ^{249}Bk(^{22}Ne,4n) reaction, was used in studies to compare the volatility of the oxychloride of Bh with those of its group 7 homologs Re and Tc in on-line isothermal gas chromatographic experiments using the OLGA system (Eichler *et al.*, 2000) conducted at the PSI cyclotron. The recoiling reaction products were sorbed on carbon particles suspended in He gas and continuously transported over a distance of a few meters to the OLGA where they were treated with HCl and oxygen to produce the volatile oxychlorides. These were conducted into the quartz chromatographic column, where their retention time is primarily dependent on the sorption interaction with the chlorinated column surface at a given isothermal temperature and the carrier gas velocity. The molecules passing through the column were attached to aerosols and then deposited stepwise on foils placed in positions on the circumference of a rotating wheel where their decay by alpha emission and SF was measured to identify them positively as ^{267}Bh based on their decay sequences to known daughter activities as reported in Wilk *et al.* (2000). Six such decay chains were observed over nearly 1 month of irradiation time. The relative yields for the trioxychlorides of ^{267}Bh as well as for those for Re and Tc obtained in similar experiments as a function of the isothermal temperatures are shown in Fig. 14.18.

A Monte Carlo program based on a microscopic model of the adsorption process was used to deduce ΔH_{ads} of –75 kJ mol^{-1} with a 68% confidence interval of –66 to –81 kJ mol^{-1} for BhO_3Cl, the most probable oxychloride under these conditions. The ΔH_{ads} values for the Tc and Re oxychlorides studied under the same conditions are –51 and –61 kJ mol^{-1}, respectively. Thus Bh oxychloride shows a stronger adsorption interaction with the chlorinated quartz

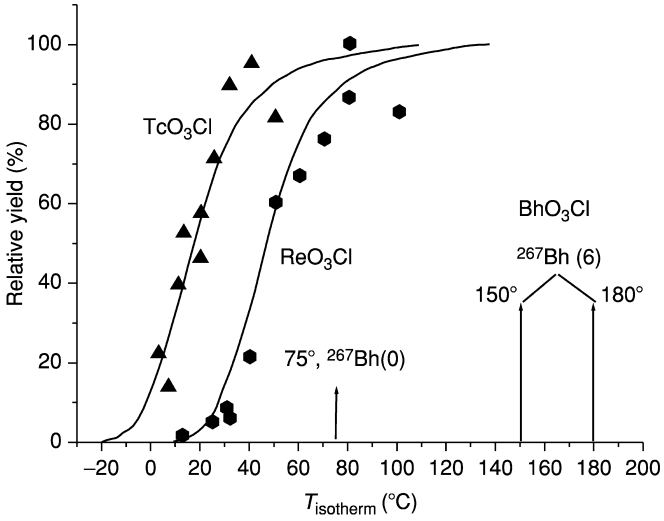

Fig. 14.18 *Relative yields vs. isothermal temperatures for TcO_3Cl (solid triangles) and ReO_3Cl (solid hexagons). A total of six events attributed to ^{267}Bh were detected at the isothermal temperatures of* 150 *and* 180°*C* (*Eichler* et al., 2000). *No events were detected at* 75°*C.*

surface than either Tc or Re compounds and it is less volatile than Re and Tc. This is in very good agreement with the calculations (Pershina and Bastug, 2000) where ΔH_{ads} of –48.2 kJ mol^{-1} for Tc and –78.5 kJ mol^{-1} for Bh were predicted, giving a volatility sequence of $TcO_3Cl > ReO_3Cl > BhO_3Cl$ (see discussion in Section 14.5.2).

(b) Hassium

Systems were developed for separating and detecting Hs as a volatile oxide based on the expectation that it would form a highly volatile tetroxide, as do its group 8-homologs osmium and ruthenium. Fully relativistic density functional calculations have been performed for MO_4 (M = Ru, Os, and Hs), as discussed in Section 14.5.2b. The volatility sequence for the tetroxides was predicted to be $HsO_4 \geq OsO_4 > RuO_4$ based on the calculated adsorption enthalpies of –(36.7 ± 1.5), –(38.0 ± 1.5), and –(40.4 ± 1.5) kJ mol^{-1}, respectively (Pershina *et al.*, 2001).

In preparation for experiments with Hs, Kirbach *et al.* (2002) developed the Cryo-Thermochromatographic Separator (CTS) to perform on-line investigations of the oxides of the α-emitters ^{171,172}Os (8 s,19 s) produced in ^{118,120}Sn (^{56}Fe,3–5*n*) reactions at the LBNL 88-Inch Cyclotron. The CTS consists of a channel formed by two facing rows of 32 PIN (Positive Implanted N-type silicon) diode α-particle detectors upon which a negative temperature gradient

from 247 K at the entrance to 176 K at the exit was maintained. The volatile species deposit on the detector surfaces at a characteristic temperature and are identified from their measured α-decay energies.

After pre-separation with the BGS to remove unwanted transfer reaction products and scattered beam particles, the separated Os ions were stopped in the RTC (described earlier) in a mixture of He gas containing 10 vol% O_2 at 100 kPa. The Os activities were transferred in a continuously flowing He/O_2 mixture through a Teflon capillary to a quartz tube heated to 1200 K where OsO_4 was formed and then transported through another capillary to the CTS. The detector pair in which the activity was deposited and the alpha spectra at each position were recorded to identify these activities. The temperature was determined from thermocouple measurements and also from the measured resistances of the PIN diodes. Monte Carlo fits to the adsorption distributions were obtained by adjusting the model to more closely approximate the slit-like CTS cross section and resulted in an adsorption enthalpy of $-(40.2 \pm 1.5)$ kJ mol^{-1} for quartz surfaces.

Düllmann *et al.* (2002a) devised the *In-situ* Volatilization and On-line detection apparatus (IVO) in which products recoiling from a nuclear reaction are thermalized and stopped in a recoil chamber containing He gas while the high-energy beam particles travel directly through the chamber to a beam stop, thus removing them from the system. The thermalized recoil products are then converted *in situ* to the volatile species to be studied and are swept by the carrier gas to a chromatography column. Volatile species pass through the column to a recluster chamber where they are sorbed on aerosols and transported via gas jet either to an additional quartz column to measure the retention times of the volatile species or directly to an on-line detection system. Short-lived Os isotopes were used to test IVO for future chemical studies with Hs. From the Monte Carlo simulations an adsorption enthalpy of $-(38.0 \pm 1.5)$ kJ mol^{-1} was obtained for $^{173}OsO_4$ on quartz surfaces, in agreement within the uncertainty limits with the value of $-(40.2 \pm 1.5)$ kJ mol^{-1} obtained by Kirbach *et al.* (2002). Subsequent to these prototype experiments, an international team of scientists (Düllmann *et al.*, 2002b) conducted the first studies of the chemistry of hassium, the heaviest element to date whose chemistry has been successfully investigated. The $^{248}Cm(^{26}Mg,5n,4n)$ reactions with estimated production cross sections of only a few picobarns were used to produce $\sim$10 s ^{269}Hs reported previously (Hofmann *et al.*, 1996, 2002) and possibly ^{270}Hs ($\sim$4 s) (Türler *et al.*, 2003) at the UNILAC at GSI. Three ^{248}Cm targets were positioned on a rotating wheel to increase the production rate. The IVO device was used to transport recoiling products to a quartz wool plug where Os and Hs were oxidized to the tetroxides by treatment with oxygen at 600°C. They were transported in helium through a Teflon capillary to the entrance to the Cryo On-Line Detector (COLD) TC formed by 12 pairs of opposing Si PIN-photodiode detectors with an outermost layer of Si_3N_4 positioned so that the gas flow was confined to the active detector surfaces. A schematic diagram of the system is shown in Fig. 14.19.

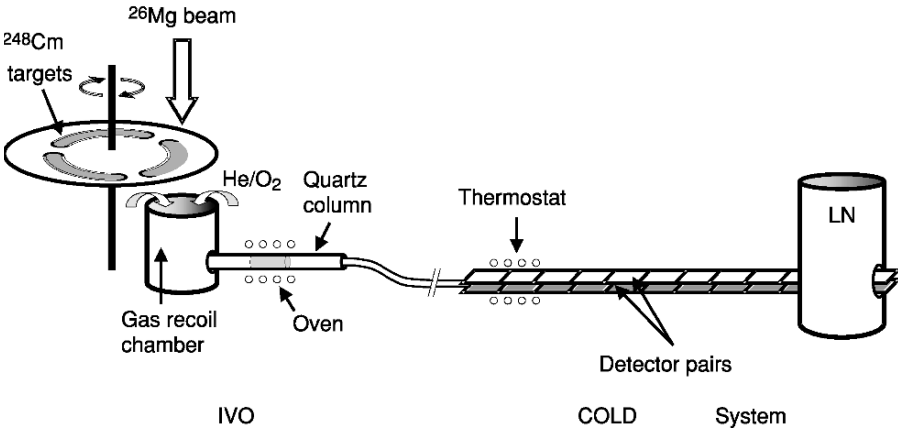

Fig. 14.19 *Schematic of IVO-COLD system for study of gas-phase properties of HsO_4 and lighter homologs* (*adapted from Düllmann* et al., 2002*b*).

Spectra of the alpha particles and SFs of the species deposited within each of the detectors of the array were measured and recorded to provide identification of the ^{269,270}Hs isotopes. The detection efficiency was about 77% for detection of a single alpha particle. A negative temperature gradient from –20 to –170°C was established along the TC formed by the detector array and measured at five positions. The system was checked at the beginning and at the end of the experiment by on-line measurements of the short-lived Os isotopes. In the 64 h experiment performed to produce Hs, three $\alpha-\alpha$-correlated decay chains were detected and assigned to the decay of ^{269}Hs. Two others, possibly due to the new nuclide ^{270}Hs or an isomer of ^{269}Hs, were detected, but a definite assignment could not be made. Based on detection of the three decay chains attributable to ^{269}Hs and two to a new nuclide ^{270}Hs (Türler *et al.*, 2003), HsO_4 was found to condense at a higher temperature than OsO_4 under similar conditions, indicating that the Hs oxide is less volatile than that of Os. The data for Hs and Os are shown in Fig. 14.20.

The Monte Carlo simulations that best fit these data give an adsorption enthalpy of $-(39 \pm 1)$ kJ mol^{-1} for OsO_4 on the silicon nitride surface, in good agreement with the previously measured values for SiO_2. An adsorption enthalpy of $-(46 \pm 2)$ kJ mol^{-1} was deduced for HsO_4 using only the three events assigned to ^{269}Hs and a $t_{1/2}$ value of 11 s in the analysis. This value is considerably more negative than the predicted value of $-(36.7 \pm 1.5)$ kJ mol^{-1} and suggests that HsO_4 is less volatile than OsO_4, in disagreement with calculations (Pershina, 1998a) that indicated that they should be nearly the same. More data and a better half-life measurement for ^{269}Hs are needed to investigate this discrepancy further. The possibility of different behaviors of HsO_4 on the Si_3N_4 detector surface compared to the SiO_2-coated detector surfaces should

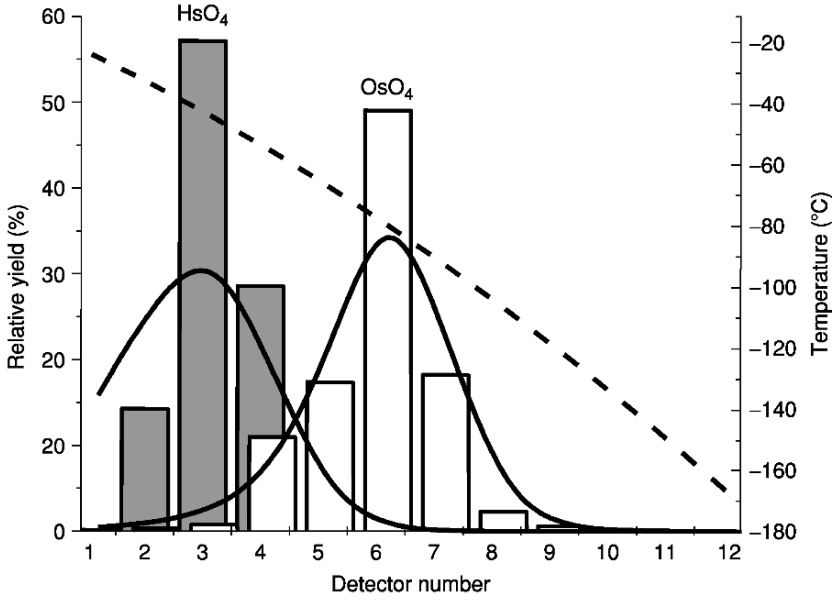

Fig. 14.20 *Combined thermochromatograms for Hs and Os oxides based on deposition positions (temperatures) for each of the* 12 *detector pairs. Dashed line indicates the temperature profile. The bars represent measured values and the curves result from Monte Carlo simulations of the migration process along the column.*

be considered and experiments with the tetroxide of Ru, predicted to be more volatile than those of either Os or Hs, should be conducted on both surfaces to investigate possible differences and the possibility that other oxides may be formed.

14.6.5 Summary of measured compared to predicted chemical properties

(a) Gas-phase studies

Observed trends in the volatility of the compounds of groups 4 through 8 compared to the theoretical predictions are summarized in Table 14.11. It can be seen that the measured and predicted trends in volatilities of the halide and oxyhalide compounds are in excellent agreement. However, in the case of the presumed tetroxides of Os and Hs there appears to be a discrepancy. This discrepancy emphasizes the need for additional investigations because few Hs disintegrations events were measured and their nuclear characteristics have not been unequivocally established.

Table 14.11 *Comparison of measured and predicted trends in volatilities of the compounds of Rf, Db, Sg, Bh, and Hs and their lighter homologs in periodic table groups* 4 *through* 8.

Group	*Compounds*	*Predicted volatility*	*Reference*	*Measured volatility*	*Reference*
4	MCl_4, MBr_4	Rf>Hf	Pershina and Fricke (1999)	Rf >Hf	Kadkhodayan *et al*. (1996); Sylwester *et al*. (2000)
5	ML_5 (L = Cl, Br)	Db >Ta > Nb	Pershina *et al*. (1992b)	(DbO_3Br)	Türler *et al*. (1996)
		$DbCl_5 > DbOCl_3$	Pershina *et al*. (1992b)	$DbCl_5$>$DbOCl_3$	Türler *et al*. (1996)
6	MO_2Cl_2	Mo > W > Sg	Pershina and Fricke (1996)	Mo > W > Sg	Schädel *et al*. (1997a); Türler *et al*. (1999)
7	MO_3Cl	Tc > Re > Bh	Pershina and Bastug (2000)	Tc > Re > Bh	Eichler *et al*. (2000)
8	MO_4	Hs = Os >Ru	Pershina *et al*. (2001)	Os > Hs	Düllmann *et al*. (2002b)

(b) Aqueous-phase studies

The measured trends in hydrolysis, complex formation, and extraction of complexes of Rf, Db, and Sg and their lighter homologs in groups 4 through 6 of the periodic table under a variety of experimental conditions compared to theoretical predictions for the same systems are summarized in Table 14.12. Care must be taken to ensure that the conditions for the experimental studies are the same as for the theoretical predictions since small differences in pH, purity of halide solutions, etc. can affect the equilibria that determine whether hydrolysis or complex formation dominates and whether the resultant complexes are neutral or charged. The order of extraction into organic solvents and sorption in cation- and anion-exchange chromatography differs greatly, depending on the charge on the complex. In general, agreement of the experimental results with the predictions is excellent when these factors are carefully controlled, as discussed in Section 14.5.3c.

There are some prospects for studies of the aqueous chemistry of elements heavier than 106 as well as for more detailed studies of elements 104, 105, and 106 using shorter-lived isotopes that may have higher production rates. The RTC (Kirbach *et al.*, 2002) coupled with the BGS could be used so that the separated isotopes can be transported to different rapid chemical separation systems such as SISAK-III described earlier (Omtvedt *et al.*, 2002) for few-second liquid–liquid extractions or other automated systems such as ARCA. This might permit detailed studies of complex formation of elements Bh and Hs that would be of special interest in acid solutions.

14.6.6 Prospects for experimental studies of chemistry of Mt through element 112

(a) Predictions of half-lives and production modes

Prospects for chemical studies of Mt depend on the confirmation of longer-lived isotopes than ^{268}Mt, currently the longest-lived known isotope of Mt. This isotope decays primarily by alpha emission, with a half-life reported to be about 40 ms; it was detected as the alpha-decay product of ^{272}111 produced with a cross section of 2.5 pb in the ^{209}Bi(^{64}Ni,n) reaction (Hofmann *et al.*, 2002). The half-lives of the ^{264}Bh daughter and the ^{260}Db granddaughter of ^{268}Mt are only about 1 s, so even techniques involving chemical separation of the daughters to infer the parent chemical properties do not appear feasible. Longer-lived isotopes of Mt are expected around the deformed nuclear shell at 162 neutrons and might be produced using the ^{238}U(^{37}Cl,4n) or the ^{249}Bk (^{26}Mg,4n) reaction to make ^{271}Mt. The half-life of this odd-proton, odd-neutron isotope was estimated from interpolation of Smolańczuk's (1997) calculations

Table 14.12 *Comparison of measured with predicted trends in hydrolysis and complex formation of some compounds of Rf, Db, and Sg and their lighter homologs in periodic table groups* 4 *through* 6.

Group	*Complexes*	*Experimental conditions*	*Predictions*	*Reference*	*Measured*	*Reference*
4	hydrolysis of M^{4+}	$pH \leq 2$	Zr > Hf > Rf	Pershina *et al.* (2002b)	Zr > Hf > Rf	Czerwinski (1992a)
	$MF_x(H_2O)_{8-x}^{z-x} (x \leq 4)$	$[HF] < 10^{-1}$ M	Zr > Hf > Rf	Pershina *et al.* (2002b)	Zr > Hf > Rf	Strub *et al.* (2000)
	MF_6^-	$[HF] > 10^{-3}$ M	Rf ≥ Zr > Hf	Pershina *et al.* (2002b)	Rf ≥ Zr > Hf	Trubert *et al.* (1999)
	MCl_6^-	4–8 M [HCl]	Zr > Hf > Rf	Pershina *et al.* (2002b)	Rf > Zr > Hf	Haba *et al.* (2002)
5	hydrolysis of M^{5+}	all pH	Nb > Ta > Db	Pershina (1998a)	Nb > Ta	Baes and Mesmer (1976)
	$M(OH)_2Cl_4^-$	all [HCl]	Pa >> Nb ≥ Db > Ta	Pershina (1998b)	Pa >> Nb ≥ Db >Ta	Paulus *et al.* (1999)
	$MOCl_4^-$, MCl_6^-					
6	hydrolysis of M^{6+}	$0 < pH < 1$	Mo > W > Sg	Pershina and Kratz (2001)	Mo > W > Sg	Schädel *et al.* (1998)
	hydrolysis of $MO_2(OH)_2$	$pH > 1$	Mo > Sg > W	Pershina and Kratz (2001)	Mo > W	Baes and Mesmer (1976)

for even proton–even neutron nuclides to be a few seconds and decay primarily by alpha emission. The cross section for the first reaction is expected to be similar to that of 2.5 pb, measured for the ^{238}U(^{34}S, 5n)$\rightarrow$^{267}Hs reaction (Lazarev *et al.*, 1995) as the enhancement of the cross section due to the extra two neutrons in ^{37}Cl compared to ^{34}S is expected to balance the decrease due to the higher Z of Mt. Based on this cross section, detection of two or three chains a week might be expected using multiple ^{238}U targets in the BGS. The BGS is capable of positively separating and identifying such a new nuclide based on measurement of the known alpha-decay chain of its daughters even if the ^{271}Mt half-life is as short as a few tenths of a second. The overall yield for the reaction with the highly radioactive target ^{249}Bk will be much lower because the cross section is expected to be only a few tenths of 1 pb and it is much more difficult to use multiple targets.

The production of longer-lived isotopes of elements 110, 111, and 112 with half-lives in the range of seconds to minutes have now been reported using 'warm/hot' fusion reactions or as decay products of elements 114 and 115. (See Table 14.2 and Fig. 14.2(b) and discussion in Section 14.1.) It may be possible to produce ^{277}110 directly in the 'warm' fusion reaction ^{232}Th(^{48}Ca,3n), but the cross section may be low and the systematics of these reactions need to be investigated further. The isotope ^{280}110 with a half-life of 7.6 s has been reported as the granddaughter of ^{288}114 produced in a four neutron out reaction in the bombardment of ^{244}Pu targets with ^{48}Ca (Oganessian *et al.*, 2000a; Oganessian, 2001), but this indirect production method is not favorable for chemical studies. Currently, there appear to be no suitable reactions for direct production of the very neutron-rich isotopes of Ds.

Some isotopes of the odd-proton element 111 should have half-lives of seconds or more and hindrances toward fission and alpha decay should exist. An isotope with mass number 280 and with a half-life of 3.6 s has been reported in the alpha-decay chain of ^{288}115 produced in the bombardment of ^{243}Am with ^{48}Ca projectiles (Oganessian *et al.*, 2004a).

SF activity attributed to ^{283}112 produced in the ^{238}U(^{48}Ca,3n) reaction and from the alpha decay of ^{287}112 produced via the ^{242}Pu(^{48}Ca,3n) reaction has been reported by Oganessian *et al.* (1999a,c, 2004b) who obtained a half-life of $\sim$5 min by averaging these results. However, as discussed in Section 14.1, it is difficult to positively identify a new nuclide that decays only by SF and even if this assignment is verified, its positive identification in chemical studies would be equally difficult and likely to be inconclusive. The production of 112 isotopes in ^{238}U(^{48}Ca,xn) reactions should be investigated further to determine the cross sections and if there is an alpha branch in ^{283}112 or ^{284}112. Then more definitive chemical studies could be undertaken. Such experiments would also help to assess the usefulness of 'warm' fusion reactions for production of a broad range of heavy element reactions for chemical studies.

(b) Chemical methods

Even though it appears that isotopes of the elements from Mt through element 112 can exist with half-lives long enough for chemical studies, the most difficult problem will be to increase the production rates and to perform on-line experiments with continuous separation and detection capabilities that can be operated for times long enough to obtain statistically significant results. These times will be of the order of weeks or months and will certainly require computer-controlled automated systems to carry out both gas-phase and solution chemistry. As the production cross sections for the elements of interest become ever smaller, the use of some pre-separation technique – either physical such as BGS or chemical such as IVO – will become mandatory in order to separate out the multitude of unwanted products before use of the more selective systems mentioned below.

The stable oxidation states of these elements both in the gas phase and in solution are predicted to vary widely, as shown in Table 14.10. From element 107 on, the maximum oxidation state is expected to be relatively unstable in aqueous solutions. Experimental studies designed simply to try to determine the most stable oxidation states in aqueous solution should be devised. Thus, for example, the stability of Bh(IV) relative to Bh(VII), or Hs(IV) relative to Hs(VIII) could be investigated by performing anion-exchange separations from HCl solutions in which the 4+ states might form negatively charged complexes that would be retained on the anion column. The relative positions of the peaks of the elution curves associated with reduction would give information about relative stabilities of lower oxidation states. Complex formation can also be studied for elements 109 and heavier. The imaginative gas-separation techniques developed for study of Bh and Hs can be applied to Mt and Ds, which are predicted to form volatile hexafluorides and octafluorides, as discussed in Section 14.5.2b.

Some preliminary chemical experiments on element 112 have been reported by Yakushev *et al.* (2001) and by Yakushev (2002) using the spontaneously fissioning nuclide $^{283}112$ ($\sim$5 min) reported by Oganessian *et al.* (1999a, 2004b) to be formed in the $^{238}U(^{48}Ca,3n)$ reaction with a cross section of 5 pb. The experiment was designed to determine whether element 112 behaved similarly to its periodic table homolog Hg, which had been shown to deposit on Au- or Pd-coated silicon surface barrier detectors (Yakushev *et al.*, 2001), or whether it behaved as a noble gas like Rn and remained in the gas phase. An unambiguous answer about the physical or chemical properties of element 112 was not obtained. The system was improved by introducing a special ionization chamber after the silicon detectors to measure alpha decays and SF events of nuclei remaining in the gas. More than 95% of the simultaneously produced Hg isotopes were deposited on the first Au-coated detector. Again, no events attributable to element 112 were detected on either the Au- or the Pd-coated

silicon detectors, but eight SF events were registered in the ionization chamber (Yakushev, 2002). These SF events were attributed to element 112, which indicates that it is more chemically inert than Hg and remained in the gas phase. The ΔH_{ads} of element 112 was deduced to be more positive than –55 kJ mol^{-1}. Further experiments with a temperature gradient in the chromatography column are now planned to better define ΔH_{ads}. It is also important to confirm that the observed SF events actually belong to element 112. If an alpha-decaying isotope of element 112 with a suitable half-life and production rate can be identified it would be much more suitable for chemical studies because it could be positively identified from its half-life and characteristic alpha-decay chain.

Experiments on element 112, similar to those conducted in Dubna, are planned by researchers at PSI (Soverna *et al.*, 2001) using a chromatographic column with a negative temperature gradient from 35 to –190°C. Silicon detectors coated with Au and Pd will be placed along the chromatographic column to detect element 112 and its deposition temperature will be determined relative to those of Hg at 115°C and Rn at –115°C in order to deduce ΔH_{ads}.

Eichler and Schädel (2002) investigated the adsorption of Rn on polycrystalline surfaces of transition metals and found the strength of adsorption to decrease in the order: Ni > Pd ≈ Cu > Au > Ag. They suggest that low-temperature vacuum thermochromatographic techniques could be used to rapidly separate element 112 from 114 and Rn and to determine whether its behavior is more like its lighter homolog Hg or an inert noble gas.

Isotopes of Hg have been studied by carrying them on Pd aerosols to serve as a model system for possible studies of elements 112 or 114 (Düllmann *et al.*, 2002a). Recoiling Hg isotopes produced in ^{168}Yb(^{22}Ne,xn)$^{190-x}$Hg reactions in the IVO setup at the PSI Philips cyclotron were thermalized in He, swept through an isothermal quartz column at 800°C to the re-cluster chamber, and transported on Pd aerosols to a suitable detection device for measurement of alpha spectra. The short-lived nuclides $^{183-185}$Hg were identified, indicating that volatile metals such as Hg can be transported in gas-flow systems without the presence of aerosol particles and then quickly adsorbed on metal aerosols if the enthalpy of adsorption is sufficiently large. The aerosols can then be transported to a detection system for measurements at low pressure and room temperature. Such a technique may also be applicable to measurements of transactinides with $Z = 112$ to 117.

Plans to separate elements with $Z > 108$ as noble metals by electrochemical deposition from aqueous solutions have been described (Kratz, 1999a). The choice of an appropriate electrode material is very important and estimates of suitable electrodes have been made for lighter homologs of the heaviest elements (Eichler and Kratz, 2000). Pd and Pt were found to be suitable electrode metals for the deposition of Hg, Tl, Pb, Bi, and Po, the homologs of elements 112 through 116.

14.7 FUTURE: ELEMENTS BEYOND 112 (INCLUDING SHEs)

14.7.1 Predictions of electronic structures and chemical properties

(a) Introduction

The ground state configurations of the free neutral atoms of elements 113 through 184 obtained from relativistic DF calculations are summarized in Table 14.13.

Table 14.13 *Dirac–Fock ground state configurations of free neutral atoms of elements* 113 *through* 184.[a]

Rn 'core' + $5f^{14} + 6d^{10} + 7s^2$ +								*Element* 120 *'core'* + $5g^{18} + 8p_{1/2}^2$ +					
	$5g$	$6f$	$7p_{1/2}$	$7p_{3/2}$	$7d$	$8s$	$8p_{1/2}$		$6f$	$7d$	$9s$	$9p_{1/2}$	$8p_{3/2}$
113			1					145	3	2			
114			2					146	4	2			
115			2	1				147	5	2			
116			2	2				148	6	2			
117			2	3				149	6	3			
118			2	4				150	6	4			
119			2	4		1		151	8	3			
120			2	4		2		152	9	3			
121			2	4		2	1	153	11	2			
122			2	4	1	2	1	154	12	2			
123		1	2	4	1	2	1	155	13	2			
124		3	2	4		2	1	156	14	2			
125	1	3	2	4		2	1	157	14	3			
126	2	2	2	4	1	2	1	158	14	4			
127	3	2	2	4		2	2	159	14	4	1		
128	4	2	2	4		2	2	160	14	5	1		
129	5	2	2	4		2	2	161	14	6	1		
130	6	2	2	4		2	2	162	14	8			
131	7	2	2	4		2	2	163	14	9			
132	8	2	2	4		2	2	164	14	10			
133	8	3	2	4		2	2	165	14	10	1		
134	8	4	2	4		2	2	166	14	10	2		
135	9	4	2	4		2	2	167	14	10	2	1	
136	10	4	2	4		2	2	168	14	10	2	2	
137	11	3	2	4	1	2	2	169	14	10	2	2	1
138	12	3	2	4	1	2	2	170	14	10	2	2	2
139	13	2	2	4	2	2	2	171	14	10	2	2	3
140	14	3	2	4	1	2	2	172	14	10	2	2	4
141	15	2	2	4	2	2	2	...					
142	16	2	2	4	2	2	2	...					
143	17	2	2	4	2	2	2	184	172 'core' + $6g^5 7f^4 9d^3$				
144	18	1	2	4	3	2	2						

[a] Fricke (1975).

Chemical properties for elements 113 through 121, as predicted by various researchers, are summarized in Table 14.14. A rather complete discussion and summary of the chemical properties predicted for these elements as of 1986 was given by Seaborg and Keller (1986).

(b) Elements 113 through 115

In elements 113 through 118, the filling of the 7p shell is expected to takes place. Chemistry of these elements will be strongly influenced by relativistic effects: the large relativistic stabilization of the $7s^2$ electron pair (a large 7s–7p gap hindering the hybridization) and a very large SO splitting of the 7p levels into $7p_{1/2}$ and $7p_{3/2}$, reaching 11.8 eV for element 118 (Fig. 14.21). Since the electrons occupying the $7p_{1/2}$ orbital will then form a closed subshell, an enhanced stability of lower oxidation states of these elements is expected. However, destabilization of the 6d levels would contribute to a more transition element character for the earlier 7p elements (Han *et al*., 1999b; Seth *et al*., 1999).

(*i*) *Element* 113

Element 113 has one electron in the $7p_{1/2}$ valence shell. Due to relativistic stabilization of the $7p_{1/2}$ electrons, its first IP of 7.306 eV, as shown in Table 14.15, is the largest in group 13 (Eliav *et al*., 1996a). The 1+ state is thus predicted to be the most stable.

The CCSD calculations (Eliav *et al*., 1996a) revealed a dramatic reduction in the excitation energy of an electron from the d^{10} shell: the $d^{10}s \rightarrow d^9s^2$ energy of 113^{2+} is 0.1 eV as compared to 8 eV for Tl^{2+}. It is, therefore, predicted that divalent or trivalent compounds of element 113 with an open $6d^9$ shell could exist. The calculated EA of Tl and element 113 are 0.4 and 0.68 eV, respectively.

The very large SO splitting of the 7p orbital will influence the chemistry of element 113 compounds by destabilizing the binding energy by almost 1 eV in the monohydride 113H. In this molecule, the 6d and 7s orbitals were shown to participate little in bonding (Han *et al*., 1999a,b, 2000; Seth *et al*., 1999) and all the effects are defined by the large participation of the $7p_{1/2}$ shell. Element 113 was calculated to be more electronegative than Ga, In, Tl, and even Al among all the monohydrides. Involvement of the 6d electrons in bonding in element 113 was confirmed by PP calculations (Han *et al*., 1999b; Seth *et al*., 1999) for $113H_3$, $113F_3$, and $113Cl_3$. As a consequence, a T-shape geometric configuration rather than a trigonal planar was predicted for these molecules. The stability of a high-coordination compound MF_6^- with the metal in the 5+ oxidation state is foreseen. $113F_5$ will probably be unstable since the energy of the reaction $113F_5 \rightarrow 113F_3 + F_2$ is only –53.4 kJ mol^{-1} (Seth *et al*., 1999). The calculated energies of the decomposition reaction $MX_3 \rightarrow MX + X_2$ (M = B, Al, Ga, In, Tl and element 113) confirmed a decrease in the stability of the 3+ oxidation state in group 13.

Table 14.14 *Predicted chemical properties of elements* 113 *through* 121.

	113	114	115	116	117	118	119	120	121
Chemical group	13	14	15	16	17	18	1	2	3
stable oxidation states[a,b,c]	**1**,3	**2**,0,(4)	**1**,3	**2**,4	**1**,**3**,5,(–1)	**4**,2,–1,(6)	**1**,3	2,4	**3**
first ionization potential (eV)[d]	7.306[d]	8.539[d]	5.58[d]	7.5[c]	7.7[c]	8.7[c]	4.53[e]	6.0[c]	4.45[f]
standard electrode potential in aqueous solution (V)	+0.6	+0.9	–1.5	+0.1	–0.25, 0.5		–2.7	–3.0	+2.1
	+0.6	+0.9	–1.5	+0.1	–0.25, 0.5		–2.7	–3.0	+2.1
ionic radius of indicated ion (Å)	1.4(1+)	1.2(2+)	1.5(1+) 1.0(3+)	0.83(4+) 0.58(7+)	0.80(4+) 0.58(7+)		1.8(1+)	1.6(2+)	
atomic radius (Å)[b]	1.7	1.6	2.0				2.4[c]	2.0[c]	
density (g cm^{-3})[b]	18 (16[c])	22 (14[c])	11 (13.5[c])	12.9[c]			3[c]	7[c]	
ΔH_{sub} (kJ mol^{-1})[b]	142(129[c])	42	142	197[c]			42	138	
boiling point (K)[b]	1400	420	~1400		883	263			
melting point (K)[b]	700	340	~700		623–823[c]	258[c]	273–303[c]	953[c]	

[a] Bold type: most stable in gas phase; underlined = most stable in aqueous solutions; non-bold: less stable; ( ) = least stable.
[b] Keller and Seaborg (1977) and Seaborg and Keller (1986).
[c] Fricke (1975).
[d] See Table 14.15.
[e] Lim *et al.* (1999).
[f] Eliav *et al.* (1998a).

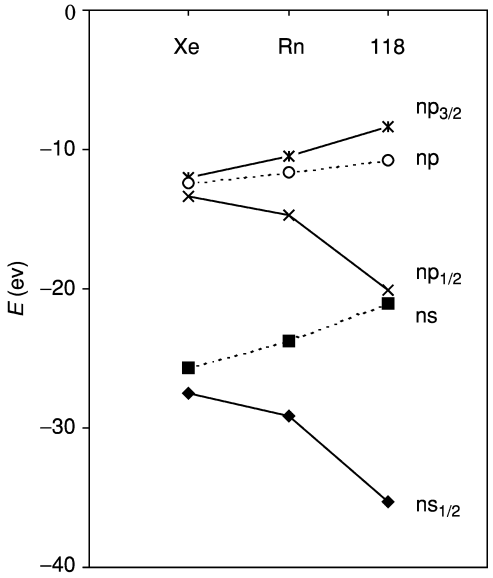

Fig. 14.21 *Relativistic stabilization of the ns and* $np_{1/2}$ *orbitals and the spin–orbit splitting of the np orbitals for the noble gases Xe, Rn, and element* 118. *DF atomic energies* (—) *are from Desclaux* (1973) *and HF values* (---) *are from Schwerdtfeger and Seth* (1998).

The standard electrode potential $E^{\circ}(113^{+}/113)$ was predicted to be +0.6 eV and 113^{+} is expected to be more easily complexed than Tl^{+} and to be similar to Ag^{+} (Keller *et al.*, 1970). For example, the solubility of TlCl in water is not increased much by adding excess HCl (Alekseeva *et al.*, 1972) or NH_3, whereas AgCl dissolves when NH_3 is added. Element 113 is expected to be more like silver in this respect. The smallest sublimation enthalpy in the group was predicted for element 113 by extrapolation (Keller *et al.*, 1970) and can be explained by the relativistic stabilization of the $7p_{1/2}$ orbital.

(*ii*) *Element* 114

The most interesting among the 7p elements is element 114 where a very large SO splitting of the 7p orbital and the relativistically stabilized 7s and $7p_{1/2}$ electrons result in a closed-shell ground state $7s^2 7p_{1/2}{}^2$, suggesting that the element should be rather inert. This is also reflected by the largest IP in group 14 (Table 14.15). One of the most striking features seen in Table 14.14 is the great decrease in boiling point in going from element 113 to element 114. This decrease was predicted by Keller *et al.* (1970) on the basis of extrapolations of the heats of sublimation of the group 13 and 14 elements versus periods of the periodic system. The boiling points were then calculated using Trouton's rule. This effect is a result of adding a second $7p_{1/2}$ electron in element 114 to form a

Table 14.15 *Ionization potentials* (*in* eV) *for the* 7*p elements.*

Calculated	113	114	115	116	117	118	*Reference*
DF	7.4[a]	8.5[a]	5.5[a]	7.5[a]	7.7	8.7	Fricke (1975)
MCDF	7.11	8.04 (8.51[b])	4.65	5.96	6.51	7.74 (7.6[b])	Pyper and Grant (1981)
CCSD	7.306[c]	8.539[d]	5.58[e]	–	–		Eliav *et al*. (1996a),[c] Eliav *et al*. (1998b),[d] Landau *et al*. (2001)[e]

[a] DF values corrected for the difference between theoretical and experimental values for the elements of the 6th period.
[b] Relativistic CI version of RECP (Nash and Bursten, 1999a).
[c] Eliav *et al*. (1996a).
[d] Eliav *et al*. (1998b).
[e] Landau *et al*. (2001).

closed-shell $7p_{1/2}{}^2$ configuration, similar to the s^2 one, making this configuration responsible for much weaker bonding in a metallic state.

The group 14 elements show increasing stability of the 2+ oxidation state relative to the 4+ state as one goes to higher atomic numbers. Lead is known to be most stable of the group 14 elements in the 2+ oxidation state. Due to the very large 7s orbital stabilization, the sp^3 hybridization energy needed for the 4+ valence is very large in element 114, so that the 4+ oxidation state of element 114 is expected to be unstable, while the 2+ state should be the most stable in the group. Recent calculations (Liu *et al*., 2001) have, indeed, shown $114O_2$ to be thermodynamically unstable in contrast to PbO_2. Energies of the decomposition reactions $MX_4 \rightarrow MX_2 + X_2$ and $MX_2 \rightarrow M + X_2$ (M=Ge, Sn, and Pb; X = H, F, and Cl) were calculated at the PP level (Seth *et al*., 1998b; Nash and Bursten, 1999a). The results confirm a trend of decreasing stability of the 4+ oxidation state in the group. The neutral (monatomic) state was calculated to be more stable for element 114 than for Pb. Element 114 should also have a greater tendency to form complexes in solutions than Pb. Because the stability of the 2+ state increases within group 14, element 114 would probably form MX^+, MX_2, MX_3^-, or MX_4^{2-} (X = Cl, Br, and I) by analogy with Pb. $114F_6^{2-}$, suggested by Seth *et al*. (1998b), will probably be unstable in the aqueous phase due to strong hydrolysis of the fluorides in aqueous solutions. Thus, aqueous complexes of element 114 such as $114Br_3^-$ or $114I_3^-$ should be preferentially formed. Pitzer (1975a) predicted stable $(114)X_2$ (X = F, Cl, and Br). The standard electrode potential $E^\circ(114^{2+}/114)$ was estimated as +0.9 V by Keller *et al*. (1970). We thus see that relativistic effects on the $7p_{1/2}$ electrons cause a diagonal relationship to be introduced into the periodic table near element 114, causing 114^{2+} to be somewhere between Hg^{2+} or Cd^{2+} and Pb^{2+} in its chemistry and causing 113^+ to act more like Ag^+ than Tl^+.

(*iii*) *Element* 115

In element 115, one electron is located in the relativistically destabilized $7p_{3/2}$ orbital and, therefore, is loosely bound,while $7p_{1/2}{}^2$ serves as an inert pair. Thus, the 1+ oxidation state of element 115, like that of Tl^+, should be preferred. This is also supported by a drastic decrease in the first IP between 114 and 115 (Fig. 14.8). Furthermore, calculations show that element 115 has the smallest IP in group 15 and in the 7th period, as shown in Table 14.15 and Fig. 14.8. Keller *et al*. (1974) made some detailed predictions of the chemical properties of element 115 based on extrapolations of the properties of group 15 elements and relativistic atomic DS and DF calculations. Their results indicate that the chemical properties of element 115 should be analogous through a diagonal relationship to those of Tl (group 13) as well as to those of Bi. They predicted a standard electrode potential $E^\circ(115^+/115) = -1.5$ V, indicating that element 115 metal should be quite reactive. They also suggested that 115(III) should be relatively stable and have some chemical properties somewhat similar

to Tl(III), but that its chemical properties will be closer to those of Bi(III). The 5+ state seems unlikely. Melting and boiling points of the metal should be close to those of element 113.

(c) Elements 116 through 118

The chemistry of elements 116 through 118 will be defined mostly by the participation of the $7p_{3/2}$ orbital in bonding. Certain predicted volatility characteristics of elements 116, 117, and 118 or their compounds may offer advantages for chemical identification. This will be especially true for element 118. The chemical properties of element 116 can be deduced by extrapolations from Po, though the 2+ state should be more stable than the 4+ state because the $7p_{1/2}^2$ electrons are expected to be rather inert. Estimates of formation enthalpies of MX_2 and MX_4 (X = F, Cl, Br, I, SO_4^{2-}, CO_3^{2-}, NO_3^-, and PO_4^{3-}) for Po and element 116 (Grant and Pyper, 1977) on the basis of the MCDF atomic calculations are consistent with the expected instability of 116^{4+}. The chemistry of element 116 is expected to be mainly cationic, i.e. the relative ease of formation of the divalent compounds should approach that of Be or Mg, and tetravalent compounds such as $116F_4$ should be formed only with the most electronegative atoms.

In element 117, the 1– oxidation state becomes less important than that of the lighter group 17 halide ions due to the destabilization of the $7p_{3/2}$ orbital. The EA of element 117 is the smallest in the group (2.6 eV as predicted by Cunningham, 1969 and 1.8 eV as given by Waber *et al.*, 1969). Therefore, the 3+ state should be at least as important as the 1– state, so that element 117 might resemble Au^{3+} in its ion-exchange behavior in halide media. The trend to decreasing participation of the $np_{1/2}$ orbital bonding in group 17 was found to be continued further with element 117 (Hoffman, 1996; Saue *et al.*, 1996; Nash and Bursten, 1999c; Han *et al.*, 2000). In the group HI, HAt, and H117, an increasing trend in R_e and a decreasing trend in D_e are continued with H117. Analogous to its lighter homologs, Element 117 should form dimers X_2. The DCB CCSD(T) calculations for X_2 (X = F through At) (Visscher *et al.*, 1996) found a considerable antibonding σ-character in the HOMO of At_2 due to the SO coupling while without the SO coupling it is an antibonding π-orbital. The bonding in $(117)_2$ is predicted to continue this trend and have a strong π-character.

The elements in the noble gas group become less inert with increasing Z. Earlier predictions of properties of element 118 were made by extrapolation from lighter homologs within the group (Grosse, 1965; Pitzer, 1975a,b). Early calculations of Penneman and Mann (1976) indicated that ionization energies of element 118 should be less than the experimental values for xenon, and that chemical compounds should be expected for 118. The first IP of element 118 is 8.7 eV (see Table 14.15), about the same as the IP(114) = 8.54 eV and smaller than IP(Rn) = 10.74 eV and IP(112) = 11.97 eV. The outer 8s orbital of element 118 is relativistically stabilized to give the atom a positive EA of 0.056 eV, as

shown by recent CCSD calculations (Eliav *et al.*, 1996b). The polarizability of 118 is expected to be the largest in group 18. Its largest polarizability, together with its smallest IP, implies that it will have the highest reactivity in the group. It should be stable in the 4+ oxidation state, and should form stable tetrafluorides and tetrachlorides as well. Recent RECP calculations (Han and Lee, 1999) of free energies of the reactions $M + F_2 \rightarrow MF_2$ and $MF_2 + F_2 \rightarrow MF_4$, where M = Xe, Rn, and element 118, confirmed an increase in the stabilities of the 2+ and 4+ oxidation states in group 18. The SO effects were shown to stabilize $118F_4$ by a significant amount, about 2 eV, though they elongate R_e by 0.05 Å. The influence of the SO interaction on the geometry of MF_4 was investigated by RECP calculations (Han and Lee, 1999; Nash and Bursten, 1999a,b). It was found that the D_{4h} geometrical configuration for XeF_4 and RnF_4 becomes slightly unstable for $118F_4$. A T_d configuration was shown to be more stable than D_{4h} by about 0.20 eV. The reason was the availability of only stereochemically active $7p_{3/2}$ electrons for bonding. An important observation was made that the fluorides of element 118 will most probably be ionic rather than covalent as is the case of Xe. Therefore, they are predicted to be non-volatile.

(d) Elements 119 through 121

In elements 119 and 120, the filling of the 8s shell will take place, so that these elements should be homologs of the alkali and alkaline earth elements in groups 1 and 2 and will be stable in the 1+ and 2+ oxidation states, respectively. Their first IPs (Fricke, 1975) should be about 0.5 eV higher than those of Fr and Ra, respectively, due to the relativistic stabilization of the 8s electrons, and closer to the values of Rb and Sr. Thus, an upturn in the IPs from Cs to element 119 and from Ba to element 120 (see Fig. 14.22) was predicted (Penneman and Mann, 1976). Recent DK CCSD calculations (Lim *et al.*, 1999) showed the first IP of element 119 to be relativistically increased from 3.31 to 4.53 eV, while polarizability is decreased from 693.94 to 184.83 a.u. Due to the relativistic stabilization of the 8s orbital, the EA for element 119, of 662 meV, is 20 meV higher (being the highest in the group) than that for Fr, according to recent DCB CCSD calculations (Landau *et al.*, 2001).

The atomic radii of elements 119 and 120 are expected to be 2.4 and 2.0 Å, respectively, very similar to the values of Rb and Sr, as shown in Fig. 14.23. They show the same reversal of the trend (a downturn from Cs/Ba to 119/120) as do the IPs in groups 1 and 2 (Fricke, 1975). Thus, the chemical properties of elements 119 and 120 should be close to those of Rb and Sr, respectively, rather than to Fr and Ra in the 1+ and 2+ oxidation states. On the other hand, the ions will have larger radii than Rb^+ and Sr^{2+} because of the larger extension of the filled 7p shell compared to the lower p-shells. Another important point is that due to the relatively small ionization energy of the outer $7p_{3/2}$ electrons and their spatial extension, higher oxidation states like 3+ or 4+, respectively, could be reached in elements 119 and 120.

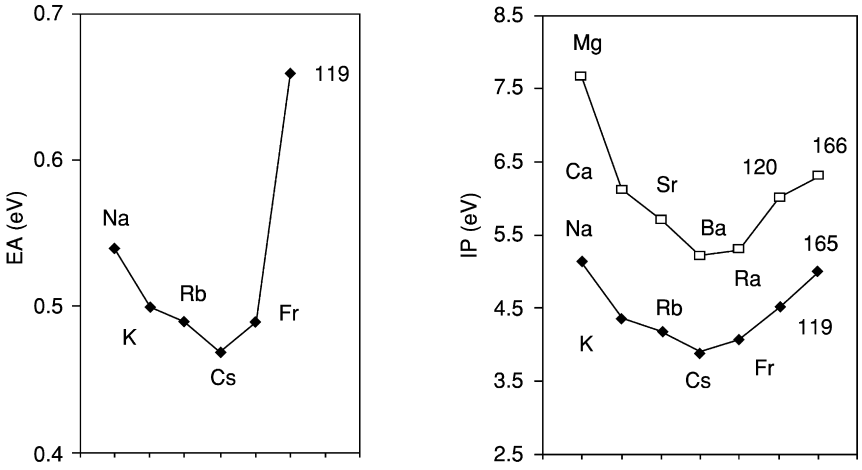

Fig. 14.22 *Electron affinities* (*EAs*) *and ionization potentials* (*IPs*) *for alkali and alkaline-earth elements. The data for Na through Fr and Mg through Ra are experimental. The value for Element* 119 *is from DF CCSD calculations* (*Landau* et al., 2001). *The values for elements* 120, 165 *and* 166 *are from DF calculations* (*Fricke,* 1975).

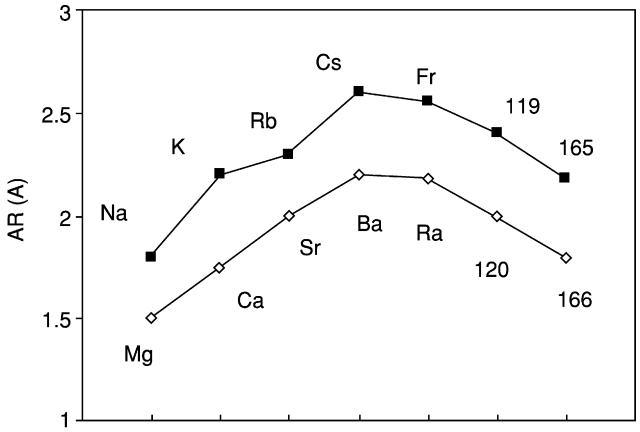

Fig. 14.23 *Atomic radii* (*AR*) *of alkali and alkaline earth elements. The data for Na through Cs and Mg through Ra are experimental. The other data are from DS calculations.* (*Redrawn from Fricke,* 1975).

The next element, 121, will have a relativistically stabilized 8p electron in its ground state electronic configuration $8s^2 8p_{1/2}$ (see Table 14.13) in contrast to that of $8s^2 7d$ predicted by a simple extrapolation within the group. As early as 1969, Griffin *et al.* (1969) showed that the large SO splitting brings an 8p

electron into the stable atomic ground state. Recent CCSD calculations for element 121 (Eliav *et al.*, 1998a) gave $IP_1 = 4.45$ eV and EA = 0.75 eV, the highest EA in group 3. Griffin *et al.* also showed that large changes occur in the spatial distribution of the valence orbitals in going from element 120 to 121. For example, the effective radius of the 5g electrons changes from 25 Bohr units for element 120 in the excited configuration $8s^15g^1$ to 0.8 Bohr units for element 121 in the configuration $8s^17d^15g^1$. This phenomenon, called 'radial collapse', occurs as late as element 125 as a consequence of indirect relativistic effects. Due to the proximity of the valence levels, higher oxidation states are possible.

(e) Superactinide elements and beyond

Element 122 belongs to a very long, unprecedented transition series that is characterized by the filling of not only 6f but also 5g orbitals with partially filled $8p_{1/2}$ orbitals, which is a direct relativistic effect. These elements were dubbed 'superactinides' by Seaborg (1968) as early as 1968. Quite a number of theoretical calculations of the ground state electronic configurations (Griffin *et al.*, 1969; Mann, 1969; Mann and Waber, 1970; Fricke *et al.*, 1971) were performed for this region and the results have been summarized by Fricke (1975). The calculated ground state configurations of the free neutral atoms of elements 113 through 184 are listed in Table 14.13. Here, at the beginning of the superactinides, not only two but four electron shells, namely $8p_{1/2}$, $7d_{3/2}$, $6f_{5/2}$, and $5g_{7/2}$, are expected to compete simultaneously. These open shells, together with the 8s electrons, determine the chemistry.

As shown in Table 14.13, a 7d electron is added to the ground state in element 122 and the 8p electron is relativistically stabilized so that the configuration is $8s^27d8p$, in contrast to the $7s^26d^2$ state of Th. This is the last element where accurate CCSD calculations (Eliav *et al.*, 2002) exist. The first four calculated IPs of element are 5.6, 11.3, 20.4, and 27.14 eV as compared to the first and the fourth IPs, 6.54 and 28.75 eV, of Th. A decrease in the first IP from Th to element 122 is due to the ionized $8p_{1/2}$ electron.

Elements 122 through 152 might have chemical properties somewhat similar to those of the actinides but there will be some differences. The very small binding energies of all the valence electrons will cause the higher oxidation states to be reached in these elements. This will be a continuation of the trend from the lanthanides (where 3+ states are highest) to the superactinides.

For ionic compounds it is important to establish which external orbitals are left after all outer s-, p-, and d-electrons are removed. Will there be some g- and f-electrons left or will they be easily excited to an outer electron shell, so that they can be removed as well? Some investigations showed that for element 126 in the divalent state, one g-electron will move to an f-electronic state, and the 8s electrons will not be the first to be removed. Thus, the divalent ions are expected

to act as soft Lewis acids and possibly form covalent complex ions readily. From some calculations of excited states, it is assumed that very high oxidation states may be possible around element 128 in complex compounds, but that normally these elements will have 4+ as their main oxidation state in ionic compounds. The maximum valence will be reduced to 6+ at element 132 and in the region of 140, it will be 3+ to 4+. At the end of the superactinide series, the normal oxidation states are expected to be only 2+ because the 6f shell will be buried deep inside the electron core and the 8s and $8p_{1/2}$ orbitals will be strongly bound. At element 156, only two 7d relativistically destabilized electrons will be available for bonding. This behavior should be similar to that of the low oxidation states of elements at the end of the actinides. Thus, at the end of the superactinide series, the elements will be more noble.

A contraction of bond lengths, analogous to the actinide contraction, is expected for the superactinide series. The total effect will be very large because of the 32 electrons, with the expected contraction of 0.02 Å per element. The predictions of chemical properties by extrapolation will be very difficult und unreliable in this area, since most of the elements have no homologs. From atomic calculations, one can already say that the behavior will be very different due to the stronger relativistic effects.

The fifth series of transition elements is expected to begin beyond the superactinides. Several early DF calculations in this region were performed. In elements 155 to 164, the filling of the 7d shell will take place so that they will be the d transition elements of the 8th period. The 8s and $8p_{1/2}$ electrons will be bound so strongly in these elements that they will not participate in the chemical bonding in contrast to the 7s electrons of the 7th period. Nevertheless, the 9s and $9p_{1/2}$ states will be easily available in 164 for hybridization so that the chemical behavior is expected to be similar to that of other d-elements. From DF calculations of excited states of element 164, Penneman and Mann (1976) suggested that the 7d orbitals will be chemically very active. Thus, in aqueous solutions, strong ligands can form tetra- and hexavalent bonds in addition to the predominant bivalent bonds. Consequently, tetrahedral $164(CO)_4$, $164(PF_3)_4$, and linear $164(CN)_2^{2-}$ might be prepared, which would be a striking contrast to lead (Fricke, 1975). The softness of element 164 should be similar to that of Hg, so that its location in the same group in the periodic table is justified. The metallic state of element 164 should have a larger cohesive energy than almost any other element because of covalent bonding, so that the melting point should be high (Fricke and Waber, 1971). The same authors indicated that the properties of elements 118 and 164 might also be analogous.

In elements 165 and 166, the 9s shell will be filled, suggesting that they should be homologs of group 1 and 2 elements and that their IPs and IR (Fricke, 1975) will be similar to those of the group 1 and 2 elements, respectively. Nevertheless, because of the underlying 7d shell, elements 165 and 166 might exhibit

properties similar to those of the group 13 and 14 elements. Therefore, higher oxidation states than 1+ and 2+, respectively, might occur.

In elements 167 through 172 the $9p_{1/2}$ shell will fill before the $8p_{3/2}$ shell. The energies of these orbitals are so close to each other that this situation is analogous to the nonrelativistic p-shell in the 3d period. Thus, the common oxidation states of elements 167 to 179 will be 3+ to 6+. Element 171 is expected to have many states from 1– to 7+, as do halogens. H(171) would form due to its high electron affinity of 3.0 eV (Fricke *et al.*, 1971). Compounds with F and O are also expected. Element 172 might be a noble gas similar to Xe due to the similar values of their IPs. The major difference is that element 172 is predicted to be a liquid or a solid at normal temperatures because of its large atomic weight.

Mann reported that his program was unable to go beyond $Z = 176$. Model calculations of Fricke and Waber (1972) took into account a phenomenological formulation of quantum electrodynamic effects and made it possible to extend the DF calculations to even higher elements. They calculated the DF ground state for element 184, as shown in Table 14.13. The 10s and $10p_{1/2}$ electrons do not appear in the ground state configuration and only $8d^3$ and $7f^4$ electrons might be available for chemical bonding. The chemical behavior will be then even simpler than that of the early superactinides. With increasing ionization of the 184 ion, a redistribution of electrons occurs between the 6g and 7f shells so that the number of electrons in the 6g shell increases. Since the 6g electrons are very deep inside the ion, only 7f electrons will be available for bonding. By analogy to U, the 5+ and 6+ states may be easily reached, but in aqueous solution the 4+ oxidation state will be the most stable. Higher oxidation states are not likely because the binding energy of the electrons in the deeply buried 6g shell will increase rapidly with higher ionization. Thus, in the very long SHE transition series, where many outer electron shells are being filled simultaneously in the neutral atom, a large increase in ionization energies will occur so that extremely high or unusual oxidation states are not expected.

In summary, in the area of the SHEs, the relativistic effects are so strong that any classification based on the knowledge of their electronic configurations or extrapolations of properties from the known elements is inappropriate. It is interesting to note that even without relativistic effects, the chemistry of the heaviest SHEs would be different from that of their lighter homologs due to very large shell-structure effects. The nonrelativistic expansion and destabilization of the *n*s valence orbitals and contraction and stabilization of the *n*d, *n*f, and orbitals of higher angular quantum number *l* with very large *n* also would have drastically changed the properties of the SHEs. However, due to the opposite actions of relativistic and shell-structure effects, the relativistic and nonrelativistic changes are predicted to go in opposite directions. A more detailed periodic table up to element 172 was given by Fricke (1975). Some discussions of the chemistry of SHEs can be found in Penneman *et al.* (1971),

Fricke (1975), and Jorgensen (1968), and more recently in a review of the evolution of the periodic table by Seaborg (1996).

14.7.2 Prospects for experimental studies of chemistry of elements beyond element 112, including SHEs

The prerequisites for successful studies of the chemistry of elements beyond 112 will be similar to those discussed previously for Mt through 112. These include the existence of isotopes with long enough half-lives for chemical studies, knowledge of their nuclear decay properties so that they can be positively identified as belonging to the element being studied, synthesis reactions with the highest possible cross sections, techniques for increasing the production rates such as cooled, multiple targets, the highest possible beam currents at accelerators with facilities for conducting these studies, and, ideally, dedicated beamlines for optimal utilization of facilities by international groups of scientists. After the chemistry of a given element is known, the atomic number of new isotopes can be positively assigned based on their established chemical properties and detailed studies of nuclear properties such as SF can be conducted on chemically separated samples.

(a) Chemical methods

A useful technique that should prove invaluable in the study of very low-yield, short-lived elements is pre-separation of the nuclides of interest from the host of unwanted activities using a dedicated on-line separator such as the BGS at the appropriate accelerator. At the focal plane the separated isotopes can be stopped in an RTC containing an appropriate gas and can even be treated chemically to adjust oxidation states and volatility. The resultant volatile species can then be rapidly and continuously transported to a cryo-thermochromatographic separator or any other desired chemical separation/detection system.

The ingenious isothermal gas-phase techniques that have already been applied in the studies of volatile Hs oxides can be used to study other volatile species that can be similarly swept in carrier gas directly to an on-line detection system or to a cryogenic TC composed of the particle detectors. In this way, simultaneous on-line measurements can be performed of the decay properties of the radioactive nuclides in the volatile species and their deposition temperature on the surface of the detectors that form the chromatography column. Vacuum cryo-thermochromatographic techniques in which the relative reactivity of elements 114 through 118 are determined based on their sorption on a variety of transition metal surfaces might be used to assess whether their behavior is more like their lighter homologs or the inert noble gases.

The continuous, computer-controlled automated procedures discussed in the previous sections can be used and other procedures designed specifically to exploit the chemistry predicted for each of these elements. Continuously

operating, rapid systems for liquid–liquid extractions followed by detection in flowing liquid-scintillation detectors such as the SISAK-III/liquid scintillation system (Omtvedt *et al.*, 1998, 2002) can be used for on-line studies of isotopes with half-lives as short as a few seconds provided chemical systems that rapidly come to equilibrium can be devised. Alternatively, they could be used to continuously purify longer-lived SHEs. A variety of computer-controlled, continuous multi-ion-exchange column techniques that include automated transport of samples to the detection equipment have been developed (Haba *et al.*, 2002; Nagame *et al.*, 2002) for performing rapid separations of isotopes with half-lives as short as a few seconds and then inferring their presence based on detection of their longer-lived daughters in subsequent chemical separations. Such continuous systems might also be adapted for processing longer-lived SHEs for subsequent off-line detection.

New methods for studying gas-phase ion chemistry in a Penning trap have been reported by Rieth *et al.* (2002) and it has been shown by the ISOLTRAP group at the Centre Européen pour la Recherche Nucléaire (CERN) (Kugler *et al.*, 1992; Bollen *et al.*, 1996) that nuclides as short as a few tenths of a second can be used with Penning trap mass spectrometers. These techniques have potential application to gas-phase studies of elements beyond 112. Kinetic data on ion–molecule interactions can be obtained with single-ion detection, and mass spectrometry can be used to unambiguously determine the stoichiometry of the reaction products. However, the reaction rates must be increased in order to make the technique viable for the low production rates of less than one atom per week expected for the heaviest elements.

(b) Predicted and reported half-lives and nuclear properties of SHEs

One of the most significant nuclear properties of elements 107 through 112 is that they decay predominantly by alpha emission rather than SF, contrary to earlier predictions. This experimental discovery sparked a renewal of interest in searching for elements beyond 112 and revived hope that the long-predicted island of SHEs might finally be reached. Armbruster and Münzenberg (1989) proposed that even though the neutron-deficient isotopes of elements 107 through 112 are probably not spherical, they should qualify as SHEs because without the stabilization of nuclear shells they would not exist. These elements have not been generally recognized as SHEs.

The discovery of longer-lived isotopes in this region, ^{265,266}Sg, ^{267}Bh, and ^{269,270}Hs, substantiated the theoretical model and calculations (Sobiczewski *et al.*, 1994; Smolańczuk *et al.*, 1995) predicting a doubly magic deformed region of extra stability in the vicinity of proton number 108 and neutron number 162 in addition to the island of spherical stability originally predicted to be around $Z = 114$ and $N = 184$, as shown in Fig. 14.24.

Evidence for three isotopes of element 114, ^{287,288,289}114, has been reported (Oganessian *et al.*, 1999a) although only one event of 21-s ^{289}114 was detected

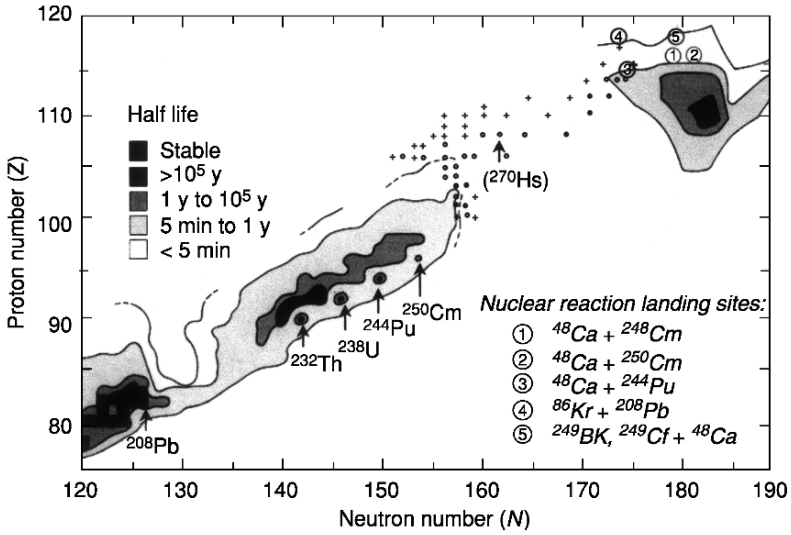

Fig. 14.24 *Updated plot of heavy element topology from* 1978 *showing some landing points for proposed reactions. Heavy element isotopes reported since* 1978 *up to mid-*2002 *are indicated with symbols denoting the following half-life ranges:* 0.1 ms to 0.1 s (+); 0.1 s to 5 min (○); > 5 min (●).

and it was not confirmed in subsequent experiments (Lougheed *et al.*, 2000). The discovery of isotopes of element 116, $^{292}116$, has been discussed by Oganessian (2002) and Oganessian *et al.* (2002, 2004c). Calculations (Smolańczuk, 1997) indicate that these isotopes are nearly spherical with deformation energies ranging from only about 0.1 MeV for $^{292}116$ to 0.3–0.2 MeV for the 114 isotopes, compared to zero deformation energy for the spherical doubly magic $^{298}114$ and 7.8 MeV for the doubly deformed magic nucleus, $^{270}108$. Thus, element 114 and 116 isotopes qualify as spherical SHEs even though they do not have the full complement of 184 neutrons. However, their existence still awaits confirmation by other groups.

Recent theoretical predictions (Chasman and Ahmad, 1997; Smolańczuk, 2001a,b) indicate that isotopes with half-lives of microseconds or longer will exist all along the way to the predicted islands of stability. However, the half-lives predicted for nuclei in the region of the spherical island of stability have decreased dramatically since the 1970s when half-lives of billions of years were predicted. For example, Smolańczuk (2001a,b) predicted that the spherical doubly magic superheavy nucleus $^{298}114$ will decay predominantly by alpha emission with a half-life of only 12 min, but that ^{292}Ds may alpha decay with a half-life of about 50 years.

Some other recent calculations (Kruppa *et al.*, 2000) predict that the strongest spherical shell effects might be at $Z = 124$ or 126 and $N = 184$ while still others

propose the maximum effect might be at $Z = 120$ and $N = 172$. Doughnut-like, toroidal nuclear shapes with lower densities or a hole in the middle to alleviate the effects of Coulomb repulsion have even been postulated. How many more elements can exist is still unclear and it is even more unclear how many of these we can actually produce.

(c) Production reactions

So-called 'cold' fusion reactions in which the compound nucleus is produced with small excitation energy and emits only a single neutron were used to discover the elements from Bh through 112 (Hofmann, 1998). After the discovery of element 112 in 1996 (Hofmann *et al*., 1996), researchers at GSI unsuccessfully attempted to produce element 113 using the cold fusion reaction ^{209}Bi (^{70}Zn,n) ^{278}113 (Hofmann and Münzenberg, 2000). From two experiments lasting about 3 weeks each, they set a limit of 0.6 pb on the cross section at a mean excitation energy of 10.5 MeV. They concluded that the cross section for production of element 116 would be only 1 femtobarn and that their experimental setup would have to be greatly improved in order to investigate this region further. Contrary to these expectations that the production cross sections for the 1n evaporation channel in cold fusion reactions to produce elements above 112 would continue to decrease exponentially with the proton number of the projectile, Smolańczuk (1999a) suggested that the cold fusion reaction ^{208}Pb(^{86}Kr,n) reaction to produce the hypothetical spherical SHE nuclide ^{293}118 with an excitation energy of only 13 MeV would have an unusually large cross section of a few hundred picobarns. The predicted increase in formation cross section was attributed to the fact that ^{86}Kr contains the magic number of 50 neutrons, which leads to a larger Q value with a subsequent increase in the transmission probability through the Coulomb barrier. He also predicted that ^{293}118 would decay by a unique decay sequence of six high-energy alpha particles. However, the results of Gregorich *et al*. (2002) setting upper limits of less than 1 pb for the formation cross section for this reaction based on detection of the predicted high-energy alpha-decay chain make the use of cold fusion reactions appear less attractive for production of SHEs. Estimates of the predicted cross section were later lowered to about 6 pb (Smolańczuk, 2001b), and it was pointed out that the excitation functions are quite narrow and have a rather sharp threshold (Smolańczuk, 1999c) so use of too low a bombarding energy might result in a negative result and the idea should not be totally abandoned.

Similar cold fusion reactions with ^{208}Pb or ^{209}Bi targets with ^{87}Rb or ^{86}Kr projectiles could be used to produce ^{294}119 (Smolańczuk, 1999a,b), whose half-life is estimated to be only microseconds. However, ^{294}119 is predicted to decay to isotopes of the new longer-lived, odd-Z elements 117, 115, and 113 via a succession of alpha emissions, ending with the known isotope 3.6-h ^{262}Lr. Production of ^{295}120 ($\sim$2 μs) via the ^{208}Pb(^{88}Sr,1n) reaction and detection of its high-energy alpha-decay chain have also been proposed (Smolańczuk, 2001a).

The reported elements 114 and 116 were synthesized using reactions of ^{244}Pu and ^{248}Cm with ^{48}Ca projectiles to form the compound nuclei ^{292}114 and ^{296}116, which then emitted four neutrons to produce 2.6-s ^{288}114 and 53-ms ^{292}116 (Oganessian *et al*., 2000a,b; Oganessian, 2001, 2002). They were calculated to have excitation energies of only 33 and 31 MeV, respectively, due to the stability of the doubly magic projectile, compared to >45 MeV for 'hot' fusion reactions. The detection limit of these experiments was about 0.5 pb, several orders of magnitude more sensitive than in the unsuccessful attempt reported in 1984 by an international group of nuclear scientists, both chemists and physicists (Armbruster *et al*., 1985), who conducted an exhaustive 'final' investigation of the reaction of ^{248}Cm with ^{48}Ca projectiles to produce SHEs. Oganessian also proposed that the reaction of ^{48}Ca with ^{249}Cf targets be used to produce element ^{294}118 via the '3n out' reaction. However, the viability of the '3n out' reactions in this region has yet to be confirmed. Loveland *et al*. (2002) set a limit of <2 pb for SF and alpha events for the ^{238}U(^{48}Ca,3n)^{283}Ds reaction. Hot fusion reactions between ^{48}Ca projectiles and ^{249}Bk and ^{249}Cf targets to produce elements ^{293,294}117 and ^{293,294}118, respectively, are under investigation by the Dubna/LLNL group.

The ^{237}Np and ^{249}Bk targets with ^{48}Ca projectiles can probably be used to make the odd-proton element 113 and more neutron-rich isotopes of element 117, respectively. Other highly radioactive targets such as ^{249}Cf or even ^{254}Es with appropriate projectiles might be used to make more neutron-rich isotopes of elements as heavy as 118, but considerable development work will be required.

Reactions that can produce a higher ratio of neutrons to protons will certainly be most advantageous and need to be investigated. Myers and Swiatecki (2000) have suggested that so-called 'unshielded' reactions in which the Coulomb barrier has sunk below the bombarding energy may result in enhanced production yields for some of the higher Z elements. Their hypothesis that the cross section for ^{277}112 produced in the symmetric reaction ^{142}Ce(^{136}Xe,n) might be much larger than that for the 112 discovery reaction ^{208}Pb(^{70}Zn, n)^{277}112 should be tested experimentally. If so, the unshielded reaction ^{170}Er (^{136}Xe,n) reaction to make ^{305}122, which has 183 neutrons, might be a method for getting closer to these regions. It should decay by successive alpha emission to the isotope ^{289}114, reported by the Dubna/LLNL group. Whether additional SHEs can be produced depends very much upon whether the cross sections for the 'cold' fusion reactions in which only a single neutron is emitted and the 'warm'/'hot' fusion reactions with three or four neutrons emitted are large enough to permit detection.

It now appears likely that many more relatively long-lived nuclides can exist than are presently known, but a major research effort to explore new types of production reactions, imaginative techniques for optimizing overall yields by using multiple targets and higher beam currents, innovative chemical separations, and a dedicated on-line installation for chemical studies at an appropriate

accelerator with access to a pre-separator will be required in order to fully explore their chemical properties. If, on the other hand, relatively long-lived new elements are discovered, then methods for 'stockpiling' them for off-line studies or producing them as by-products of other experiments must be devised to facilitate studies of their chemistry. The prospect lies ahead of a whole new landscape for the exploration of the chemical properties of the heaviest elements and their compounds, determining the influence of relativistic effects, assigning their positions in the periodic table, and extending and further defining the architecture of the periodic table.

REFERENCES

Adloff, J. -P. and Guillaumont, R. (1993) *Fundamentals of Radiochemistry*, CRC Press, Boca Raton, pp. 327–52.

Ahrland, S., Liljenzin, J. O., and Rydberg, J. (1973) in *Comprehensive Inorganic Chemistry*, vol. 5 (ed. J. Bailar), Pergamon Press, Oxford, pp. 519–42.

Alekseeva, T. E., Arkhipova, N. F., and Rabinovitch, V. A. (1972) *Russ. J. Inorg. Chem.* **17**, 140–1.

Alstad, J., Skarnemark, G., Haberberger, F., Herrmann, G., Nähler, A., Pense-Maskow, M., and Trautmann, N. (1995) *J. Radioanal. Nucl. Chem. Articles*, **189**, 133.

Alzitzoglou, T., Rogowski, J., Skålberg, M., Alstad, J., Herrmann, G., Kaffrell, N., Skarnemark, G., Talbert, W., and Trautmann, N. (1990) *Radiochim. Acta*, **51**, 145–50.

Amble, E., Miller, S. L., Schawlaw, A. L., and Townes, C. H. (1952) *J. Chem. Phys.,* **20**, 192.

Armbruster, P., Agarwal, Y. K., Brüchle, W., Brügger, M., Dufour, J. P., Gäggeler, H., Hessberger, F. P., Hofmann, S., Lemmertz, P., Münzenberg, G., Poppensieker, K., Reisdorf, W., Schädel, M., Schmidt, K. H., Schneider, J. H. R., Schneider, W. F. W., Sümmerer, K., Vermeulen, D., Wirth, G., Ghiorso, A., Gregorich, K. E., M., D. L., Leino, M., Moody, K. J., Seaborg, G. T., Welch, R. B., Wilmarth, P., Yashita, S., Frink, C., Greulich, N., Herrmann, G., Hickmann, U., Hildebrand, N., Kratz, J. V., Trautmann, N., Fowler, M. M., Hoffman, D. C., Daniels, W. R., Gunten, H. R. V., and Dornhöfer, H. (1985) *Phys. Rev. Lett.,* **54**, 406–9.

Armbruster, P. and Münzenberg, G. (1989) *Sci. Am,* **66**, 66–72.

Armbruster, P., Hessberger, F. P., Hofmann, S., Leino, M., Münzenberg, G., Reisdorf, W., and Schmidt, K.-H. (1993) *Pure Appl. Chem*., **65**, 1822–4.

Autschbach, J., Siekierski, S., Seth, M., Schwerdtfeger, P., and Schwarz, W. H. E. (2002) *J. Comput. Chem*., **23**, 804–13.

Baerends, E. J., Schwarz, W. H. E., Schwerdtfeger, P., and Snijders, J. G. (1990) *J. Phys. B,* **23**, 3225–40.

Baes, C. F. and Mesmer, R. E. (1976) *The Hydroysis of Cations*, Wiley Interscience, New York, pp. 152–91.

Barber, R. C., Greenwood, N. N., Hrynkiewicz, A. Z., Jeannin, Y. P., Lefort, M., Sakai, M., Ulehla, I., Wapstra, A. H., and Wilkinson, D. H. (1991) *Pure Appl. Chem*., **63**, 879–86.

Barber, R. C., Greenwood, N. N., Hrynkiewicz, A. Z., Jeannin, Y. P., Lefort, M., Sakai, M., Ulehla, I., Wapstra, A. H., and Wilkinso, D. H. (1992) *Prog. Part. Nucl. Phys*., **29**, 453–530.

Barber, R. C., Greenwood, N. N., Hrynkiewicz, A. Z., Jeannin, Y. P., Lefort, M., Sakai, M., Ulehla, I., Wapstra, A. H., and Wilkinso, D. H. (1993) *Pure Appl. Chem.,* **65**, 1757–813.

Bastug, T., Heinemann, D., Sepp, W.-D., Kolb, D., and Fricke, B. (1993) *Chem. Phys. Lett*., **211–224**, 119–24.

Bemis, C. E. Jr, Silva, R. J., Hensley, D. C., Keller, O. L. Jr, Tarrant, J. R., Hunt, L. D., Dittner, P. F., Hahn, R. L., and Goodman, C. D. (1973) *Phys. Rev. Lett.,* **31**, 647–50.

Bemis, C. E. Jr, Dittner, P. F., Silva, R. J., Hahn, R. L., Tarrant, J. R., Hunt, L. D., and Hensley, D. C. (1977) *Phys. Rev. C,* **16**, 1146–57.

Bilewicz, A., Kacher, C. D., Gregorich, K. E., Lee, D. M., Stoyer, N. J., Kadkhodayan, B., Kreek, S. A., Lane, M. R., Sylwester, E. R., Neu, M. P., Mohar, M. F., and Hoffman, D. C. (1996) *Radiochim. Acta*, **75**, 121–6.

Bollen, G., Becker, S., Kluge, H.-J., Konig, M., Moore, R. B., Otto, T., Raimbault-Hartmann, H., Savard, G., Schweikhard, L., and Stolzenberg, H. (1996) *Nucl. Instrum. Methods A,* **368**, 675–97.

Bratsch, S. G. and Lagowski, J. J. (1986) *J. Phys. Chem.,* **90**, 307–12.

Bratsch, S. G. (1989) *Phys. Chem. Ref. Data,* **18**, 1–21.

Brown, D. (1973) *Comprehensive Inorganic Chemistry*, vol. 3, Pergamon Press, Oxford, pp. 553–622.

Brüchle, W., Jäger, E., Pershina, V., Schädel, M., Schausten, B., Günther, R., Kratz, J. V., Paulus, W., Seibert, A., Thörle, P., Zauner, S., Schümann, D., Eichler, B., Gäggeler, H., Jost, D., and Türler, A. (1998) *J. Alloy Compds*, **271–273**, 300–2.

Burraghs, P., Evans, S., Hamnett, A., Orchard, A. F., and Richardson, N. V. (1974) *J. Chem. Soc. Faraday Trans.* 2, **70**, 1895.

Chasman, R. R. and Ahmad, I. (1997) *Phys. Lett. B,* **392**, 255–61.

CNIC, Commission on Nomenclature of Inorganic Chemistry of IUPAC (1997) *Pure Appl. Chem.*, **69**, 2471–3.

Corish, J. and Rosenblatt, G. M. (2003) *Pure Appl. Chem*., **75**, 1613–15.

Corish, J. and Rosenblatt, G. M. (2004) *Pure Appl. Chem*. **76**, 2101–3.

Cunningham, B. B. (1969) in *Proc. Robert A. Welch Foundation, XIII, The Transuranium elements – The Mendeleev Centennial*, pp. 307–22, Houston, Texas.

Czerwinski, K. R. (1992a) *Studies of Fundamental Properties of Rutherfordium (element 104) Using Organic Complexing Agents*, Doctoral Thesis, LBL-32233, Berkeley.

Czerwinski, K. R. (1992b) *Studies of Fundamental properties of Rutherfordium (element 104) Using Organic Complexing Agents*, Ph.D. Thesis, Berkeley, LBL-32233, pp. 83–102.

Czerwinski, K. R., Gregorich, K. E., Hannink, N. J., Kacher, C. D., Kadkhodayan, B. A., Kreek, S. A., Lee, D. M., Nurmia, M. J., Türler, A., Seaborg, G. T., and Hoffman, D. C. (1994a) *Radiochim. Acta,* **64**, 23–8.

Czerwinski, K. R., Kacher, C. D., Gregorich, K. E., Hamilton, T. M., Hannink, N. J., Kadkhodayan, B. A., Kreek, S. A., Lee, D. M., Nurmia, M. J., Türler, A., Seaborg, G. T., and Hoffman, D. C. (1994b) *Radiochim. Acta,* **64**, 29–35.

Desclaux, J. P. (1973) *Data Nucl. Data Tables*, **12**, 311–406.

Desclaux, J. P. (1975) *Comp. Phys. Commun*., **9**, 31–45.

Desclaux, J. P. and Fricke, B. (1980) *J. Phys.*, **41**, 943–6.
Dolg, M., Stoll, H., Preuss, H., and Pitzer, R. M. (1993) *J. Phys. Chem.*, **97**, 5852–9.
Düllmann, C. E., Eichler, B., Eichler, R., Gäggeler, H. W., Jost, D. T., Piguet, D., and Türler, A. (2002a) *Nucl. Instrum. Methods A*, **479**, 631–9.
Düllmann, C. E., Brüchle, W., Dressler, R., Eberhardt, K., Eichler, B., Eichler, R., Gäggeler, H. W., Ginter, T. N., Glaus, F., Gregorich, K. E., Hoffman, D. C., Jäger, E., Jost, D. T., Kirbach, U. W., Lee, D. M., Nitsche, H., Patin, J. B., Pershina, V., Piguet, D., Qin, Z., Schädel, M., Schausten, B., Schimpf, E., Schött, H.-J., Soverna, S., Sudowe, R., Thörle, P., Timokhin, S. N., Trautmann, N., Türler, A., Vahle, A., Wirth, G., Yakushev, A. B., and Zielinski, P. M. (2002b) *Nature,* **418**, 859–62.
Eichler, B. (1974) Dubna Report JINR P12–7767.
Eichler, B. and Rossbach, H. (1983) *Radiochim. Acta,* **33**, 121–5.
Eichler, B., Türler, A., and Gäggeler, H. W. (1999) *J. Phys. Chem. A,* **103**, 9296–306.
Eichler, B. and Kratz, J. V. (2000) *Radiochim. Acta,* **88**, 475–82.
Eichler, R., Brüchle, W., Dressler, C. E., Düllman, C. E., Eichler, B., Gäggeler, H. W., Gregorich, K. E., Hoffman, D. C., Hübener, S., Jost, D. T., Kirbach, U. W., Laue, C. A., Lavanchy, V. M., Nitsche, H., Patin, J. B., Piguet, D., Schädel, M., Shaughnessy, D. A., Strellis, D. A., Taut, S., Tobler, L., Tsyganov, Y. S., Türler, A., Vahle, A., Wilk, P. A., and Yakushev, A. B. (2000) *Nature (Lett.),* **407**, 63–5.
Eichler, R. and Schädel, M. (2002) *J. Phys. Chem. B,* **106**, 5413–20.
Eliav, E., Landau, A., Ishikawa, Y., and Kaldor, U. (1992) *J. Phys. B,* **35**, 1693.
Eliav, E., Kaldor, U., Schwerdtfeger, P., Hess, B. A., and Ishikawa, Y. (1994) *Phys. Rev. Lett.,* **73**, 3203–6.
Eliav, E., Kaldor, U., and Ishikawa, Y. (1995a) *Phys. Rev. Lett.,* **74**, 1079–82.
Eliav, E., Kaldor, U., and Ishikawa, Y. (1995b) *Phys. Rev. A,* **52**, 2765–9.
Eliav, E., Kaldor, U., Ishikawa, Y., Seth, M., and Pyykkö, P. (1996a) *Phys. Rev. A,* **53**, 3926–33.
Eliav, E., Kaldor, U., Ishikawa, Y. M., and Pyykkö, P. (1996b) *Phys. Rev. Lett.*, **77**, 5350–2.
Eliav, E., Shmulyian, S., Kaldor, U., and Ishikawa, Y. (1998a) *J. Chem. Phys.*, **109**, 3954–8.
Eliav, E., Kaldor, U., and Ishikawa, Y. (1998b) *Mol. Phys.*, **94**, 181–7.
Eliav, E., Landau, A., Ishikawa, Y., and Kaldor, U. (2002) *J. Phys. B,* **35**, 1693–700.
Ermler, W. C., Ross, R. B., and Christiansen, P. A. (1988) *Adv. Quant. Chem.,* **19**, 139–82.
Faegri, K. and Saue, T. (2001) *J. Chem. Phys.*, **115**, 2456–64.
Fiset, E. O. and Nix, J. R. (1972) *Nucl. Phys.*, **A193**, 647.
Flerov, G. N. and Zvara, I. (1971) Joint Institute of Nuclear Research, Dubna, USSR, Report D7-6031, August 1971.
Fricke, B., Greiner, W., and Waber, J. T. (1971) *Theor. Chim. Acta,* **21**, 235–60.
Fricke, B. and Waber, J. T. (1971) *Actinides Rev.*, **1**, 433–85.
Fricke, B. and Waber, J. T. (1972) *J. Chem. Phys.*, **56**, 3246.
Fricke, B. (1975) in *Structure and Bonding*, vol. 21 (ed. J. D. Dunitz), Springer-Verlag, Berlin, pp. 89–144.
Fricke, B., Johnson, E., and Rivera, G. M. (1993) *Radiochim. Acta,* **62**, 17–25.

Gäggeler, H. W. (1990) Chemistry of the transactinide elements, in *The Robert A. Welch Foundation Conference on Chemical Research XXXIV. Fifty Years with Transuranium Elements*, pp. 255–76, Houston, Texas.

Gäggeler, H. W., Jost, D. T., Kovacs, J., Scherer, U. W., Weber, A., Vermeulen, D., Türler, A., Gregorich, K. E., Henderson, R. A., Czerwinski, K. R., Kadkhodayan, B., Lee, D. M., Nurmia, M., Hoffman, D. C., Kratz, J. V., Gober, M. K., Zimmermann, H. P., Schädel, M., Bruchle, W., Schimpf, E., and Zvara, I. (1992) *Radiochim. Acta,* **57**, 93–100.

Gäggeler, H. W. (1994) *J. Radioanal. Nucl. Chem. Articles,* **183**, 261.

Gäggeler, H. W. (1997) Fast chemical separation procedures for transactinides, in *The Robert A. Welch Foundation 41st Conference on Chemical Research the Transuranium Elements*, pp. 47–51, Houston, Texas.

Gärtner, M., Boettger, M., Eichler, B., Gäggeler, H. W., Grantz, M., Hubener, S., Jost, D. T., Piguet, D., Dressler, R., Türler, A., and Yakushev, A. B. (1997) *Radiochim. Acta,* **78**, 59–68.

Ghiorso, A., Nurmia, M., Harris, J., Eskola, K., and Eskola, P. (1969) *Phys. Rev. Lett.,* **22**, 1317.

Ghiorso, A., Nurmia, M., Eskola, K., Harris, J., and Eskola, P. (1970) *Phys. Rev. Lett.,* **24**, 1498–503.

Ghiorso, A., Nurmia, M., Eskola, K., and Eskola, P. (1971) *Phys. Rev C,* **4**, 1850–5.

Ghiorso, A. and Seaborg, G. T. (1993a) *Pure Appl. Chem*., **65**, 1815–20.

Ghiorso, A. and Seaborg, G. T. (1993b) *Prog. Part. Nucl. Phys*., **31**, 233–7.

Ghiorso, A., Lee, D., Somerville, L. P., Loveland, W., Nitschke, J. M., Ghiorso, W., Seaborg, G. T., Wilmarth, P., Leres, R., Wydler, A., Nurmia, M., Gregorich, K., Czerwinski, K., Gaylord, R., Hamilton, T., Hannink, N. J., Hoffman, D. C., Jarzynski, C., Kacher, C., Kadkhodayan, B., Kreek, S., Lane, M., Lyon, A., McMahan, M. A., Neu, M., Sikkeland, T., Swiatecki, W. J., Türler, A., Walton, J. T., and Yashita, S. (1995a) *Nucl. Phys*., **583**, 861–6.

Ghiorso, A., Lee, D., Somerville, L. P., Loveland, W., Nitschke, J. M., Ghiorso, W., Seaborg, G. T., Wilmarth, P., Leres, R., Wydler, A., Nurmia, M., Gregorich, K., Czerwinski, K., Gaylord, R., Hamilton, T., Hannink, N. J., Hoffman, D. C., Jarzynski, C., Kacher, C., Kadkhodayan, B., Kreek, S., Lane, M., Lyon, A., McMahan, M. A., Neu, M., Sikkeland, T., Swiatecki, W. J., Türler, A., Walton, J. T., and Yashita, S. (1995b) *Phys. Rev. C,* **51**, R2293–7.

Girichev, G. V., Petrov, V. M., Giricheva, N. I., Utkin, A. N., and Petrova, V. N. (1981) *Zh. Strukt. Khim.,* **22**, 6.

Glebov, V. A., Kasztura, L., Nefedov, V. S., and Zhuikov, B. L. (1989) *Radiochim. Acta*, **46**, 117–21.

Gober, M. G., Kratz, J. V., Zimmermann, H. P., Schädel, M., Brüchle, W., Schimpf, E., Gregorich, K. E., Türler, A., Hannink, N. J., Czerwinski, R. K., Kadkhodayan, B., Lee, D. M., Nurmia, M. J., Hoffman, D. C., Gäggeler, H., Jost, D., Kovacs, J., Scherer, U. W., and Weber, A. (1992) *Radiochim. Acta*, **57**, 77–84.

Grant, I. P. and Pyper, N. C. (1977) *Nature (Lett.)*, **265**, 715–17.

Grant, I. P. (1986) *J. Phys. B,* **19**, 3187–205.

Grant, I. P. (1994) *Adv. Mol. Phys.,* **32**, 169–86.

Grant, I. P. and Quiney, H. (2000) *Int. J. Quant. Chem*., **80**, 283–97.

Gregorich, K. E., Henderson, R. A., Lee, D. M., Nurmia, M. J., Chasteler, R. M., Hall, H. L., Bennett, D. A., Gannett, C. M., Chadwick, R. B., Leyba, J. D., Hoffman, D. C., and Herrmann, G. (1988) *Radiochim. Acta*, **43**, 223–31.

Gregorich, K. E. (1997a) Radiochemistry of rutherfordium and hahnium, in *The Robert A. Welch Foundation 41st Conference on Chemical Research the Transuranium Elements*, pp. 95–124, Houston, Texas.

Gregorich, K. E. (1997b) Radiochemistry of rutherfordium and hahnium, in *The Robert A. Welch Foundation 41st Conference on Chemical Research the Transuranium Elements*, pp. 103–8, Houston, Texas.

Gregorich, K. E., Ginter, T., Loveland, W., Peterson, D., Patin, J. B., Folden, C. M. III, Hoffman, D. C., Lee, D. M., Nitsche, H., Omtvedt, J. P., Omtvedt, L. A., Stavsetra, L., Sudowe, R., Wilk, P. A., Zielinski, P., and Aleklett, K. (2002) *Eur. Phys. J. A,* **18**, 633–8.

Griffin, D. C., Andrew, K. L., and Cowan, R. D. (1969) *Phys. Rev.,* **177**, 62–71.

Grosse, A. V. (1965) *J. Inorg. Nucl. Chem.,* **27**, 509–20.

Guillaumont, R., Adloff, J.-P., and Peneloux, A. (1989) *Radiochim. Acta,* **46**, 169–76.

Guillaumont, R., Adloff, J.-P., Peneloux, A., and Delamoye, P. (1991) *Radiochim. Acta,* **54**, 1–15.

Günther, R., Paulus, W., Kratz, J. V., Seibert, A., Thorle, P., Zauner, S., Bruchle, W., Jager, E., Pershina, V., Schädel, M., Schausten, B., Schumann, D., Eichler, B., Gäggeler, H. W., Jost, D. T., and Türler, A. (1998) *Radiochem. Acta,* **80**, 121–8.

Haba, H., Tsukada, K., Asai, M., Goto, S., Toyoshima, A., Nishinaka, I., Akiyama, K., Hirata, M., Ichikawa, S., Nagame, Y., Shoji, Y., Shigekawa, M., Koike, T., Iwasaki, M., Shinohara, A., Kaneko, T., Maruyama, T., Ono, S., Kudo, H., Oura, Y., Sueki, K., Nakahara, H., Sakama, M., Yokoyama, A., Kratz, J. V., Schädel, M., and Brüchle, W. (2002) *J. Nucl. Radiochem. Sci.,* **3**, 143–6.

Han, Y.-K. and Lee, Y. S. (1999) *J. Phys. Chem. A,* **103**, 1104–8.

Han, Y.-K., Son, S.-K., Choi, Y. J., and Lee, Y. S. (1999a) *J. Phys. Chem.,* **103**, 9109–15.

Han, Y.-K., Bae, C., and Lee, Y. S. (1999b) *J. Chem. Phys.,* **110**, 8986–75.

Han, Y.-K., Bae, C., Son, S.-K., and Lee, Y. S. (2000) *J. Chem. Phys.,* **112**, 2684–91.

Harvey, B. G., Gunther, H., Hoff, R., Hoffman, D. C., Hyde, E. K., Katz, J. J., and Seaborg, G. T. (1976) *Science,* **193**, 271–3.

Hessberger, F. P., Hofmann, S., Ninov, V., Armbruster, P., Folger, H., Munzenberg, G., Schott, H. J., Popeko, A. G., Yeremin, A. V., Andreyev, A. N., and Saro, S. (1997) *Z. Phys. A,* **359**, 415–25.

Hoffman, D. C. (1994) *Chem. Eng. News*, 24–34.

Hoffman, D. C. (1996) *Radiochim. Acta,* **72**, 1–6.

Hoffman, D. C. and Lee, D. M. (1999) *J. Chem. Educ.,* **76**, 331–47.

Hoffman, D. C., Ghiorso, A., and Seaborg, G. T. (2000a) *The Transuranium People: The Inside Story*, Imperial College Press, London, pp. 258–98; 379–96.

Hoffman, D. C., Ghiorso, A., and Seaborg, G. T. (2000b) *The Transuranium People: The Inside Story*, Imperial College Press, London, pp. 400–17.

Hofmann, S., Ninov, V., Hessberger, F. P., Armbruster, P., Folger, H., Münzenberg, G., Schott, H. J., Popeko, A. G., Yeremin, A. V., Andreyev, A. N., Saro, S., Janik, R., and Leino, M. (1995a) *Z. Phys.,* **A350**, 277–80.

Hofmann, S., Ninov, V., Hessberger, F. P., Armbruster, P., Folger, H., Münzenberg, G., and Leino, M. (1995b) *Z. Phys.,* **A350**, 281–2.

Hofmann, S., Ninov, V., Hessberger, F. P., Armbruster, P., Folger, H., Münzenberg, G., Schott, H. J., Popeko, A. G., Yeremin, A. V., Saro, S., Janik, R., and Leino, M. (1996) *Z. Phys.,* **A354**, 229–30.

Hofmann, S. (1998) *Rep. Prog. Phys.,* **61**, 639–89.

Hofmann, S. and Munzenberg, G. (2000) *Rev. Modern Phys.,* **72**, 733–67.

Hofmann, S., Hessberger, F. P., Ackermann, D., Münzenberg, G., Antalic, S., Cagarda, P., Kindler, B., Kojouharova, J., Leino, M., Lommel, B., Mann, R., Popeko, A. G., Reshitko, S., Saro, S., Uusitalo, J., and Yeremin, A. V. (2002) *Eur. Phys. J. A,* **14**, 147–57.

Hübener, S., Taut, S., Vahle, A., Dressler, R., Eichler, B., Gäggeler, H. W., Jost, D. T., Piguet, D. T., Türler, A., Brüchle, W., Jäger, E., Schädel, M., Schimpf, E., Kirbach, U., Trautmann, N., and Yakushev, A. B. (2001) *Radiochim. Acta,* **89**, 737–41.

Hulet, E. K., Lougheed, R. W., Wild, J. F., and Landrum, J. H. (1980) *J. Inorg. Nucl. Chem.,* **42**, 79–82.

Hyde, E. K., Hoffman, D. C., and Keller, O. L. Jr (1987) *Radiochim. Acta,* **42**, 57–102.

Ionova, G. V., Pershina, V., Johnson, E., Fricke, B., and Schädel, M. (1992) *J. Phys. Chem.,* **96**, 11096–101.

Ionova, G. V., Pershina, V., Zuraeva, I. T., and Suraeva, N. I. (1996) *Sov. Radiochem.,* **37**, 282–91.

Ishikawa, Y. and Kaldor, U. in *Computational Chemistry, Reviews of Current Trends* (1996) (ed. J. Leszczynski), Worlds Scientific, Singapore, Vol. 1, pp. 1–52.

Jampolskii, V. I. (1973) Doctoral Thesis, Moscow State University.

Johnson, E., Fricke, B., Keller, O. L. Jr, Nestor, C. W. Jr, and Ticker, T. C. (1990) *J. Chem. Phys.,* **93**, 8041–50.

Johnson, E. and Fricke, B. (1991) *J. Phys. Chem.,* **95**, 7082–4.

Johnson, E., Pershina, V., and Fricke, B. (1999) *J. Phys. Chem.,* **103**, 8458–62.

Johnson, E., Fricke, B., Jacob, T., Dong, C. Z., Fritzsche, S., and Pershina, V. (2002) *J. Chem. Phys.,* **116**, 1862–8.

Jorgensen, C. K. (1968) *Chem. Phys. Lett.,* **2**, 549–50.

Kacher, C. D., Gregorich, K. E., Lee, D. M., Watanabe, Y., Kadkhodayan, B., Yang, B. J., Hsu, M., Hoffman, D. C., and Bilewicz, A. (1996a) *Radiochim. Acta,* **75**, 127–33.

Kacher, C. D., Gregorich, K. E., Lee, D. M., Watanabe, Y., Kadkhodayan, B., Wierczinski, B., Lane, M. R., Sylwester, E. R., Keeney, D. A., Hendricks, M., Hoffman, D. C., and Bilewicz, A. (1996b) *Radiochim. Acta,* **75**, 135–9.

Kadkhodayan, B., Türler, A., Gregorich, K. E., Nurmia, M. J., Lee, D. M., and Hoffman, D. C. (1992) *Nucl. Instrum. Methods,* **A317**, 254–61.

Kadkhodayan, B. (1993) *On-Line Gas Chromatographic Studies of Rutherfordium (element 104), Hahnium (element 105), and Homologs*, Doctoral Thesis, LBL-33961, Berkeley.

Kadkhodayan, B., Türler, A., Gregorich, K. E., Baisden, P. A., Czerwinski, K. R., Eichler, E., Gäggeler, H. W., Hamilton, T. M., Stoyer, N. J., Jost, D. T., Kacher, C. D., Kovacs, A., Kreek, S. A., Lane, M. R., Mohar, M. F., Neu, M. P., Sylwester, E. R., Lee, D. M., Nurmia, M. J., Seaborg, G. T., and Hoffman, D. C. (1996) *Radiochim. Acta,* **72**, 169–78.

Kaldor, U. and Eliav, E. (1998) *Adv. Quantum. Chem.,* **31**, 313–36.

Kaldor, U. and Eliav, E. (2000) Energies and other properties of heavy atoms and molecules, in *Quantum Systems in Chemistry and Physics,* vol. II (eds. A. Hernandes-Laguna, J. Maruani, R. McWeeny, S. Wilson), Kluwer, Dordrecht, vol. 1, pp. 161–176.

Karol, P. J., Nakahara, H., Petley, B. W., and Vogt, E. (2001) *Pure Appl. Chem.,* **73**, 959–67.

Karol, P. J., Nakahara, H., Petley, B. W., and Vogt, E. (2003) *Pure Appl. Chem.,* **75**, 1601–11.

Keller, O. L. Jr, Burnett, J. L., Carlson, T. A., and Nestor, C. W. J. (1970) *J. Phys. Chem.,* **74**, 1127–34.

Keller, O. L. Jr, Nestor, C. W., Carlson, T. A., and Fricke, B. (1973) *J. Phys. Chem.,* **77**, 1806–9.

Keller, O. L. Jr, Nestor, C. W., and Fricke, B. (1974) *J. Phys. Chem.,* **78**, 1845–9.

Keller, O. L. Jr and Seaborg, G. T. (1977) *Annu. Rev. Nucl. Sci.,* **27**, 139–66.

Keller, O. L. Jr (1984) *Radiochim. Acta,* **37**, 169–80.

Kirbach, U. W., Folden, C. M. III, Ginter, T. N., Gregorich, K. E., Lee, D. M., Ninov, V., Omtvedt, J. P., Patin, J. B., Seward, N. K., Strellis, D. A., Sudowe, R., Türler, A., Wilk, P. A., Zielinski, P. M., Hoffman, D. C., and Nitsche, H. (2002) *Nucl. Instrum. Methods A,* **484**, 587–94.

Kohn, W., Becke, A. D., and Parr, R. G. (1996) *J. Phys. Chem.,* **100**, 12974–80.

Kratz, J. V., Zimmermann, H. P., Scherer, U. W., Schädel, M., Brüchle, W., Gregorich, K. E., Gannett, C. M., Hall, H. L., Henderson, R. A., Lee, D. M., Leyba, J. D., Nurmia, M. J., Hoffman, D. C., Gäggeler, H. W., Jost, D., Baltensperger, U., Ya, N. Q., Türler, A., and Lienert, C. (1989) *Radiochim. Acta,* **48**, 121–33.

Kratz, J. V., Gober, M. K., Zimmermann, H. P., Schädel, M., Brüchle, W., Schimpf, E., Gregorich, K. E., Türler, A., Hannink, N. J., Czerwinski, K. R., Kadkhodayan, B., Lee, D. M., Nurmia, M. J., Hoffman, D. C., Gäggeler, H. W., Jost, D., Kovacs, J., Scherer, U. W., and Weber, A. (1992) *Phys. Rev. C,* **45**, 1064–9.

Kratz, J. V. (1999a) Fast chemical separation procedures for transactinides, in *Heavy Elements and Related New Phenomena* (eds. W. Greiner and R. K. Gupta), World Scientific, Singapore, pp. 43–63.

Kratz, J. V. (1999b) Chemical properties of the transactinide elements, in *Heavy Elements and Related New Phenomena* (eds. W. Greiner and R. K. Gupta), World Scientific, Singapore, pp. 129–93.

Krebs, B., and Hasse, K. D. (1976) *Acta Crystallogr., B* **32**, 1334

Kruppa, A. T., Bender, M., Nazarewicz, W., Reinhard, P. G., Vertse, T., and Cwiok, S. (2000) *Phys. Rev. C,* **61** 034313-1–13.

Kugler, E., Fiander, D., Jonson, B., Haas, H., Przewloka, A., Ravn, H. L., Simon, D. J., and Zimmer, K. (1992) *Nucl. Instrum. Methods. B,* **70**, 41–9.

Landau, A., Eliav, E., Ishikawa, Y., and Kaldor, U. (2001) *J. Chem. Phys.,* **114**, 2977–80.

Lazarev, Y. A., Lobanov, Y. V., Oganessian, Y. T., Utyonkov, V. K., Abdullin, F. S., Buklanov, G. V., Gikal, B. N., Iliev, S., Mezentsev, A. N., Polyakov, A. N., Sedykh, I. M., Shirokovsky, I. V., Subbotin, V. G., Sukhov, A. M., Tsyganov, Y. S., Zhuchko, V. E., Lougheed, R. W., Moody, K. J., Wild, J. F., Hulet, E. K., and McQuaid, J. H. (1994) *Phys. Rev. Lett.,* **73**, 624–7.

Lazarev, Y. A., Lobanov, Y. V., Oganessian, Y. T., Tsyganov, Y. S., Utyonkov, V. K., Abdullin, F. S., Iliev, S., Polyakov, A. N., Rigol, J., Shirokovsky, I. V., Subbotin, V. G., Sukhov, A. M., Buklanov, G. V., Gikal, B. N., Kutner, V. B., Mezentsev, A. N., Sedykh, I. M., Vakatov, D. V., Lougheed, R. W., Wild, J. F., Moody, K. J., and Hulet, E. K. (1995) *Phys. Rev. Lett.,* **75**, 1903–6.

Lazarev, Y. A., Lobanov, Y. V., Oganessian, Y. T., Utyonkov, V. K., Abdullin, F. S., Polyakov, A. N., Rigol, J., Shirokovsky, I. V., Tsyganov, Y. S., Iliev, S., Subbotin, V. G., Sukhov, A. M., Buklanov, G. V., Gikal, B. N., Kutner, V. B., Mezentsev, A. N., Subotic, K., Wild, J. F., Longheed, R. W., and Moody, K. J. (1996) *Phys. Rev. C,* **54**, 620–5.

Lijima, K. and Shibata, S. (1974) *Bull. Chem. Soc. Jpn.,* **47**, 1393.

Lijima, K. and Shibata, S. (1975) *Bull. Chem. Soc. Jpn.,* **48**, 666.

Lim, I., Pernpointner, M., Seth, M., and Schwerdtfeger, P. (1999) *Phys. Rev. A,* **60**, 2822–8.

Liu, W., Hong, G., Dai, D., Li, L., and Dolg, M. (1997) *Theor. Chem. Acc.,* **96**, 75–83.

Liu, W. and van Wüllen, C. (1999) *J. Chem. Phys.,* **110**, 3730–5.

Liu, W., van Wüllen, C., Han, Y. K., Choi, Y. J., and Lee, Y. S. (2001) *Adv. Quant. Chem.,* **39**, 325–55.

Lougheed, R. W., Moody, K. J., Wild, J. F., Hulet, E. K., McQuaid, J. H., Lazarev, Y. A., Lobanov, Y. V., Oganessian, Y. T., Utyonkov, V. K., Abdullin, F. S., Buklanov, G. V., Gikal, B. N., Iliev, S., Mezentsev, A. N., Polyakov, A. N., Sedykh, I. M., Shirokovsky, I. V., Subbotin, V. G., Sukhov, A. M., Tsyganov, Y. S., and Zhuchko, V. E. (1994) *J. Alloys Compds,* **213**, 61–6.

Lougheed, R. W., Moody, J., Wild, J. F., Stoyer, N. J., Stoyer, M. A., Oganessian, Y. T., Utyonkov, V. K., Lobanov, Y. V., Abdullin, F. S., Polyakov, A. N., Shirokovsky, I. V., Tsyganov, Y. S., Gulbekian, G. G., Gobomolov, S. L., Gikal, B. N., Mezentsev, A. N., Iliev, S., Subbotin, V. G., Sukhov, A. M., Buklanov, G. V., Subotic, K., and Itkis, M. G. K. (2000) NUCL Abstract 19, San Francisco, CA, March 27.

Loveland, W., Gregorich, K. E., Patin, J. B., Peterson, D., Rouski, C., Zielinski, P., and Aleklett, K. (2002) *Phys. Rev. C,* **66** 044617-1–5.

Mann, J. B. (1969) *J. Chem. Phys.,* **51**, 841.

Mann, J. B. and Waber, J. T. (1970) *J Chem. Phys.,* **53**, 2397.

Meldner, H. (1967) *Ark. Fys.,* **36**, 593–8.

Moore, C. E. (1958) Atomic Energy Levels, Natl. Bur. Stand. (U. S.) Circ. No. 467 (U. S. GPO, Washington, DC, 1952), Vol. II; III.

Mulliken, R. S. (1955) *J. Chem. Phys.,* **23**, 1833–46.

Myers, W. D. and Swiatecki, W. J. (1966) *Nucl. Phys.,* **81**, 1.

Myers, W. D. and Swiatecki, W. J. (2000) *Phys. Rev. C,* **6204**, 312–17.

Nagame, Y., Asai, M., Haba, H., Tsukada, K., Goto, S., Sakama, M., Nishinaka, I., Toyoshima, A., Akiyama, K., and Ichikawa, S. (2002) *J. Nucl. Radiochem. Sci.,* **3**, 129–32.

Nash, C. S. and Bursten, B. E. (1995) *New J. Chem.,* **19**, 669–75.

Nash, C. S., Bursten, B. E., and Ermler, W. C. (1997) *J. Chem. Phys.,* **106**, 5133–42.

Nash, C. S. and Bursten, B. E. (1999a) *J. Phys. Chem. A,* **103**, 402–10.

Nash, C. S. and Bursten, B. E. (1999b) *Angew. Chem. Int. Ed. Engl.,* **38**, 151–3.

Nash, C. S. and Bursten, B. E. (1999c) *J. Phys. Chem. A,* **103**, 632–6.

Nilsson, S. G., Tsang, C. F., Sobiczewski, A., Szymanski, Z., Wycech, S., Gustafsson, G., Lam, I. L., Möller, P., and Nilsson, B. (1969a) *Nucl. Phys.,* **A131**, 1.

Nilsson, S. G., Thompson, S. G., and Tsang, C. F. (1969b) *Phys. Lett.,* **28B**, 458.

Oganessian, Y. T. and Zvara, I. (1993) *Pure Appl. Chem.,* **65**, 1820–1.

Oganessian, Y. T., Yeremin, A. V., Popeko, A. G., Bogomolov, S. L., Buklanov, G. V., Chelnokov, M. L., Chepigin, V. I., Gikal, B. N., Gorshkov, V. A., Gulbekian, G. G., Itkis, M. G., Kabachenko, A. P., Lavrentev, A. Y., Malyshev, O. N., Rohac, J., Sagaidak, R. N., Hofmann, S., Saro, S., Giardinas, G., and Morita, K. (1999a) *Nature,* **400**, 242–5.

Oganessian, Y. T., Utyonkov, V. K., Lobanov, Y. V., Abdullin, F. S., Polyakov, A. N., Shirokovsky, I. V., Tsyganov, Y. S., Gulbekian, G. G., Gobomolov, S. L., Gikal, B. N., Mezentsev, A. N., Iliev, S., Subbotin, V. G., Sukhov, A. M., Buklanov, G. V., Subotic, K., Itkis, M. G., Moody, K. J., Wild, J. F., Stoyer, N. J., Stoyer, M. A., and Lougheed, R. W. (1999b) *Phys. Rev. Lett.,* **83**, 3154–7.

Oganessian, Y. T., Yeremin, A. Y., Gulbekian, G. G., Bogomolov, S. L., Chepigin, V. I., Gikal, B. N., Gorshkov, V. A., Itkis, M. G., Kabachenko, A. P., Kutner, V. B., Lavrentev, A. Y., Malyshev, O. N., Popeko, A. G., Rohac, J., Sagaidak, R. N., Hofmann, S., Münzenberg, G., Veselsky, M., Saro, S., Iwasa, N., and Morita, K. (1999c) *Eur. Phys. J. A,* **5**, 63–8.

Oganessian, Y. T., Utyonkov, V. K., Lobanov, Y. V., Abdullin, F. S., Polyakov, A. N., Shirokovsky, I. V., Tsyganov, Y. S., Gulbekian, G. G., Bogomolov, S. L., Gikal, B. N., Mezentsev, A. N., Iliev, S., Subbotin, V. G., Sukhov, A. M., Ivanov, O. V., Buklanov, G. V., Subotic, K., Itkis, M. G., Moody, K. J., Wild, J. F., Stoyer, N. J., Stoyer, M. A., and Lougheed, R. W. (2000a) *Phys. Rev. C,* **62** 041604 (R) 1–4.

Oganessian, Y. T., Utyonkov, V. K., Lobanov, Y. V., Abdulin, F. S., Polyakov, A. N., Shirokovsky, I. V., Tsyganov, Y. S., Gulbekian, G. G., Bogomolov, S. L., Gikal, B. N., Mezentsev, A. N., Iliev, S., Subbotin, V. G., Sukhov, A. M., Ivanov, O. V., Buklanov, G. V., Subotic, K., Itkis, M. G., Moody, K. J., Wild, J. F., Stoyer, N. J., Stoyer, M. A., Lougheed, R. W., Laue, C. A., Karelin, Y. A., and Tatarinov, A. N. (2000b) *Phys. Rev. C,* **63** 011301 (R) 1–2.

Oganessian, Y. T. (2001) *Nucl. Phys. A,* **685**, 17c.

Oganessian, Y. T. (2002) *J. Nucl. Radiochem. Sci.,* **3**, 5–8.

Oganessian, Y. T., Utyonkov, V. K., Lobanov, Y. V., Abdullin, F. S., Polyakov, A. N., Shirokovsky, I. V., Tsyganov, Y. S., Gulbekian, G. G., Bogomolov, S. L., Gikal, B. N., Mezentsev, A. N., Iliev, S., Subbotin, V. G., Sukhov, A. M., Ivanov, O. V., Buklanov, G. V., Subotic, K., Voinov, A. A., Itkis, M. G., Moody, K. J., Wild, J. F., Stoyer, N. J., Stoyer, M. A., Lougheed, R. W., and Laue, C. A. (2002) *Eur. Phys. J. A,* **15**, 201–4.

Oganessian, Y. T., Utyonkoy, V. K., Lobanov, Y. V., Abdullin, F. S., Polyakov, A. N., Shirokovsky, I. V., Tsyganov, Y. S., Gulbekian, G. G., Bogomolov, S. L., Mezentsev, A. N., Iliev, S., Subbotin, V. G., Sukhov, A. M., Voinov, A. A., Buklanov, G. V., Subotic, K., Zagrebaev, V. I., Itkis, M. G., Patin, J. B., Moody, K. J., Wild, J. F., Stoyer, M. A., Stoyer, N. J., Shaughnessy, D. A., Kenneally, J. M., and Lougheed, R. W. (2004a) *Phys. Rev. C,* **69**, 021601(R).

Oganessian, Y. T., Yeremin, A. V., Popeko, A. G., Malyshev, O. N., Belozerov, A. V., Buklanov, G. V., Chelnokov, M. L., Chepigin, V. I., Gorshkov, V. A., Hofmann, S., Itkis, M. G., Kabachenko, A. P., Kindler, B., Munzenberg, G., Sagaidak, R. N., Saro,

S., Schott, H.-J., Streicher, B., Shutov, A. V., Svirikhin, A. I., and Vostokin, G. K. (2004b) *Eur. Phys. J. A,* **19**, 3–6.

Oganessian, Y. T., Utyonkov, V. K., Lobanov, Y. V., Abdullin, F. S., Polyakov, A. N., Shirokovsky, I. V., Tsyganov, Y. S., Gulbekian, G. G., Bogomolov, S. L., Gikal, B. N., Mezentsev, A. N., Iliev, S., Subbotin, V. G., Sukhov, A. M., Voinov, A. A., Buklanov, G. V., Subotic, K., Zagrebaev, V. I., Itkis, M. G., Patin, J. B., Moody, K. J., Wild, J. F., Stoyer, M. A., Stoyer, N. J., Shaughnessy, D. A., Kenneally, J. M., and Lougheed, R. W. (2004c) *Phys. Rev. C,* **69**, 054607.

Omtvedt, J.-P., Alstad, J., Eberhardt, K., Fure, K., Malmbeck, R., Mendel, M., Nähler, A., Skarnemark, G., Trautmann, N., Wiehl, N., and Wierczinski, B. J. (1998) *J. Alloys Compds,* **271**, 303.

Omtvedt, J. P., Alstad, J., Breivik, H., Dyve, J. E., Eberhardt, K., Folden, C. M. III, Ginter, T., Gregorich, K. E., Hult, E. A., Johansson, M., Kirbach, U. W., Lee, D. M., Mendel, M., Nahler, A., Ninov, V., Omtvedt, L. A., Patin, J. B., Skarnemark, G., Stavsetra, L., Sudowe, R., Wiehl, N., Wierczinski, B., Wilk, P. A., Zielinski, P. M., Kratz, J. V., Trautmann, N., Nitsche, H., and Hoffman, D. C. (2002) *J. Nucl. Radiochem. Sci.,* **3**, 121–4.

Parpia, F. A., Froese-Fisher, S., and Grant, I. P. (1996) *CPC,* **94**, 249–71.

Paulus, W., Kratz, J. V., Strub, E., Zauner, S., Brüchle, W., Schädel, M., Schausten, B., Adams, J. L., Gregorich, K. E., Hoffman, D. C., Laue, C., Lee, D. M., McGrath, C. A., Shaughnessy, D. K., Strellis, D. A., and Sylwester, E. R. (1999) *Radiochim. Acta,* **84**, 69–77.

Penneman, R. A., Mann, J. B., and Jorgensen, C. K. (1971) *Chem. Phys. Lett.,* **8**, 321–6.

Penneman, R. A. and Mann, J. B. (1976) Calculational Chemistry of the Superheavy Elements; Comparison with elements of the 7th Period, in *J. Inorg. Chem. Suppl., Proc. Moscow Symp. on Chemistry of the Transuranium Elements,* pp. 257–63.

Peppard, D. F., Mason, G. W., and Maier, J. L. (1956) *J. Inorg. Nucl. Chem.,* **3**, 215.

Pepper, M. and Bursten, B. E. (1991) *Chem. Rev.,* **91**, 719–40.

Pershina, V., Sepp, W.-D., Fricke, B., and Rosen, A. (1992a) *J. Chem. Phys.,* **96**, 8367–78.

Pershina, V., Sepp. W.-D., Bastug, T., Fricke, B., and Ionova, G. V. (1992b) *J. Chem. Phys.,* **97**, 1123–31.

Pershina, V. and Fricke, B. (1993) *J. Chem. Phys.,* **99**, 9720–9.

Pershina, V. and Fricke, B. (1994) *J. Phys. Chem.,* **98**, 6468–73.

Pershina, V. and Fricke, B. (1995) *J. Phys. Chem.,* **99**, 144–7.

Pershina, V. (1996) *Chem. Rev.,* **96**, 1977–2010.

Pershina, V. and Fricke, B. (1996) *J. Phys. Chem.,* **100**, 8748–51.

Pershina, V. (1998a) *Radiochim. Acta,* **80**, 65–73.

Pershina, V. (1998b) *Radiochim. Acta,* **80**, 75–84.

Pershina, V. and Bastug, T. (1999) *Radiochim. Acta,* **84**, 79–84.

Pershina, V. and Fricke, B. (1999) Electronic Structure and Chemistry of the Heaviest Elements, in *Heavy Elements and Related New Phenomena,* vol. 1, (eds. W. Greiner and R. K. Gupta), World Scientific, Singapore, pp. 184–262.

Pershina, V., Johnson, E., and Fricke, B. (1999) *J. Phys. Chem. A,* **103**, 8463–70.

Pershina, V. and Bastug, T. (2000) *J. Chem. Phys.,* **113**, 1441–6.

Pershina, V., Bastug, T., Fricke, B., and Varga, S. (2001) *J. Phys. Chem.,* **115**, 792–9.

Pershina, V. and Kratz, J. V. (2001) *Inorg. Chem.,* **40**, 776–80.

Pershina, V., Bastug, T., Jacob, T., Fricke, B., and Varga, S. (2002a) *Chem. Phys. Lett.,* **365**, 176–83.

Pershina, V., Trubert, D., Le Naour, C., and Kratz, J. V. (2002b) *Radiochim. Acta,* **90**, 869–77.

Pershina, V. (2003) Theoretical chemistry of the heaviest elements, in *The Chemistry of Superheavy Elements* (ed. M. Schädel), Kluwer Academic Publishers, Dordrecht, The Netherland, pp. 31–94.

Pershina, V. and Hoffman, D. C. (2003) The chemistry of the heaviest elements, in *Theoretical Chemistry and Physics of Heavy and Superheavy Elements* in the series Comput. Phys. Commun. *Progress in Theoretical Chemistry and Physics* (eds. U. Kaldor and S. Wilson), Kluwer Academic Publishers, Dordrecht, The Netherlands, ch. 3, pp. 55–114.

Pfrepper, G., Pfrepper, R., Krauss, D., Yakushev, A. B., Timokhin, S. N., and Zvara, I. (1998) *Radiochim. Acta,* **80**, 7–12.

Pitzer, K. S. (1975a) *J. Chem. Phys.,* **63**, 1032–3.

Pitzer, K. S. (1975b) *J. Chem. Soc., Chem. Commun.*, 760–1.

Pyper, N. C. and Grant, I. P. (1981) *Proc. R. Soc. Lond. A,* **376**, 483–92.

Pyykkö, P. (1988) *Chem. Rev.,* **88**, 563–94.

Pyykkö, P., Tokman, M., and Labzowsky, L. N. (1998) *Phys. Rev. A,* **57**, R689–92.

Randrup, J., Larsson, S. E., Moller, P., Sobiczewski, A., and Kukasiak, A. (1974) *Phys. Scr.,* **10A**, 60–4.

Rieth, U., Herlert, A., Kratz, J. V., Schweikhard, L., Vogel, M., and Walther, C. (2002) *Radiochim. Acta,* **90**, 337–43.

Rosen, A., Fricke, B., Morovic, T., and Ellis, D. E. (1979) *J. Phys. C4, Suppl. 4,* **40**, C4/218–19.

Rosen, A. (1997) *Adv. Quant. Chem.,* **29**, 1–30.

Ryzhkov, M. V., Gubanov, V. A., and Zvara, I. (1992) *Radiochim. Acta,* **57**, 11–14.

Saue, T., Faegri, K., and Gropen, O. (1996) *Chem. Phys. Lett.,* **263**, 360–6.

Schädel, M., Brüchle, W., Schimpf, E., Zimmermann, H. P., Gober, M. K., Kratz, J. V., Trautmann, N., Gäggeler, H., Jost, D., Kovacs, J., Scherer, U. W., Weber, A., Gregorich, K. E., Türler, A., Czerwinski, K. R., Hannink, N. J., Kadkhodayan, B., Lee, D. M., Nurmia, M. J., and Hoffman, D. C. (1992) *Radiochim. Acta,* **57**, 85–92.

Schädel, M. (1995) *Radiochimica Acta,* **70/71**, 207–23.

Schädel, M., Brüchle, W., Dressler, R., Eichler, B., Gäggeler, H. W., Günther, R., Gregorich, K. E., Hoffman, D. C., Hübener, S., Jost, D. T., Kratz, J. V., Paulus, W., Schumann, D., Timokhin, S., Trautmann, N., Türler, A., Wirth, G., and Yakuschev, A. (1997a) *Nature* (*Lett.*), **388**, 55–7.

Schädel, M., Brüchle, W., Schausten, B., Schimpf, E., Jäger, E., Wirth, G., Günther, R., Kratz, J. V., Paulus, W., Seibert, A., Thorle, P., Trautmann, N., Zauner, S., Schumann, D., Andrassy, M., Misiak, R., Gregorich, K. E., Hoffman, D. C., Lee, D. M., Sylwester, E. R., Nagame, Y., and Oura, Y. (1997b) *Radiochim. Acta,* **77**, 149–59.

Schädel, M., Brüchle, W., Jäger, E., Schausten, B., Wirth, G., Paulus, W., Günther, R., Eberhardt, K., Kratz, J. V., Seibert, A., Strub, E., Thörle, P., Trautmann, N., Waldek, W., Zauner, S., Schumann, D., Kirbach, U., Kubica, B., Misiak, R., Nagame, Y., and Gregorich, K. E. (1998) *Radiochim. Acta,* **83**, 163–5.

Schädel, M. (2002) *J. Nucl. Radiochem. Sci.,* **3**, 113–20.

Schwarz, W. H. E., Van Wezenbeek, E. M., Baerends, E. J., and Snijders, J. G. (1989) *J. Phys. B,* **22**, 1515–30.

Schwarz, W. H. E. (1990) *Theoretical Models of Chemical Bonding,* Springer, Berlin, pp. 593–643.

Schwerdtfeger, P., Dolg, M., Schwarz, W. H. E., Bowmaker, G. A., and Boyd, P. W. D. (1989) *J. Chem. Phys.,* **91**, 1762–74.

Schwerdtfeger, P. and Seth, M. (1998) Relativistic effects on the superheavy elements, in *Encyclopedia on Computational Chemistry*, vol. 4, John Wiley, New York, pp. 2480–99.

Seaborg, G. T. (1968) *Annu. Rev. Nucl. Sci.,* **18**, 53.

Seaborg, G. T. and Keller, O. L. Jr (1986) Future elements, in *The Chemistry of the Actinide Elements,* 2nd edn, vol. II (eds. J. J. Katz, G. T. Seaborg, and L. R. Morss), Chapman & Hall, London, pp. 1635–43.

Seaborg, G. T. (1996) *J. Chem. Soc., Dalton Trans.*, 3899–907.

Seth, M., Schwerdtfeger, P., Dolg, M., Faegri, K., Hess, B. A., and Kaldor, U. (1996) *Chem. Phys. Lett.,* **250**, 461–5.

Seth, M., Schwerdtfeger, P., and Dolg, M. (1997) *J. Chem. Phys.,* **106**, 3623–32.

Seth, M., Cooke, F., Schwerdtfeger, P., Heully, J.-L., and Pelissier, M. (1998a) *J. Chem. Phys.,* **109**, 3935–43.

Seth, M., Faegri, K., and Schwerdtfeger, P. (1998b) *Angew. Chem. Int. Ed. Engl.,* **37**, 2493–6.

Seth, M., Schwerdtfeger, P., and Faegri, K. (1999) *J. Chem. Phys.,* **111**, 6422–33.

Shannon, R. D. (1976) *Acta Crystallogr. A,* **32**, 751–67.

Silva, R. J., Sikkeland, T., Nurmia, M., and Ghiorso, A. (1970a) *Inorg. Nucl. Chem. Lett.,* **6**, 733–9.

Silva, R., Harris, J., Nurmia, M., Eskola, K., and Ghiorso, A. (1970b) *Inorg. Nucl. Chem. Lett.,* **6**, 871–7.

Smolańczuk, R., Skalski, J., and Sobiczewski, A. (1995) *Phys. Rev. C,* **52**, 1871–80.

Smolańczuk, R. (1997) *Phys. Rev. C,* **56**, 812–24.

Smolańczuk, R. (1999a) *Phys. Rev. C,* **59**, 2634–9.

Smolańczuk, R. (1999b) *Phys. Rev. Lett.,* **83**, 4705–8.

Smolańczuk, R. (1999c) *Phy. Rev. C,* **61** 011601-1–4.

Smolańczuk, R. (2001a) *Phys. Lett. B,* **509**, 227–30.

Smolańczuk, R. (2001b) *Phys. Rev. C,* **63** 044607-1–8.

Sobiczewski, A., Smolańczuk, R., and Skalski, J. (1994) *J. Alloys Compds,* **213**, 38–42.

Soverna, S., Aebersold, H. U., Düllman, C. E., Eichler, B., Gäeggeler, H. W., Tobler, L., Türler, A., and Thi, Q. (2001) The GDCh Conference, Würzburg, Germany, September 2001.

Strub, E., Kratz, J. V., Kronenberg, A., Nähler, A., Thörle, P., Zauner, S., Brüchle, W., Jäger, E., Schädel, M., Schausten, B., Schimpf, E., Zongwei, L., Kirbach, U., Schumann, D., Jost, D., Türler, A., Asai, M., Nagame, Y., Sakara, M., Tsukada, K., Gäggeler, H. W., and Glanz, J. P. (2000) *Radiochim. Acta,* **88**, 265–71.

Strutinsky, V. M. (1966) *Sov. J. Nucl. Phys.,* **3**, 449–57.

Sylwester, E. R., Gregorich, K. E., Lee, D. M., Kadkhodayan, B., Türler, A., Adams, J. L., Kacher, C. D., Lane, M. R., Laue, C. A., McGrath, C. A., Shaughnessy, D. A., Strellis, D. A., Wilk, P. A., and Hoffman, D. C. (2000) *Radiochim Acta,* **88**, 837–43.

Timokhin, S. N., Yakushev, A. B., Xu, H. G., Perelygin, V. P., and Zvara, I. (1996) *J. Radioanal. Nucl. Chem. Lett.,* **212**, 31–4.

Trubert, D., Le Naour, C., Hussonois, M., Brillard, L., Montroy Gutman, F., Le Du, J. F., Constantinescu, O., Barci, V., Weiss, B., Gasparro, J., and Ardisson, G. (1999) in *Abstracts of the 1st Int. Conf. on Chemistry and Physics of the Transactinides*, Seeheim, September 26–30.

Türler, A., Gäggeler, H. W., Gregorich, K. E., Barth, H., Bruchle, W., Czerwinski, K. R., Gober, M. K., Hannink, N. J., Henderson, R. A., Hoffman, D. C., Jost, D. T., Kacher, C. D., Kadkhodayan, B., Kovacs, J., Kratz, J. V., Kreek, S. A., Lee, D. M., Leyba, J. D., Nurmia, M. J., Schädel, M., Scherer, U. W., Schimpf, E., Vermeulen, D., Weber, A., Zimmermann, H. P., and Zvara, I. (1992) *J. Radioanal. Nucl. Chem. Articles,* **160**, 327–39.

Türler, A. (1996) *Radiochim. Acta,* **72**, 7–17.

Türler, A., Eichler, B., Jost, D. T., Piguet, D., Gäggeler, H. W., Gregorich, K. E., Kadkhodayan, B., Kreek, S. A., Lee, D. M., Mohar, M., Sylwester, E., Hoffman, D. C., and Hübener, S. (1996) *Radiochim. Acta,* **73**, 55–66.

Türler, A., Dressler, R., Eichler, B., Gäggeler, H. W., Jost, D. T., Schädel, M., Bruchle, W., Gregorich, K. E., Trautmann, N., and Taut, S. (1998a) *Phys. Rev. C,* **57**, 1648–55.

Türler, A., Buklanov, G. V., Eichler, B., Gäggeler, H. W., Grantz, M., Hübener, S., Jost, D. T., Lubedev, V. Y., Piguet, D., Timokhin, S. N., Yakushev, A. B., and Zvara, I. (1998b) *J. Alloys Compds,* **271**, 287–91.

Türler, A., Brüchle, W., Dressler, R., Eichler, B., Eichler, R., Gäggeler, H. W., Gartner, M., Glatz, J. P., Gregorich, K. E., Hübener, S., Jost, D. T., Lebedev, V. Y., Pershina, V. G., Schädel, M., Taut, S., Timokhin, S. N., Trautmann, N., Vahle, A., and Yakushev, A. B. (1999) *Angew. Chem Int. Ed. Engl.,* **38**, 2212–13.

Türler, A., Düllman, C. E., Gäggeler, H. W., Kirbach, U. W., Yakushev, A. B., Schädel, M., Brüchle, W., Dressler, R., Eberhardt, K., Eichler, B., Eichler, R., Ginter, T. N., Glaus, F., Gregorich, K. E., Hoffman, D. C., Jäger, E., Jost, D. T., Lee, D. M., Nitsche, H., Patin, J. B., Pershina, V., Piguet, D., Qin, Z., Schausten, B., Schimpf, E., Schött, H.-J., Soverna, S., Sudowe, R., Thörle, P., Timokhin, S. N., Trautmann, N., Vahle, A., Wirth, G., and Zielinski, P. (2003) *Eur. Phys. J. A,* **17**, 505–8.

Varga, S., Engel, E., Sepp, W.-D., and Fricke, B. (1999) *Phys. Rev. A,* **59**, 4288–94.

Varga, S., Fricke, B., Hirata, M., Bastug, T., Pershina, V., and Fritzsche, S. (2000) *J. Phys. Chem. A,* **104**, 6495–8.

Visscher, L., Lee, T. J., and Dyall, K. G. (1996) *J. Chem. Phys.,* **105**, 8769–76.

Waber, J. T., Cromer, D. T., and Liberman, D., (1969) *J. Chem. Phys.* **51**, 664.

Waber, J. T. and Averill, F. W. (1974) *J. Chem. Phys.,* **60**, 4460–70.

Wierczinski, B. and Hoffman, D. C. (1996) Instrumentation for atom-at-a-time chemistry of the heavy elements, in *IANCAS Frontiers in Nuclear Chemistry* (eds. D. D. Sood, P. K. Reddy, and A. V. R. Pujari), Perfect Prints, Thane, India, pp. 171–91.

Wilk, P. A., Gregorich, K. E., Türler, A., Laue, C. A., Eichler, R., Ninov, V., Adams, J. L., Kirbach, U. W., Lane, M. R., Lee, D. M., Patin, J. B., Shaughnessy, D. A., Strellis, D. A., Nitsche, H., and Hoffman, D. C. (2000) *Phys. Rev. Lett.,* **85**, 2697–700.

Wilson, S., Grant, I. P., and Gyoffry, B. L. (1991) *The Effects of Relativity in Atoms, Molecules and the Solid State,* Plenum, New York.

Wood, C. P. and Pyper, N. C. (1981) *Chem. Phys. Lett.,* **84**, 614–21.

Yakushev, A. B., Timokhin, S. N., Vedeneev, M. V., Xu, H. G., and Zvara, I. (1996) *J. Radioanal. Nucl. Chem. Articles,* **205**, 63–7.

Yakushev, A. B., Buklanov, G. V., Chelnokov, M. L., Chepigin, V. I., Dmitriev, S. N., Gorshkov, V. A., Hübener, S., Lebedev, V. Y., Malyshev, O. N., Oganessian, Y. T., Popeko, A. G., Sokol, E. A., Timokhin, S. N., Türler, A., Vasko, V. M., Yeremin, A. V., and Zvara, I. (2001) *Radiochim. Acta,* **89**, 743–5.

Yakushev, A. B. (2002) Workshop on Recoil Separator for Superheavy Element Chemistry, March 20–21, 2002, Darmstadt.

Zharskii, I. M., Zasorin, E. Z., Spiridonov, V. P., Novikov, G. I., and Kupreev, V. N. (1975) *Koord. Khim.,* **1**, 574.

Zhuikov, B. L., Chuburkov, Y. T., Timokhin, S. N., Jin, K. U., and Zvara, I. (1989) *Radiochim. Acta,* **46**, 113–17.

Zhuikov, B. L., Glebov, V. A., Nefedov, V. S., and Zvara, I. (1990) *Radioanal. Nucl. Chem. Articles,* **143**, 103–11.

Zimmermann, H. P., Gober, M. K., Kratz, J. V., Schädel, M., Brüchle, W., Schimpf, E., Gregorich, K. E., Türler, A., Czerwinski, K. R., Hannink, N. J., Kadkhodayan, B., Lee, D. M., Nurmia, M. J., Hoffman, D. C., Gäggeler, G., Jost, D., Kovacs, J., Scherer, U. W., and Weber, A. (1993) *Radiochimica Acta,* **60**, 11–16.

Zvara, I., Chuburkov, Y. T., Tsaletka, R., and Shalaevskii, M. R. (1969) *Sov. Radiochem.,* **11**, 161–70.

Zvara, I., Chuburkov, Y. T., Belov, V. Z., Buklanov, G. V., Zakhvataev, B. B., Zvarova, T. S., Maslov, O. D., Caletka, R., and Shalaevsky, M. R. (1970) *J. Inorg. Nucl. Chem.,* **32**, 1885–94.

Zvara, I., Belov, V. Z., Domanov, V. P., Korotkin, Y. S., Chelnokov, L. P., Shalaevsky, M. R., Shchegolev, V. A., and Hussonois, M. (1972) *Sov. Radiochem.,* **14**, 115–18.

Zvara, I., Aikhler, V., Belov, V. Z., Zvarova, T. S., Korotkin, Y. S., Shalaevskii, M. R., Shchegolev, V. A., and Yussonnua, M. (1974) *Sov. Radiochem.,* **16**, 709–15.

Zvara, I., Belov, V. Z., Domanov, V. P., and Shalaevskii, M. R. (1976) *Sov. Radiochem.,* **18**, 328–34.

Zvara, I. (1985) *Radiochim. Acta,* **38**, 95–101.